Specific Detection of 14-3-3 Proteins by ssDNA Aptamers

Ross Stevenson

PhD Thesis

The University of Edinburgh

2006

Acknowledgements

I would like to acknowledge Prof. Robert Baxter for the opportunity to carry out this PhD and I would like to thank him for his continued support and supervision. I would also like to thank Dr. Dominic Campopiano and Dr. Helen Baxter for their additional support, advice and guidance during the course of this work.

Without the following people this work would not have been completed.
Prof. Alastair Aitken and Dr. Shaun Mackie for generously donating their time and resources to help with the 14-3-3 Proteins.

The Aptamer library was synthetically produced with the kind help and supervision of both Prof. Tom Brown and Dr. Dorkus Brown at the Chemistry Department in the University of Southampton.

Early Radioactive work was carried out under the supervision of Dr. Sandeep Varma, a visiting academic from the Institute of Kanpur, India

To all members of Lab 229, both past and present, who have contributed to a friendly working environment. Special thanks go to Paul, Dave, Rachel, Bev and Cecile

To my Mum, Paul and Katy for their support. Also thanks to Jill and Leanna.

Abstract

A library of ssDNA aptamers has been screened and a number of molecules which show high binding affinity to 14-3-3 proteins have been isolated.

The mammalian 14-3-3 γ protein modified by $(His)_6$ tagging, was overexpressed in *E.coli* and purified to homogeneity. The recombinant 14-3-3 γ was characterised using a series of techniques ensuring that the expressed protein had similar physical and immunological characteristics to that of wild type 14-3-3 γ.

An ssDNA aptamer library was synthesised and aptamers selected following an adapted SELEX (systematic evolution of ligands by exponential enrichment) protocol. After 16 selection rounds, aptamers contained within the enriched pool were cloned and sequenced for further analysis.

A sample of twenty of the sequenced aptamers were synthesised and biotinylated and their interaction with $(His)_6$14-3-3γ analysed by surface plasmon resonance and enzyme linked oligonucleotide assay (ELONA). The two aptamers showing the greatest association to $(His)_6$14-3-3γ were further analysed against all 14-3-3 isoforms using ELONA and by dot-blot analysis.

The high affinity aptamer, S16-8, was used to affinity purify recombinant 14-3-3 spiked into ovine serum albumin and wild type 14-3-3 in mouse brain homogenate and to detect and concentrate 14-3-3 protein in a scrapie positive cerebrospinal fluid (CSF) sample. The results of this work suggest that this aptamer could be used as a probe to detect isoforms of wild-type 14-3-3 proteins from a range of biological fluids.

Abbreviations

ATP - Adenosine 5'-triphosphate

Bp - Base pair(s)

BSE – Bovine spongiform encephalopathy

CD – Circular dichroism

CJD – Creutzfeldt-Jakob disease

CNBr – Cyanogen bromide

CSF – Cerebrospinal fluid

CWD – Chronic wasting disease

Da – Daltons

DMSO – Dimethyl sulfoxide

DMTr – Dimethoxytrityl group

DNA – Deoxyribonucleic acid

dNTPs – Deoxynucleotide triphosphates

EDTA – Ethylene diaminetetraacetic acid

ELISA – Enzyme Linked immunosorbent assay

ELONA – Enzyme Linked oligonucleotide assay

ES-MS – Electrospray ionization mass spectrometry

FFI - Fatal familial insomnia

GSS - Gerstmann-Sträussler-Scheinker disease

HIV – Human immunodeficiency virus

HPLC – High performance liquid chromatography

HRP – Horse radish peroxidase

IMAC – Immobilised metal affinity chromatography

IgG – Monomeric Immunoglobulin G

IPTG – Isopropyl-1-thio-β-D-galactopyransoside

LB – Luria Bertani

MALDI – Matrix-assisted laser desorption ionisation

MAP Kinase – Mitogen Activated Protein kinase

MBH – Mouse brain homogenate

NF-κB – Nuclear Factor- κB

NTA – Nitrilotriacetic acid

ORF – Open reading frame

PAGE – Polyacrylamide gel electrophoresis

PBS - Phosphate buffered saline

PBSM - Phosphate buffered saline with magnesium chloride

PCR – Polymerase chain reaction

PKC – Protein kinase C

PNK – Polynucleotide kinase

PrP^{C} – Prion protein, normal undiseased cellular structure

PrP^{Sc} – Disease associated form of prion protein

PVDF - Polyvinylidine difluoride

Q-TOF – Quadrupole time of flight

RNA – Ribonucleic acid

RP – Reverse phase

RT – Reverse transcriptase

RU – Response units

Rpm – Revolutions per minute

SDS – Sodium dodecyl sulphate

SELEX – Systematic evolution of ligands by exponential enrichment

SPR – Surface plasmon resonance

ssDNA – Single stranded DNA

Tar – Trans activation response element

TCEP- Tris (2-carboxyethyl) phosphine hydrochloride

TFA – Trifluoroacetic acid

TOF – Time of flight

Tris – Tris [hydroxymethyl] aminomethane

TMB - 3,3,5,5 Tetramethylbenzidine

TTF1 - Thyroid transcription factor 1

TSE – Transmissible spongiform encephalopathy

VEGF – Vascular endothelial growth factor

Contents

Declaration ii
Acknowledgements iii
Abstract iv
Abbreviations v
Contents vii
List of Figures x
List of Tables xiii

Chapter 1: 14-3-3 Proteins; not just a number 1

1.1 14-3-3 Proteins, an Introduction 1

1.2 14-3-3 Proteins in the Cell 2

1.3 14-3-3 Family Conservation 3

1.4 14-3-3 Structure 6

1.5 14-3-3 Ligand Interactions 9

1.6 The Mechanism of 14-3-3 Interaction 12

1.7 14-3-3 in Human Disease 15

1.7.1 Prion Diseases 15

1.7.2 14-3-3 Proteins as Surrogate Markers 20

1.7.3 Current Detection Methods for 14-3-3 Proteins 21

Chapter 2: Aptamers 26

2.1 Aptamers, an Introduction 26

2.2 DNA or RNA aptamer 30

2.3 The SELEX Approach 33

2.3.1 The Aptamer library 33

2.3.2 The ssDNA SELEX cycle 35

2.3.3 Modifications for an RNA SELEX 38

2.3.4 Considerations of the SELEX Approach 39

2.4 Aptamer Structures 41

2.4.1 Thrombin Aptamer 41

2.4.2 Crystal Structure of the G-tetrad 43

2.4.3 HIV-1 RT Aptamer 43

2.5 Aptamer Technology 45

2.5.1 Aptamers versus Antibodies 45

2.5.2 Aptamers as Therapeutics 46
2.5.3 Analytical Applications of Aptamer 48
2.5.3.1 Chiral Selection 48
2.5.3.2 Affinity chromatography 49
2.5.3.3 ELONA 49
2.5.3.4 MALDI-MS 50
2.5.3.5 Signaling Aptamers/Molecular Beacons 50
2.5.3.6 Surface Plasmon Resonance 51
2.5.3.7 Aptamer Modified Gold Nanoparticles 52

Chapter 3: Materials and Methods 53

Chapter 4: Results and Discussion 81
4.1 Cloning, Expression and Purification of 14-3-3 γ 81
4.1.1 Cloning 14-3-3 γ 82
4.1.2 14-3-3 γ Purification 85
4.1.3 Characterisation of $(his)_6$ 14-3-3 γ 86
4.1.3.1 Mass Spectrometry of 14-3-3 γ 87
4.1.3.2 Circular Dichroism of 14-3-3 γ 89
4.2 Recognition of 14-3-3 γ by Antibodies 90
4.2.1 Surface Plasmon Resonance 90
4.3 SELEX 93
4.3.1 The SELEX Approach 93
4.3.2 SELEX Counter Selection 97
4.3.3 Development of Radiolabelling Technique 98
4.3.4 Clone Analysis 102
4.4 Cycle 16 clone analysis by Surface Plasmon Resonance 115
4.5 Aptamer Characterisation using Enzyme Linked Assay 117
4.5.1 ELISA 117
4.5.2 ELONA 118
4.5.3 14-3-3 Isoform Analysis using ELONA 121
4.6 Protein Blot Analysis with Aptamer S16-8 123
4.7 Gel Filtration Analysis 125
4.8 Affinity Purification 128

4.9 Scrapie CSF Analysis 132
4.10 Summary, conclusions and suggestions 134

Chapter 5: Bibliography 138

Appendix: Structural Comparison of Cycle 16 Aptamers 153
Appendix: Tryptic Digest MS Data 156
Appendix: Publication 158
Appendix: Training Record 159

List of Figures

Figure 1.1: 14-3-3 Sequence alignment

Figure 1.2: 14-3-3 ζ Crystal structure

Figure 1.3: 14-3-3 Basic pocket

Figure 1.4: Crystal structure of a 14-3-3 monomer unit with bound peptide

Figure 1.5: A representation of 14-3-3 working as a molecular anvil

Figure 1.6: The two models of the Prion hypothesis with a brief explanation

Figure 1.7: 14-3-3 ζ

Figure 1.8: CSF 14-3-3 detection in sCJD and vCJD

Figure 1.9: Sensitivity and specificity of CSF 14-3-3 detection

Figure 2.1: TAR decoy RNA aptamer preventing TAT protein from binding viral TAR RNA

Figure 2.2: Theophylline and Caffeine

Figure 2.3: The ssDNA SELEX approach

Figure 2.4: X-ray crystal structure of the thrombin binding aptamer

Figure 2.5: Crystal structure of the G-tetrad

Figure 2.6: The NMR structure of the RNA aptamer interacting with HIV-1 RT

Figure 4.1: 14-3-3 γ gene

Figure 4.2: 14-3-3 γ amino acid sequence

Figure 4.3: Plasmid pGEX 4T1

Figure 4.4: Plasmid pQE-30

Figure 4.5: Schematic representation of pQE30/14-3-3γ gene

Figure 4.6: pQE30/14-3-3γ amino acid sequence

Figure 4.7: Chromatogram of 14-3-3 IMAC

Figure 4.8: SDS-Page and Western blot of 14-3-3 γ

Figure 4.9: LC-MS of $(His)_6$14-3-3γ

Figure 4.10: Circular dichroism of 14-3-3 γ

Figure 4.11: Chromatogram of repeatable results using antibody KK1106

Figure 4.12: Comparison of four anti 14-3-3 antibodies by SPR

Figure 4.13: The SELEX cycle with counter selection

Figure 4.14: RS977R; Aptamer starting library

Figure 4.15: Scintillation results for SELEX rounds 2-4

Figure 4.16: Absorbance results for SELEX cycles
Figure 4.17: The promoter and multiple cloning site of pGEM-T Easy Vector
Figure 4.18: Digested cycle 11 clones
Figure 4.19: Sequence alignment of cycle 11 clones
Figure 4.20: Aptamer S11
Figure 4.21: Comparison of the cycle 11 SELEX (S11) clone against the aptamer starting library
Figure 4.22: The sequence alignment of cycle 16 clones
Figure 4.23: Phylogenetic tree of Aptamer sequences
Figure 4.24: Comparison of the cycle 11 consensus clone (S11) versus S16.1
Figure 4.25: Cycle 16 Clone 1 concentration analysis
Figure 4.26: S16-1, Biotinylated comparison
Figure 4.27: SPR of biotinylated aptamer
Figure 4.28: The 14-3-3γ ELISA standard curve
Figure 4.29: Analysis of 10 different SELEX clones by ELONA
Figure 4.30: ELONA saturation curve
Figure 4.31: Comparison of the different 14-3-3 isoforms by ELONA
Figure 4.32: Comparison of 14-3-3 isoforms with aptamer S16-8 in sandwich enzyme assay
Figure 4.33: Protein blot analysis of different 14-3-3 isoforms with S16-8
Figure 4.34: Gel Filtration analysis of 14-3-3 and aptamer S16-8
Figure 4.35: The Mouse Brain Homogenate immunoprecipitation reaction
Figure 4.36: Ovine cerebrospinal fluid spiked with 14-3-3 immunoprecipitation
Figure 4.37: Western Blot amalgamation of the affinity purified mouse brain homogenate and spiked ovine CSF
Figure 4.38: Analysis of Scrapie fraction F125
Figure 4.39: Scrapie affinity purified 14-3-3 protein
Figure I: Aptamer S16.1 and S16.8
Figure II: A diagrammatical representation of aptamer S16-8 forming a g-quartet structure
Figure III: The mfold predicted structure for S16-28 and diagrammatical representation of a possible G-Quartet structure
Figure IV: MALDI ToF data from affinity purified gel

Figure V: MALDI TOF data from scrapie affinity purified gel

List of Tables

Table 1.1: 14-3-3 binding partners

Table 1.2: Reported cases of CJD in the United Kingdom from 1990

Table 1.3: 14-3-3 antibodies and their epitopes

Table 1.4: Comparison of the sensitivity and specificity of a 14-3-3 γ specific antibody for the detection of spCJD

Table 2.1: Current aptamer affinities and structures

Table 2.2: Current aptamers as therapeutics

Table 4.1: SELEX scintillation results

Table 4.2: Absorbance results for SELEX cycles

Table 4.3: Clones 1 to 97 with their ratio of nucleotides determined

Table 4.4: The K_d^{app} of selected cycle 16 aptamers

Chapter 1: 14-3-3 Proteins; not just a number

1.1 14-3-3 Proteins, an Introduction

14-3-3 proteins are a family of ubiquitously expressed regulatory molecules found in eukaryotic organisms. They are acidic, dimeric proteins that can modulate interaction between proteins involved in cell signaling and other functions, playing a role in many vital regulatory processes, including apoptotic cell death, cell cycle control and mitogenic signal transduction.

14-3-3 proteins were first discovered in 1967, in the course of the systematic classification of bovine brain proteins by Moore and Perez.[1] The unusual name is based on the elution and migration pattern following two-dimensional DEAE-cellulose chromatography and subsequent starch gel electrophoresis.

Nothing was known of the role of 14-3-3 proteins until Ichimura and co-workers ascribed the family its first function in 1987.[2] They had discovered a protein cofactor responsible for the activation of tryptophan and tyrosine hydroxylases, which are involved in the synthesis of many neurotransmitters including dopamine. Characterisation of this cofactor led to its identification as a 14-3-3 protein and led the group to clone the first 14-3-3 gene (the η isoform) in 1988, a major breakthrough in determining the role of 14-3-3 proteins in the cell.[3]

There were significant advances in uncovering the role of 14-3-3 proteins in regulatory processes in the following years. In 1990 Aitken and co-workers, along with Toker and co-workers, showed that 14-3-3 proteins were involved in the inhibition of protein kinase C (PKC).[4,5] PKC's are involved in the phosphorylation of a wide range of proteins leading and as such are involved in the control of many

signaling and regulatory pathways. In 1992 Morgan and co-workers found that 14-3-3's were stimulators of calcium dependant exocytosis, and another significant discovery was made in 1994 when the family was shown to co-associate with Raf, an activator of the MAP kinase pathway.[6,7]

To date more than 200 interacting partners have been identified for 14-3-3 proteins showing that 14-3-3 is involved in a vast range of cellular processes (see **section 1.5**). It has been suggested that perhaps the greatest challenge remaining for 14-3-3 researchers, could be to define the precise role of 14-3-3 in cell biology.[8]

1.2 14-3-3 Proteins in the Cell

14-3-3 proteins are amongst the most abundant proteins within the neuronal tissues, comprising approximately 1% of the brains total soluble protein.[9] Mammalian 14-3-3 proteins exist as a family of highly similar yet distinct protein isoforms each encoded by their own gene.[10] Seven human isoforms have been identified to date, and these are named after their elution pattern on reversed phase high performance liquid chromatography (HPLC) (β, ε, τ, σ, γ, ζ, η).[11] Two other isoforms, α and δ, had been previously described, however work in 1995 by Aitken and co-workers showed that these were actually post-translationally phosphorylated forms of β and γ.[12] Including the seven human isoforms, more than 153 14-3-3 isoforms have been detected in 48 species of multicellular organisms (correct as of 2000) including amoebae, plants, yeasts, nematodes, flies, frogs and mammals, to date no isoforms have been detected in prokaryotes.[13]

Mammalian 14-3-3 proteins have a typical monomeric mass around 30 000 Da (28kDa to 33kDa), containing between 246 to 249 amino acids, and have an isoelectric point around 4.5. In their native state the proteins are either homo- or

hetero- dimers. Many 14-3-3 ligands bind to specific 14-3-3 isoforms with different affinities, and this means that 14-3-3 hetero-dimers provide unique recognition motifs allowing two different proteins to be brought close enough to interact with each other.[14] This is a major point for 14-3-3 function and as such will be further discussed later in the chapter.

14-3-3 proteins are predominantly located in the neuronal cells of the brain, however they are no longer considered brain specific proteins and appear to be expressed in almost all mammalian tissues including heart, liver and the testes.[15,16] Two of the human 14-3-3- isoforms, τ and σ, are present at only low levels in the brain and are instead detected predominantly in T cells and epithelial cells respectively.[17,18] 14-3-3 proteins are most abundant at the cytoplasmic compartment but have also been detected at the plasma membrane, nucleus and at the Golgi apparatus.

1.3 14-3-3 Family Conservation

14-3-3 proteins are very well conserved across a broad range or organisms (the human ε isoform and the S*accharomyces cerevisiae* BMH1 are approximately 70% similar at the amino acid level).[13,19] The seven human isoforms are around 50% similar across the whole family but as high as 86% between isoforms β and ζ (the human 14-3-3 sequence alignment is shown in **Figure 1.1**). Wang and Shakes compared 50 of the available 14-3-3 sequences using a phylogenic tree to determine the evolutionary relationships among specific isoforms in different organisms. They discovered that the family contained five highly conserved sequence blocks (conservation of each block varies from 53.8% to 89.9%) across all species. When correlated with the three dimensional 14-3-3 structures, the conserved regions match with the internal "binding domain" regions of the dimer which are essential for dimerisation and ligand binding

(refer to **Figure 1.2**). The outer helices that are less well conserved, supporting the previous observation by Liu and co-workers in 1995 that the internal region of the dimer the most conserved region.[20] Many functionally important residues are found in the conserved regions, however there are subtle differences between isoforms, including the phosphorylation sites that may lead to isoform binding specificity.

The N and C terminal regions contain the least well conserved amino acid regions across all species. Liu *et al.* suggested that the C-terminus, which shares little sequence conservation but is uniformly acidic in character, may serve to regulate the function of 14-3-3 by interacting with a basic cluster of residues contained within the dimer.

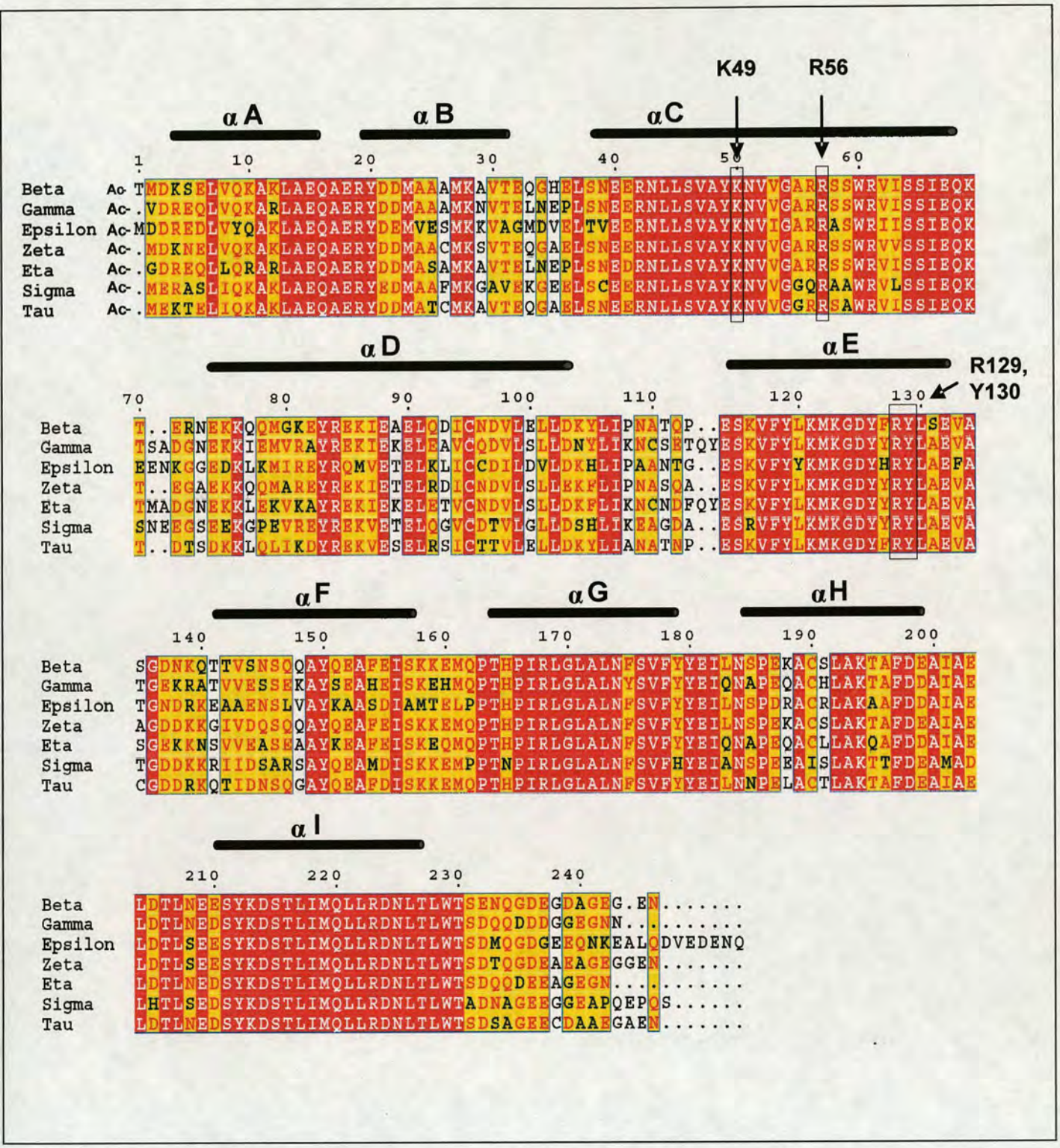

Figure 1.1: 14-3-3 sequence alignment. The human 14-3-3 sequences were aligned using ClustalW.[21] Black bars above sequences indicate α-helices. Some key residues (see **section 1.5**) have also been highlighted.

1.4 14-3-3 Structure

In 1995, the crystal structures of two 14-3-3 isoforms, τ and ζ, were solved by Xiao and co-workers and Liu and co-workers respectively.[22,20] The structures are very similar, leading to the suggestion that all 14-3-3 proteins share a similar tertiary dimeric structure, resembling a flattened 'U' shape as shown in **Figure 1.2**.

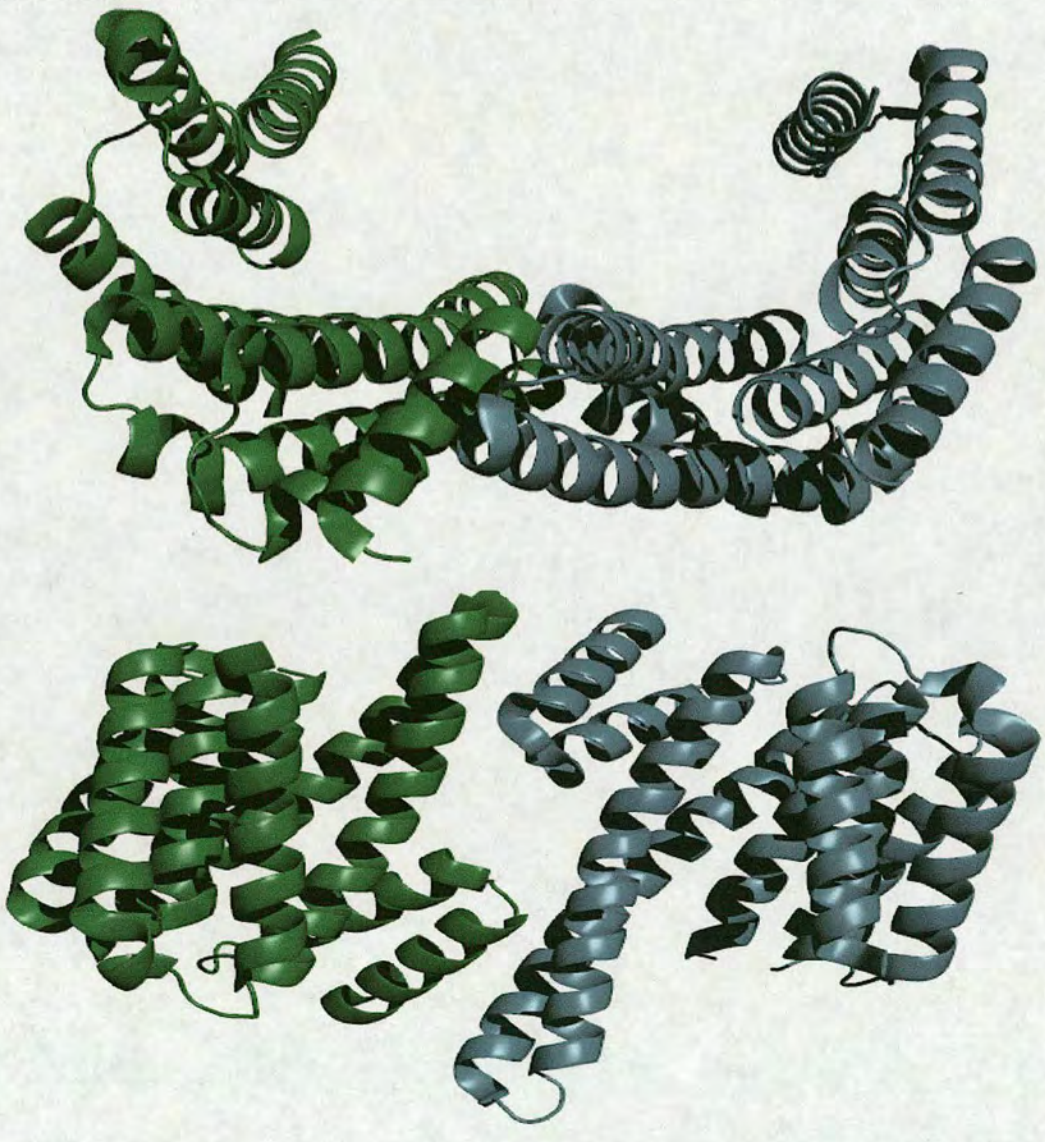

Figure 1.2: 14-3-3 ζ Crystal Structure. Shown are two images of a 14-3-3 ζ homo dimer. Each monomer unit is represented by either the colour green or blue. The second image was obtained by rotating the first image by 90° relative to the plane of the paper, effectively viewing the image from above.

Each 14-3-3 monomer unit consists of nine anti-parallel α-helices, with a highly conserved inner concave surface and a variable outside surface. As shown in Figure 1.2, the N-terminal region helix 1 (specifically residues 5-21) interacts directly with helices 3 and 4 of the corresponding monomer unit (specifically residues Ser58-Gly89), leaving a negatively charged channel about 7Å wide in the centre, which is surrounded by amino acids which are almost totally conserved across the whole family. The conserved inner region of the 14-3-3 monomer unit contains an amphipathic groove, 35Å long by 35Å wide by 20Å depth, with polar residues on one side (helices 3 and 5), and the other side (helices 7 and 9) containing a cluster of hydrophobic residues.[20] The five conserved sequence blocks previously mentioned are helices 3, 5, 7, 9 along with the connecting loop of helices 1 and 2, itself an integral element in dimer formation. By analyzing the crystal structure of 14-3-3 ζ with ligand attached, Yaffe and co-workers suggested that the ligand interacts directly in the groove between Lys49 and Arg56 in helix 3 and with Arg129 and Tyr130 in helix 5 (highlighted in Figures 1.3 and 1.4), a model confirmed by further co-crystallisation experiments and by mutagenesis of the residues involved in ligand binding.[23,24,25] These residues form a basic cluster of residues within an otherwise acidic molecule, suggesting that ligand serine/threonine phosphorylation could act as molecular switch controlling ligand binding. Interestingly, co-crystal studies using unphosphorylated ligands, show binding at the same highly conserved sites, suggesting that other residues of the protein may aid ligand:14-3-3 interaction.[26]

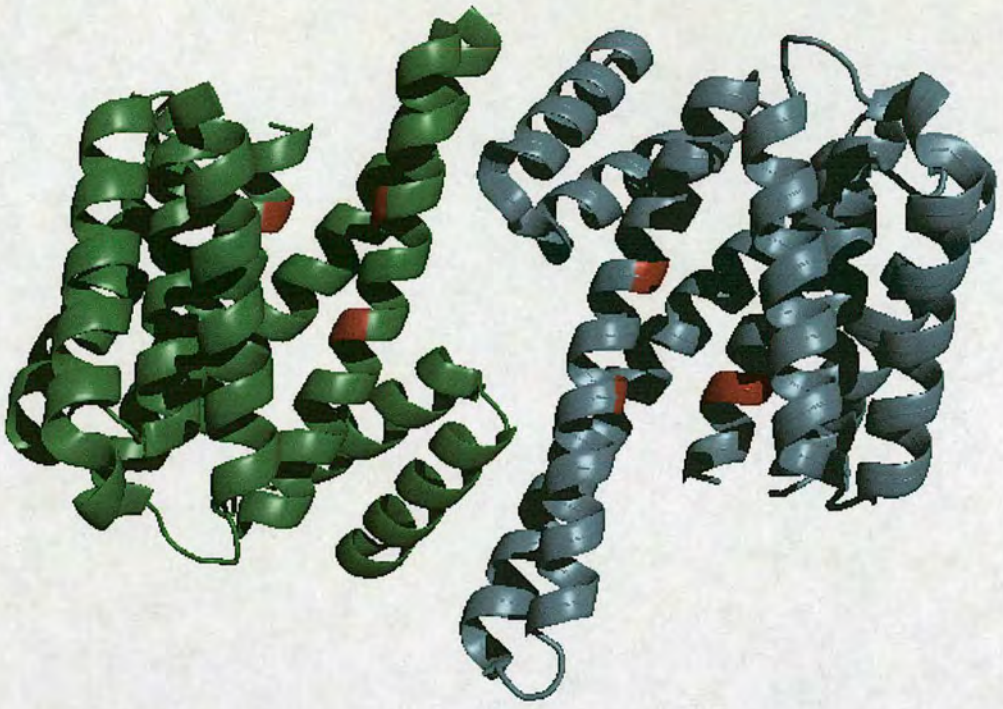

Figure 1.3: 14-3-3 Basic pocket. Residues Lys-49, Arg-56, Arg-129 and Tyr-130 have been highlighted red showing the phosphate binding site.

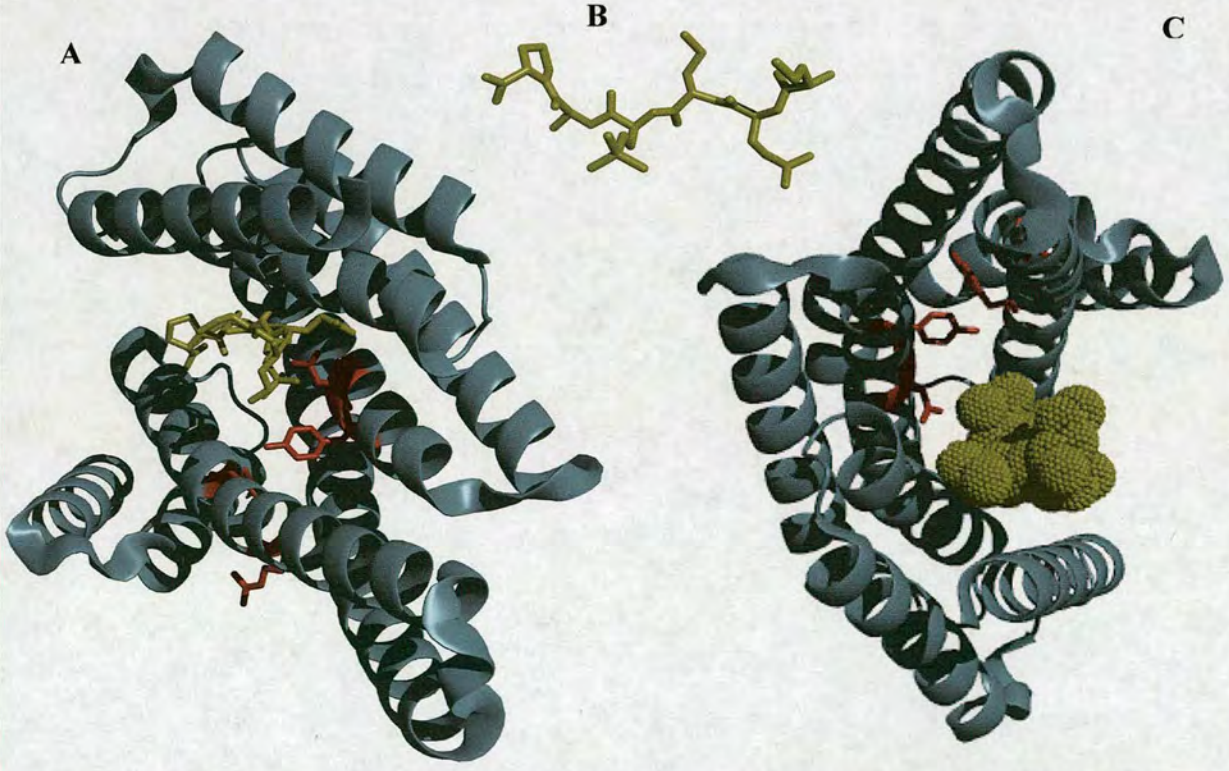

Figure 1.4: Crystal Structure of a 14-3-3 monomer unit with bound peptide. Image A shows the bound peptide, B is a structure of the free peptide ligand and image C shows the peptide in space fill.

1.5 14-3-3 Ligand Interactions

The history of 14-3-3 proteins has been a series of rediscoveries expanding the roles played by the family. The findings that 14-3-3 proteins inhibit PKC's, co-associate with Raf and middle T-antigen implicating a role in DNA damage response, caused an explosion in interest in the family.[27] The mid 90's brought many publications showing that the 14-3-3 family interacted with a range of protein kinases, phosphatases and other signaling proteins and led to the suggestion that 14-3-3 molecules were a novel type of dimeric scaffold protein that could modulate interaction between kinases and other signalling proteins.[11,28]

In 1996 Muslin and co-workers suggested that because the 14-3-3 family has so many binding partners, some of which are very similar, it would be reasonable to propose a common binding determinant that mediates contact.[29] They deduced the recognition motif from a 15-mer Raf-1 peptide. Their work and that of Yaffe and co-workers in 1997 led to the discovery of two specifically phosphorylated motifs that are present (or very close matches are present) in more than half of the 14-3-3 ligands established to date.[30,31] The motifs, RSx[pS/pT]xP and RxΦx[pS/pT]xP (where x can be any amino acid, S is serine, T is threonine, P is proline, R is arginine, the symbol p represents a phosphorylated amino acid and Φ denotes aromatic or aliphatic amino acids), appear to be recognised by all 14-3-3 isotypes. The arginine at -3 or -4 from pS/T is obligatory for 14-3-3 interaction whereas the proline at +2 is dispensable, although the K_d is increased when this amino acid is present.[32]

It should be noted however, that many ligands bind to 14-3-3 isoforms using drastic variations from this motif some phosphorylated and some unphosphorylated. It should also be noted that the affinity of non phosphorylated ligands can be similar to those of phosphorylated ligands. Two main motifs have been found for such

unphosphorylated interactions, those ligands that contain cysteine rich domains (CRD's) such as Raf and ligands which can interact through acidic residues such as ExoS ADP-ribosyltransferase.[7,33] Phage display library experiments have shown that phosphorylation is not required in peptides containing many acidic residues, especially those that are Glu rich, and this explains the affinity of 5-phosphatase, an unphosphorylated 14-3-3 ligand containing the binding motif RSESEE.[24] **Table 1.1** gives just some of proteins found to interact with 14-3-3 to date.

14-3-3 molecules are predominantly dimeric in nature, with two ligand binding sites, occupied by either two different ligands or by a single ligand with two recognition sites. Many examples exist of ligands that contain a single binding motif. Ligands such as Raf, BAD and Cbl are bidentate and contain two high affinity recognition motifs. In contrast the protein Cdc25B is a ligand which contains a high affinity binding site and a second, lower affinity motif that serves to aid binding.[34] This is discussed later in the context of the anvil/gatekeeper hypothesis. As a result of the phospholigand-binding discovery by Muslin and Yaffe, 14-3-3 proteins were redefined as the first phosphoserine/phosphothreonine binding molecule, suggesting a key role for the molecule in the control of intracellular signal transduction.[35]

In 2004, Pozuelo Rubio and co-workers were able to identify over 200 human phosphoproteins that bind 14-3-3 proteins by affinity chromatography.[36] In their study proteins were identified by passing crude extract human HeLa cells through a 14-3-3 sepharose affinity column (containing the two *Saccharomyces cerevisiae* isoforms), then eluting the bound proteins by addition of a 14-3-3 binding

phosphopeptide (ARAApSAPA). Interestingly, they found that when the purified proteins were dephosphorylated, they lost their ability to bind to 14-3-3.

Table 1.1 14-3-3 binding partners. This is not a complete list and shows just a slice of the 14-3-3 ligands established to date, adapted from Aitken *et al.*[37]

Target Protein and Category	Binding Motif
Protein Kinases	
BCR	RSQSTPSEQ
PKCμ (PKD)	RLpSNVS, TRSpSAELpS
PKCζ	RHDMpSYMP
c-Raf-1 kinase	RSTpSTP, RSApSEP
Phosphatases	
PTPHI, tyrosine phosphotase	RSLpSVE, RVDpSEP
Cdc25A cell-cycle dual-specificity phosphotase	RSPpSMP
Cdc25C cell-cycle phosphotase	RSPpSMP
Receptors and related proteins	
Exoenzyme-S, ADP-ribosylation	DALDL
Insulin growth factor I receptor	S VPLDPSASSSpSLP
RAS effector protein RINI	RSMpSAA
Nuclear receptor (Nur77)	RLPpSKP
Apoptosis-regulating proteins	
BAD, apoptosis-regulating	RHSpSYP, RSRpSAP, RRMpSDFE
Apoptosis signal-regualting kinase I (ASKI)	RSIpSLP
Adaptor Proteins	
KSR (kinase suppressor of RAS)	RSKpSHE, RTEpSVP
Cbl	RHpSLPFpS, RLGpSTFpS
Transcription factors and nuclear proteins	
Forkhead transcription factor (FKHRLI)	RPRSCpTWP, RRRAVpSMD
Nuclear factor of activated T-cells (NFAT3)	RRYpSpSpS, RRGpS
p53 tumour-suppressor/transcription factor	KGQSTpSRH/G
Enzymes and others	
43 kDa inositol polyphosphotase 5-phosphotase	ELVLRSESEEKW
Middle T antigen, polyoma virus	RSHpSYT
Tyrosine hydroxylase	RRAVpSELD

1.6 The Mechanism of 14-3-3 Action

14-3-3 proteins are currently believed to have 5 major roles of action:

1) 14-3-3 binding can alter the ability of the target protein to interact with other proteins through sequestration (binding) or modification of the target protein. This mechanism can be demonstrated by the 14-3-3 interaction to BAD.[38] BAD is sequestered by 14-3-3, preventing binding of BAD to the anti-apoptic protein Bcl-2. Introduction of the protein phosphotase PP2A, dephosphorylates BAD which leads to the release of 14-3-3 and binding of 14-3-3 to Bcl-2.

2) 14-3-3 can control the subcellular localisation of target by masking a targeting sequence, inhibiting ligand relocation. Release of the target allows subcellular movement. 14-3-3 has been shown to play a role in nuclear retention of tobacco DNA-binding protein phosphatase 1 and in protein shuttling in cytoplasm/mitochondrion, cytoplasm/nucleus, cytoplasm/plasma membrane and endoplasmic reticulum/plasma membrane.[39] The cytoplasm/nucleus movement of this cell cycle protein Cdc25C provides an example of the scenario.[40]

3) 14-3-3 can act as a phosphorylation dependant scaffold to bridge two proteins together. This has been demonstrated for Raf-BCR interactions.[41]

4) 14-3-3 regulates the catalytic activity of the target ligand, enhancing or inhibiting its function. For example 14-3-3 has been shown to increase the binding affinity of p53 for DNA.[42]

5) 14-3-3 can shield the target sequence and protect it from further modifications, such as dephosphorylation and proteolysis.[28]

In 2002, Yaffe proposed two models for the mechanism of 14-3-3 interactions, namely gatekeeper phosphorylation and the molecular anvil hypothesis, models that

rely heavily on the dimeric nature of 14-3-3 proteins.[31] As mentioned previously, some ligands including BAD and Raf contain two ligand binding sites, making possible the interaction of a single protein with both monomer units in the 14-3-3 dimer.[43] Comparison of synthetic phosphopeptides with one and two 14-3-3 binding motifs showed that the bidentate ligand interaction was 30 times tighter.[30] Similarly, point mutations in one of the binding sites have been shown to impair 14-3-3/ligand function.[25]

The molecular anvil model proposes that 14-3-3 dimers are capable of altering the enzymatic activity or masking/revealing functional motifs by altering the conformation of bound bidentate ligands. It is suggested that 14-3-3 dimers are very rigid due to the plethora of interacting forces between the α-helices, lending to the distortion of bound ligands without self-deformation. When such a ligand binds, its conformation is changed enough to facilitate a process that was not available to the unbound ligand. **Figure 1.5** shows a diagrammatical representation of the molecular anvil hypothesis. The second site binding to 14-3-3 protein causes a change in the ligand structure, revealing an active site that was previously inaccessible.

The gatekeeper hypothesis can be explained using the protein Cdc25B. This is one of a range of molecules containing high affinity and lower affinity 14-3-3 binding motifs. The high affinity region is proposed to bind to a 14-3-3 monomer unit, acting as a gatekeeper and allowing the lower affinity motif to bind 14-3-3 more easily due to its proximity, making a secondary contact which would not be as stable without the primary interaction.

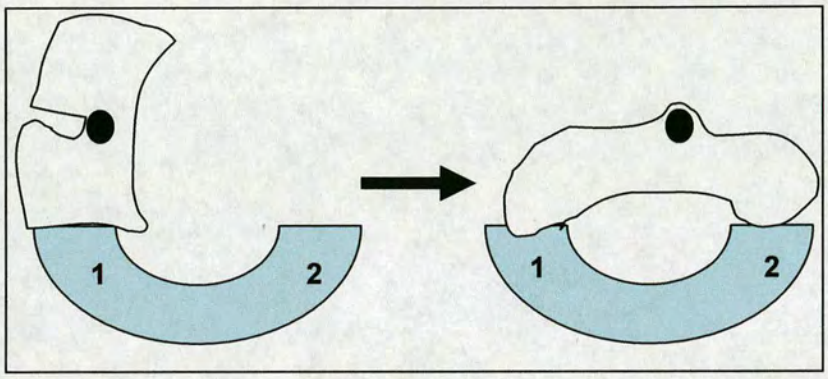

Figure 1.5: A representation of 14-3-3 working as a molecular anvil. The numbers 1 and 2 represent ligand binding sites of a 14-3-3 dimer initially interacting at one site of a bidentate ligand.

Aitken *et al.* have shown that specific 14-3-3 isoforms differ in their preference for homo- and hetero dimerisation, with particular heterodimers forming at the expense of others.[14] They proposed that because ligands generally have different affinities for each 14-3-3 isoform, populations of specific hetero-dimers may alter which two interacting proteins that are brought together, possibly resulting in long term changes in cell signalling.

1.7 14-3-3 Proteins in Human Disease

Changes in the expression levels of specific 14-3-3 proteins in human plasma, has been used for early diagnosis for a range of disorders.[44] Elevated levels of 14-3-3 proteins are detected in the Cerebrospinal fluid (CSF) of patients suffering neurodegeneration, caused by diseases including Creutzfeldt-Jakob disease (CJD), Alzheimers disease and Parkinsons disease. Some epithelial cancers can be detected by monitoring the expression levels of 14-3-3σ since downstream gene silencing of this gene is proposed to play an important role in the onset of carcinogenesis.[45,46] Patients who suffer from AIDS dementia complex or cytomegalovirus encephalitis also show specific 14-3-3 isoform expression patterns in the CSF.[47] Other diseases where 14-3-3 proteins have been used as markers include herpes simplex encephalitis, acute ischematic stroke and paraneoplastic neurological disorders.[45]

1.7.1 Prion Diseases

Transmissible Spongiform Encephalopathies (TSE's) or Prion disease are a family of fatal neurodegenerative diseases, characterised by spongiform degeneration of the brain (microcavitation), neuronal loss, astrocytosis and the build up of PrP^{Sc} (scrapie prion protein) an atypical form of PrP^{c} (the native, protease-sensitive, normally expressed form of PrP) in the central nervous system.[48]

Prion diseases are unique in that they differ from viral and other neurodegenerative and infectious diseases. Prions unlike viruses do not require a nucleic acid code necessary for self perpetuation, they cause no inflammatory reaction and do not succumb to radiography as would an infectious disease, and they are capable of transferring between human-human and human-animals unlike most

neurodegenerative diseases characterised to date. Although they have relatively low incidence rate (1 in a million), the transmissibility of prion diseases causes them to be considered a significant risk to public health. In 1967 it was first suggested that the infectious agent was not a living organism but was instead an abnormal protein, later coined a prion in 1982 by Pruisner.[49,50] Two popular models exist for the Prion hypothesis, adapted from Aguzzi and co-workers are shown in **Figure 1.6.**[51] The current favoured model is the seeding mechanism; PrP^{Sc} is an infectious agent capable of self-propagation by converting PrP^{c} to itself (PrP^{Sc} and PrP^{c} have the same amino acid chain yet a post translational modification is capable of taking the native α-helical protein and converting it to β-sheet structure that is nuclease resistant and causes insoluble aggregates) catalysed by physical interaction with PrP^{Sc}. The conversion mechanism is not fully understood however it is suggested that PrP^{Sc} aggregates serve as templates for the ordered aggregation of PrP^{c}. The Prion hypothesis is still to be fully accepted and will remain controversial until PrP^{Sc} proteins are successfully taken from an infected donor, purified in vitro added to a recipient, causing new Prion growth. Recent studies by Legname and co-workers in 2004 and by Castilla and co-workers in 2005 come close to achieving that goal and proving the hypothesis.[52,53] For more detailed information on Prion diseases and their possible therapies, two very good reviews are available from Aguzzi and co-workers and Cashman and Caughey.[51,48]

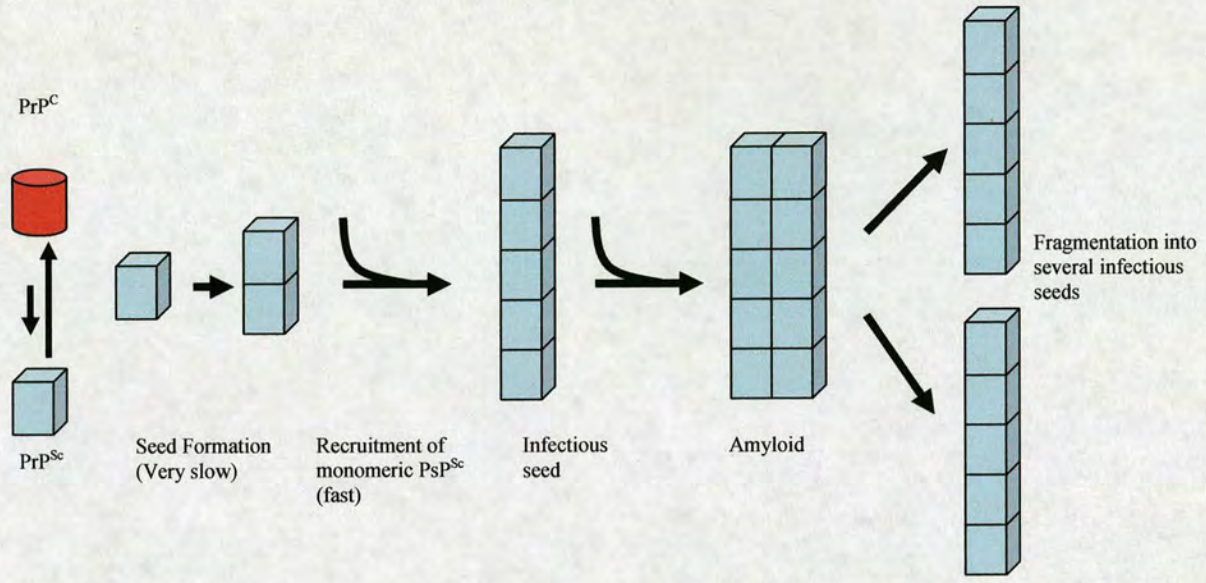

Model A: The Nucleation Polymerisation or Seeding Mechanism; PrP^{C} and PrP^{Sc} are in reversible thermodynamic equilibrium. If several PrP^{Sc} monomers are mounted into a highly ordered seed then further monomeric PrP^{Sc} can be recruited to form an amyloid. Fragmentation of the amyloid, increase the number of seed nuclei that can recruit further PrP^{Sc} and thus results in apparent replication of the agent.

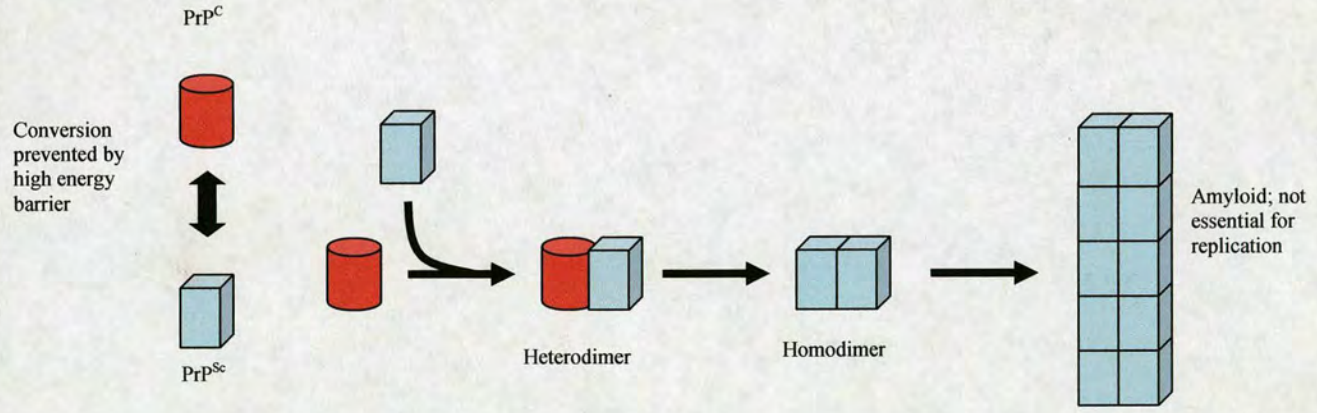

Model B: The Template Assisted or Refolding Mechanism; An interaction between exogenously introduced PrP^{Sc} and endogenous PrP^{C}, induces PrP^{C} to transform itself into further PrP^{Sc}.

Figure 1.6: The two models of the Prion hypothesis with a brief explanation. The proposed mechanism of each is described within.

Prion diseases effect both humans and animals, examples include; sporadic CJD, iatrogenic CJD, new variant CJD, familial CJD, in humans, bovine spongiform encephalopathies (BSE) in cattle, scrapie in sheep and chronic wasting disease (CWD) in elk and deer. Other human TSE's include the now almost extinct Kuru and the inherited disorders Gerstmann-Sträussler-Scheinker disease (GSS) and fatal familial insomnia (FFI), both of which caused by a mutation of the PrP gene.

Most common of the human Prion diseases is sporadic CJD (sCJD) which has a worldwide annual incidence rate of around one case per million.[54] It is a fatal disorder of the central nervous system, typical onset between 45 to 75 years, characterised by a rapidly progressive dementia and a case fatality greater than 90% within the first year. In 1996, a new variant CJD (vCJD) was identified, which has to date been detected in the United Kingdom, France, the Republic of Ireland, Hong Kong, Italy, the United States and Canada.[55] vCJD affects younger patients and has a longer clinical course than its sporadic equivalent, it has over 150 UK individuals to date and is believed to derive from consumption of BSE contaminated neuronal tissues.[56]

The primary UK vCJD epidemic appears to have peaked in 2000 (as shown in **Table 1.2**), although much concern remains about a secondary epidemic caused by blood, tissue, or organ donation, or by treatment using contaminated instruments.[57] The only current definitive diagnosis for spCJD and vCJD are obtained by post-mortem neuropathological examination of brain tissue. There is a need for an effective pre-mortem diagnosis to prevent hospital acquired infections of CJD (iatrogenic CJD) and prevent the spread of BSE, scrapie and CWD throughout the world. It has been suggested that proteins used as surrogate markers could be used for early detection of

CJD, leading to a prolonged onset of disease, possibly providing a better quality of life for suffers and preventing the avoidable transmission of prion diseases.

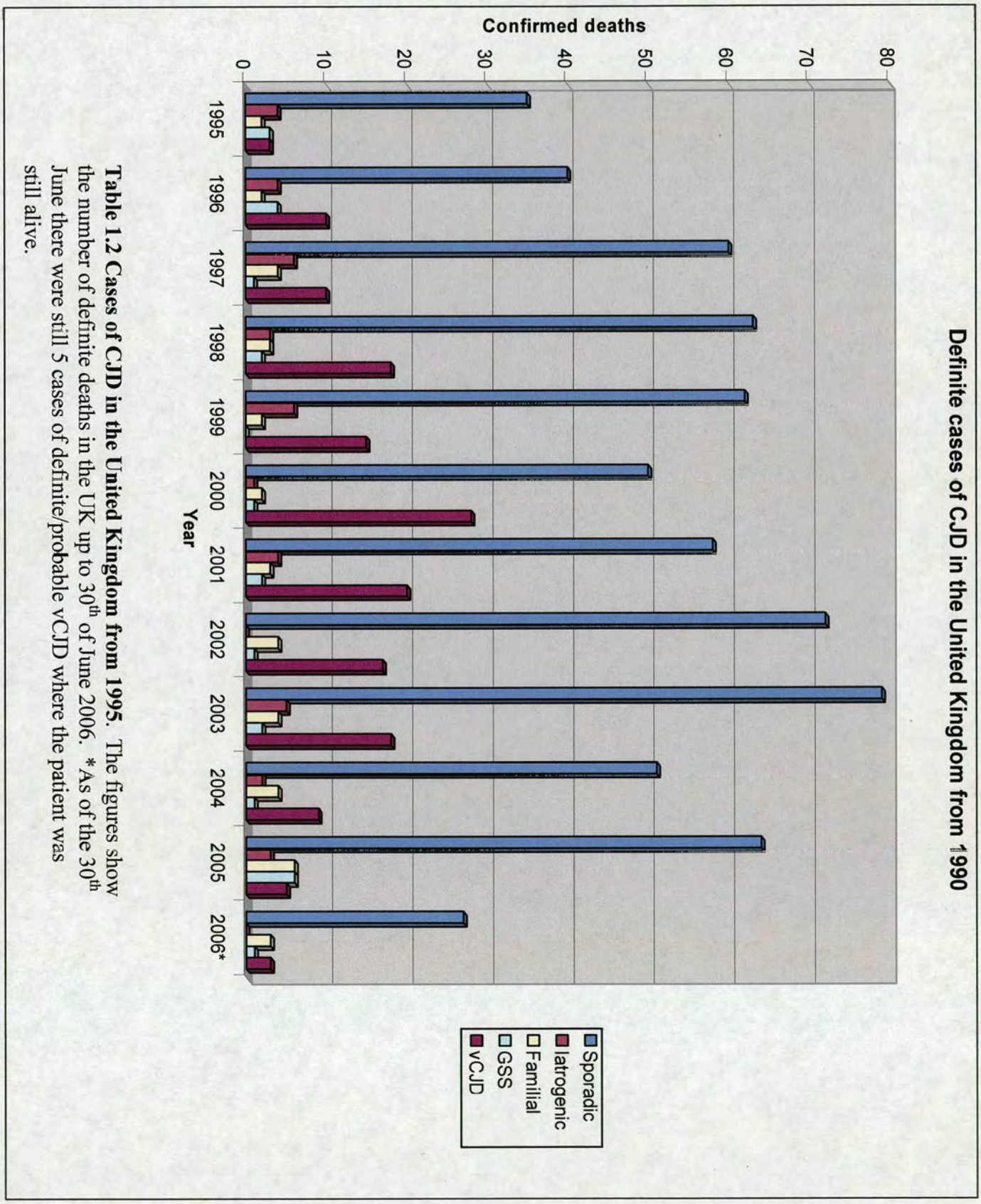

Table 1.2 Cases of CJD in the United Kingdom from 1995. The figures show the number of definite deaths in the UK up to 30th of June 2006. *As of the 30th June there were still 5 cases of definite/probable vCJD where the patient was still alive.

1.7.2 14-3-3 Proteins as Surrogate Markers

Detection of PrP^{Sc}, as a marker for vCJD, in blood and peripheral tissues poses significant problems. Among the complicating factors are that there are no current antibodies uniquely specific for PrP^{Sc} and the very low levels of the abnormally folded PrP^{Sc} compared to PrP^{c}. For classical immunodetection methods to be useful, this necessitates the removal of the interfering PrP^{c} typically by limited proteolysis. Alternatively concentration of the PrP^{Sc} can be achieved by selective precipitation in a complicated and lengthy procedure that provides best case concentrations that lie in the lower limits of sensitivity for immunoassay detection.[58]

A number of proteins found in the CSF of patients with neurodegenerative disorders have been considered as possible surrogate markers for prion disease detection. These include 14-3-3 proteins, S-100b, neuron specific enolase and Tau protein. Among these markers, it was found that 14-3-3 proteins have the highest sensitivity and specificity in pre-mortem spCJD diagnoses, leading the World Health Organization (WHO), in 1998 to revise its clinical criteria for the diagnosis of **probable** spCJD to include 14-3-3 detection in the cerebrospinal fluid (CSF).[59] The use of 14-3-3 proteins as a surrogate marker of vCJD is less attractive since only about 50% of vCJD patients have detectable 14-3-3 levels in their CSF.

Of the seven human 14-3-3 isoforms, six are normally found in the brain, β, γ, ε, ζ, τ and η, and only the β, γ, ε and η isoforms are present in CSF of spCJD patients, with γ being the most abundant. This may suggest that the pathway from the neuron may be isoform specific.[60]

1.7.3 Current Detection Methods for 14-3-3 Proteins

Numerous studies have highlighted the importance of the 14-3-3 assay in the diagnosis of spCJD, however debate continues regarding the claim that the assay is not sufficiently specific in large populations to be used as a true diagnostic test.[61,62] Western blotting is the current technique of choice for detecting 14-3-3 proteins in the CSF, but this method is unable to detect the small changes in 14-3-3 levels in the early stages of spCJD and vCJD. In the Western blot procedure, the proteins are first denatured, separated electrophoretically, then transferred to nitrocellulose and detected using a anti-14-3-3 antibody coupled to a detection system.

ELISA's (enzyme linked immunosorbent assays) have been developed for the quantitative detection of CSF 14-3-3, however to date they lack the sensitivity of Western blotting.[63] An added problem is that CSF contains a heterogeneous mixture of dimeric 14-3-3 isoforms complexed with other interacting proteins making untreated (non-denatured) CSF not as amenable to 14-3-3 determination by ELISA as by Western Blot.

A number of antibodies have been raised against a range of epitopes on differing 14-3-3 isoforms. Table 1.3 shows a range of 14-3-3 antibodies that have been used in the detection of 14-3-3 proteins.[64] It is apparent from the table that most isoform specific antibodies have an epitope close to the N-terminus which poses a problem for the isoform specific detection of native state 14-3-3 dimers. As discussed in **Section 1.5**, the interface necessary for dimer formation uses parts of helices 1 and two, meaning that the epitope used for detection of the protein is blocked by the corresponding dimer unit, highlighted in **Figure 1.7**. This is why the Western blots, where the

proteins are denatured allowing antibodies to interact with their epitopes, have a higher sensitivity than the quantitative ELISA using un-denatured material.

Antibody	Epitope	Position	Specificity
C-629 (anti-β)	KSELVQKAKLAEQAERYDD	4-22	Cross-reaction with γ, ε, ζ, η
an	Purified brain 14-3-3		Raised against a mixture of brain isoforms
C-628 (anti-β)	LTLWTSENQGDEGDAGEGEN	226-245	Specific for β
199	Ac-MDKSELVQKAC	2-11	Specific for β, low level of cross-reaction with ζ
2042	Ac-TMDKSELVC	1-8	Specific for alternative start of β
C-731 (anti-γ)	LWTSDQQDDDGGEGNN	231-245	Cross-reaction with η
1005	Ac-VDREQLVQKAC	1-10	Specific for γ
C-1019 (anti-γ)	AGDDKKGIVDQSQQAY	134-159	Probable cross reaction with β
1002	Ac-MDKNELVQKAC	1-10	Low level cross reaction with β
C-1020 (anti-ε)	TGNDRKEAAENSLVAY	137-152	No reaction with standard containing ε
2025	Ac-MDDREDLVYQAKC	1-12	Specific for ε
ct	CGEEQNKEALQDVEDENQ	238-254	Specific for ε
2	Ac-GDREQLLQRARC	1-11	Specific for η
C-732 (anti-τ)	TSDSAGEECDAAEGAEN	228-245	Cross reacts with other isoforms
197 (anti-τ)	Ac-MEKTELIQKAC	1-10	Specific for τ
789	Ac-MERASLIQKAC	1-10	

Table 1.3: 14-3-3 antibodies and their epitopes. Antibodies specific for more than one isoform have their cross-reactivity shown.

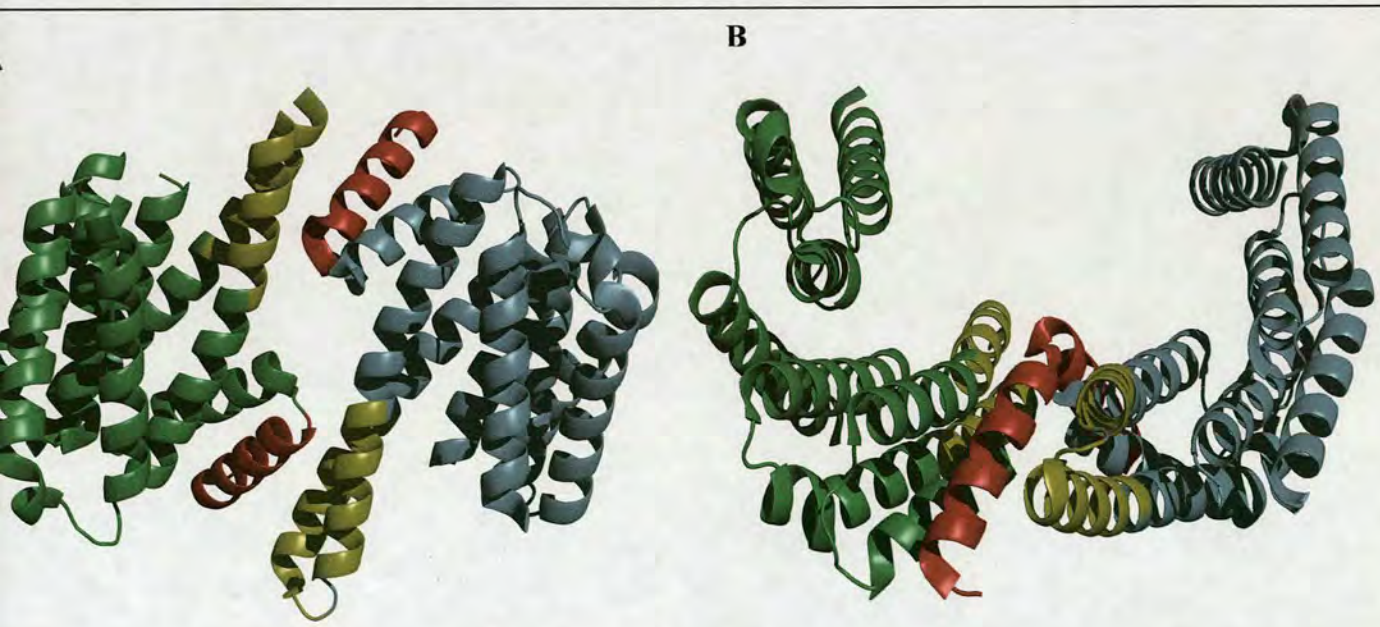

Figure 1.7: 14-3-3ζ: Helix 1 has been coloured in red and parts of helices 3 and 4 have been coloured in yellow in each monomer unit. Images A and B illustrate how close both helix 3 and 4 are to helix 1 and thus can interfere with epitope recognition.

Controversy remains regarding the suitability of 14-3-3 detection for differential diagnosis of CJD, some groups have suggested that the assay gives too many false positives and false negatives to be of value.

A study in 2005 by Van Everbroeck and co-workers involved the use of 52 spCJD and 201 control patients in whom definite diagnosis had already been made to compare the sensitivity of a γ specific antibody against commercially available anti-14-3-3 antibodies SC-731 and CJ31.[65] The experiment was carried out by both immunoblotting and a sandwich ELISA technique both of which gave comparable results. The results are shown in **Table 1.4**.

		SC-731		CJ31		γ 14-3-3	
Diagnosis	**N**	**Pos**	**Neg**	**Pos**	**Neg**	**Pos**	**Neg**
sCJD	52	51	1	50	2	50	2
Sensitivity (%)		98		96		96	
Controls	201	30	171	16	185	15	186
Specificity (%)		85		92		93	
PPV (%)		63		76		77	
Dementia	140	14	126	5	135	5	135
Specificity (%)		90		96		96	
PPV (%)		78		91		91	
OND	61	16	45	11	50	10	51
Specificity (%)		74		82		84	
PPV (%)		76		82		82	

Table 1.4: Comparison of the sensitivity and specificity of a 14-3-3 γ specific antibody for the detection of spCJD. (OND, other neuronal disorder; PPV, positive predictive value). The results show that a γ specific antibody increases the specificity without impairing the sensitivity of the assay

Work by Green and co-workers in 2002 used a capture assay to compare the viability of the 14-3-3 surrogate marker for detecting spCJD and vCJD.[66] Greens results and explanations are shown in Figure 1.8 and Table 1.5.

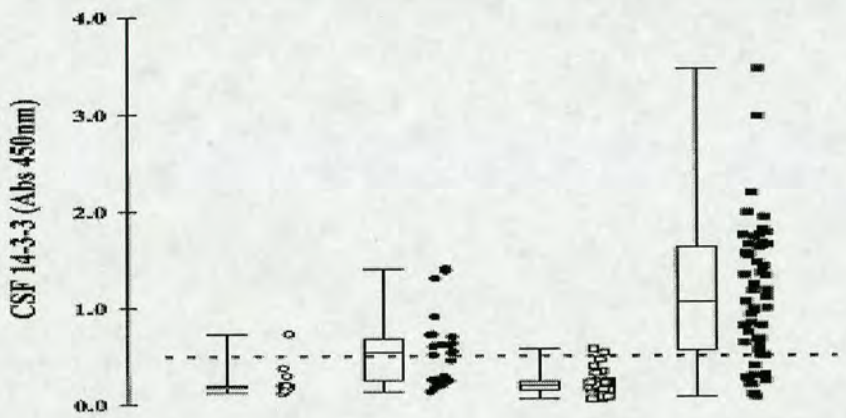

Figure 1.8: CSF 14-3-3 detection in sCJD and vCJD. Combined scatter and box and whiskers plots of CSF 14-3-3 γ detected by protein capture assay in vCJD control patients (○), in vCJD patients (●), in spCJD control patients (□), and in spCJD patients (■). The boxes represent the 25th–75th quartile,divided horizontally by the median, the whiskers represent the range and the adjacent scatter plots represent the individual values from which the boxes and whiskers are derived. The horizontal dotted line represents the cut-off absorbance of 0.5.

CSF 14-3-3γ results in patients with either variant or sporadic CJD and appropriate controls[a]

	spCJD			vCJD		
	Capture assay	Western blot	Combined assays	Capture assay	Western blot	Combined assays
Definite CJD (*n*/tn)	45/55	49/55	50/55	15/26	15/26	20/26
Controls (*n*/tn)	2/32	1/32	3/32	1/13	1/13	1/13
Sensitivity (%)	82	89	91	58	58	77
Specificity (%)	94	97	91	92	92	92
PPV (%)	96	98	86	94	94	96
NPV (%)	75	84	78	52	52	66
Efficiency (%)	86	92	87	69	69	82

Figure 1.9: Sensitivity and specificity of CSF 14-3-3. Detection of 14-3-3 γ in the CSF of patients with spCJD (n = 55) or vCJD (n = 26) and in sporadic control patients (n = 32) or vCJD control patients (n = 13) using Western blot analysis and the protein capture assay. The sensitivity, specificity, positive predictive value, negative predictive value and efficiency of both methods were calculated using the number of positive results/total number. PPV, positive predictive value; NPV, negative predictive value; n/tn, number of positive results/total number.

Green's results show that although vCJD gives a less sensitive response in the 14-3-3 assay, it can still be used in the detection of the disease.

For the 14-3-3 CJD assay to gain worldwide acceptance, a specific, sensitive method is required that can detect small levels of changes of 14-3-3 proteins in the CSF in an isoform specific manner. Recent antibodies are capable of detecting 14-3-3 to a level of 3.1±2.9 ng/ml using the ELISA technique. Although this is suitable for detecting the changes in CSF levels for sCJD, much smaller changes occur with vCJD and the current antibodies do not provide the sensitivity required for definitive diagnosis.

We propose to use an oligonucleotide alternative to antibodies, namely aptamers, and we aim to use them to provide a detection method capable of detecting native state 14-3-3 protein from CSF with sensitivity comparable to the current antibody equivalents.

Chapter 2: Aptamers

2.1 Aptamers, an Introduction

Aptamers are RNA or DNA oligonucleotides which bind to other molecules with high affinity and specificity. The theory of aptamer production is simple – a very large population (library) of synthetic oligonucleotides is screened and the candidates with the desired binding properties are isolated and identified. However this is not practical unless some kind of selective enrichment of oligonucleotides with the desired properties is incorporated in the procedure. The systematic evolution of ligands by exponential enrichment (SELEX) process, which is described later in this chapter, involves the sequential amplification of sequences in the library with high target affinity at the expense of those of lower affinity. This relies on the fact that DNA oligonucleotides can be faithfully amplified by the polymerase chain reaction and, in the case of RNA aptamers, that these can be converted to and transcribed from their DNA counterparts.

Aptamers were first described in 1990. Tuerk & Gold and Ellington & Szostak demonstrated the *in vitro* screening of large libraries of RNA oligonucleotides for RNA ligands that bind T4 DNA polymerase and a variety of small organic dye molecules respectively.[67,68] Both groups showed that by using the SELEX process they could identify individual nucleic acid sequences which showed selective target binding from very large random sequence nucleic acid libraries. Although the idea of using artificial evolution to select highly specific and selective oligonucleotides ligands against a target molecule was a new concept at that time, the idea of the potential therapeutic use of small nucleic acid ligands for biomolecular targets was not. Studies on HIV and adenovirus in the 1980s had found that these viruses

encoded small, structured RNAs which bind to viral or cellular proteins with high affinity and specificity. Such RNAs were shown to modulate the activity of proteins essential for their replication or to inhibit the activity of proteins involved in the cellular antiviral response. In 1990, Sullenger *et al.* published novel work which described the overexpression of one such HIV RNA ligand.[69] The HIV-encoded *tat* gene product is a potent *trans*-activator of viral gene expression. To function, *tat* must directly bind to a *cis* acting RNA target called TAR (*trans* activation response), which is encoded in the first 60 nucleotides of the viral RNA transcript. In a case of "intracellular immunisation", Sullenger managed to overexpress an RNA species encoding the TAR sequence, and used it as a decoy to bind to *tat*, preventing *tat* binding to the TAR sequence encoded by the viral RNA, inhibiting HIV-1 replication. Sullenger's work was seminal showing (in advancing the concept that) nucleic acid ligands could play a role in modulating the activity of clinically active proteins, and they could act like antibodies in selecting a target with high selectivity and specificity.

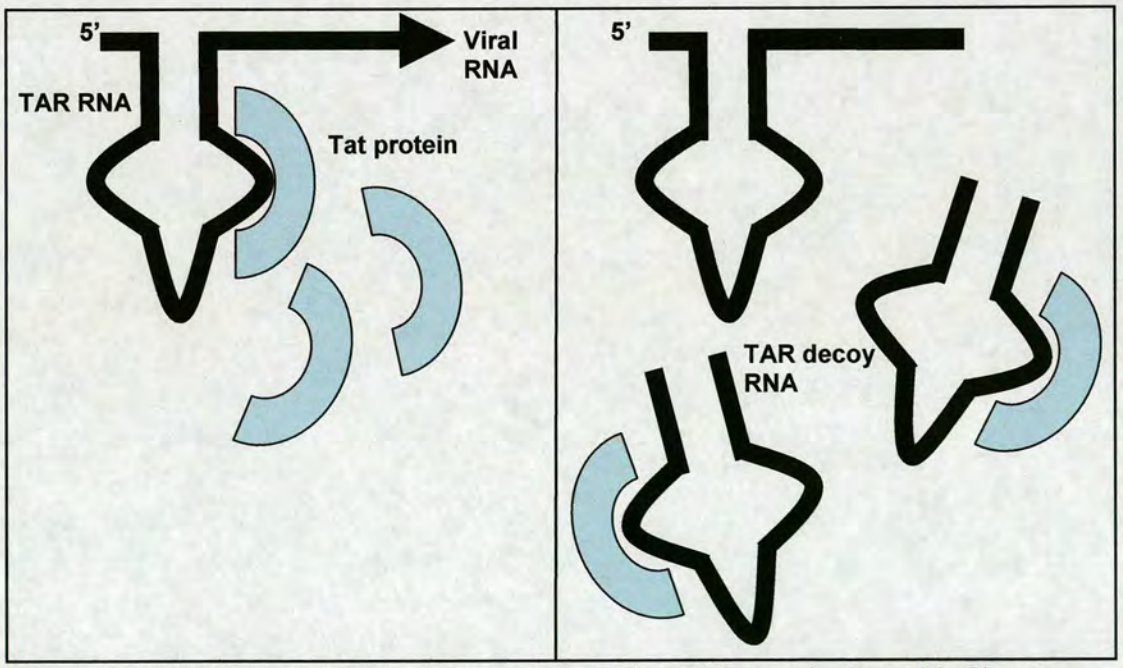

Figure 2.1: TAR decoy RNA aptamer preventing Tat protein from binding to viral TAR RNA. By inhibiting the TAR-Tat interaction the aptamer inhibits HIV RNA transcription and replication.

It should be noted here that natural nucleic acid-protein interactions, such as the tat-TAR case, are generally reversible allowing gene regulation, whereas the aim of an artificial aptamer-target selection may be to obtain the strongest binding sequence in vitro and thus selection of tighter binding sequences is possible.[70] In principle the generation of a suitable high-affinity aptamer requires no previous knowledge about the properties of the target, its structure or how it interacts with or recognises its own natural ligands. It seems reasonable that if aptamer-target interactions can be selected that such features as such as association rate, dissociation rate and affinity for the target and lack of affinity to a closely related target could be selected for by carefully selecting the selection/partitioning methods.

The affinity of published aptamers varies widely according to the choice of target.[71] Perhaps unsurprisingly, aptamers to nucleic-acid binding or heparin binding molecules generally have the strongest affinities, typically in the high picomolar to low nanomolar range. Non nucleic-acid binding proteins often have affinities in the higher nanomolar range, whereas aptamers against small molecules have affinities generally in the micromolar range. Examples of each are cited in **Table 2.1**. The KGF binding aptamer deserves special attention for binding in the femtomolar range, 300fM, an interaction encroaching on that of streptavidin-biotin binding, to date the strongest published interaction.[72]

Ligand	Nucleic Acid	Affinity K_d [μM]	3D Structure, PDB accession number	Reference
Theophylline	RNA	~0.3	NMR, 1EHT	73
FMN	RNA	~0.5	NMR, 1FMN	74
AMP	DNA	~6	NMR, 1AW4	75
	RNA	~10	NMR, 1AMO, 1RAW	76,77
Arginine	DNA	~125	NMR, 1OLD, 2ARG	78,79
	RNA	~60	NMR, 1KOC	80
Citrulline	RNA	~65	NMR, 1KOD	76
Tobramycin	RNA	~0.009	NMR, 1TOB	81
		~0.012	2TOB	82
Neomycin B	RNA	~0.115	NMR, 1NEM	83
HIV-1 Rev peptide	RNA	~0.004	NMR, 1ULL, 484D	84
HTLV-1 Rex peptide	RNA	~0.025	NMR, 1C4J	85
MS2 Coat protein	RNA	-	X-ray, 5-7MSF	86
Thrombin	DNA	~0.025	NMR, 148D	87
			X-ray, 1HAO	88
Argininamide	DNA		NMR, 1DB6	89
Vitamin B12	RNA	~0.9	X-ray, 1DDY	90
Tetramethylrosamine	RNA		X-ray, 1F1T	91
Biotin	RNA		X-ray, 1F27	92
HIV-Tat	RNA		NMR, 1NBK	93
Streptomycin	RNA		X-ray, 1NBT	94
Nf-Kb(P50)2	RNA		X-ray, 100A	95
KGF	RNA	~0.0003		72

Table 2.1; Current aptamer affinities and structures. Adapted from Hermann and Patel.[73] PDB is the Research Collaboratory for Structural Bioinformatics protein data bank, a database here all protein crystal structures solved to date.

Aptamers have been shown to have remarkable specificity for interaction between very closely linked molecules. There is evidence of the ability of aptamers to

differentiate enantiomers, L- and D-arginine have a 16 000 fold difference in their K_d values.[78] Aptamers can differentiate very similar enzymes, α-thrombin can be distinguished over γ-thrombin, aptamers have also been shown to differentiate very similar small molecules.[87] One of the most commonly quoted examples is that of the theophylline aptamer which has a 10,000 fold greater affinity over the affinity of the same aptamer for caffeine, a molecule which differs by a single methyl group (see **Figure 2.2**).[73] Hydrogen bonding between a cytosine residue in the aptamer and the purine like theophylline provides a pseudo base pair, where the aptamer and the small molecule both provide a bonding partner. In comparison, caffeine contains a bulky N-methyl substituent which makes the pairing no longer viable.

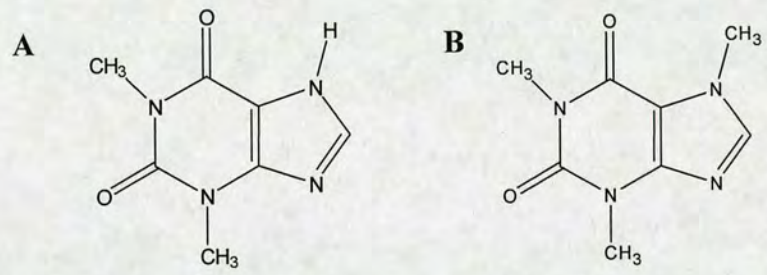

Figure 2.2: Theophylline and Caffeine. Theophylline (A) differs from Caffeine (B) by a single methyl substitution.

2.2 DNA or RNA Aptamers

Aptamers make the ideal starting molecules for combinatorial chemistry. They differ from organic libraries in that they have their own genetic code needed for their own amplification and they contain the blueprint necessary for their improvement and optimisation. Antisense nucleic acid molecules have similar chemistries however

they are considered linear molecules capable of blocking transcription by following the Watson-Crick model of DNA as opposed to forming intricate tertiary structures that bind targets like aptamers. Organic molecules have inherent limitations to the number of tertiary structures available and limits to the options of chemically synthesised derivatives that can be use in an aptamer library because of the necessity for the library to interact with nucleic acid polymerase enzymes.

Biological DNA is almost exclusively an informational macromolecule and is structured as a base paired duplex. Single stranded DNA is a rare commodity in nature and a ssDNA molecule that can form a structure and carry out a functional role is even more unusual. It is generally accepted that DNA has a limited number of intra molecular structures because of the molecules rigidity and the availability of bond donors/acceptors, however the publication of the human genome led to the belief that other structures of DNA may be possible. Only 1-2% of the complete human genome codes for proteins, leaving questions regarding the function the remaining 98% of human DNA. Recent evidence regarding the ability of DNA to form quadraplexes, sequence dependant, structurally stable complexes built around guanine residues, has brought to light the ability of DNA to form unique structures that are biologically active (the crystal structure of a g tetrad is shown in **Section 2.4.2**). Shafer and co-workers have shown that such structures exist in the human genome, are present in areas such as the telomeres, where they protect chromosomal DNA from exonucleolytic degradation, and they also have the potential to interact with regulatory regions, involving them in gene regulation, an example being the argument that they have position upstream from the P1 promoter for the *c-myc* oncogene.[96]

It is generally accepted that RNA can form a wide variety of intricate and functional structures due to the combined use of Watson-Crick pairing, non-standard base

pairing (for instance Hoogstein), and a variety of non-covalent contacts involving phosphates, ribose oxygens and cationic metals. The 2' hydroxyl of the ribose group plays an important role in building structures, acting as either a hydrogen bond donor, or as an acceptor, increasing the diversity of the structure forming potential. It should be noted that nature has its own, recently discovered, structure dependant RNA aptamers termed riboswitches.[97] Riboswitches are part of an mRNA molecule capable of binding a small target molecule, whose binding affects a genes activity. Ligand binding causes a structural change in the mRNA which directly regulates gene expression often as part of a negative feedback control.

Natural RNA (and to a lesser extent DNA) has the very real problem of phosphodiester bond hydrolysis. The reaction, which breaks the spine of the nucleic acid, is catalysed by ribonucleases found in biological fluid. The predominant nucleases in biological fluids are pyrimidine specific, so introducing a modification at the reactive 2' position of pyrimidine nucleotides prevents degradation of aptamer molecules. Enhanced stability aptamers (those modified at the 2' position by either 2'-amino, 2'-O-methyl or 2'-fluoro functional groups) have been successfully selected from SELEX libraries.[98] Attachment of a benzoyl group at the C-5 position of pyrimidine is another common modification as it appears to be tolerated by the enzymes used in amplification.[99] Another challenge facing aptamer chemists is the fact that nucleic acids have uniform hydrophobicity and low p*I*, factors that can be changed with the clever use of modified nucleosides. For a comprehensive revue of modified ribonucleosides see Eaton and Pieken.[100]

A further method used to create nuclease resistant aptamers has spawned the term spiegelmers, involving a very clever method of selecting nuclease-resistant L-ribose aptamers, first described in 1996 by Klussmann *et al.*[101]

2.3 The SELEX Approach

2.3.1 The Aptamer Library

The process of aptamer selection typically begins with a random sequence oligonucleotide library obtained by the combinatorial synthesis of DNA or RNA. The library, generally of defined length oligonucleotides, is synthesised by solid phase oligonucleotide methods. A typical aptamer library sequence contains a 'core' randomised region of length *N*, encased by 5' and 3' fixed 'flanking' regions which are generally 15-20nt in length and which are necessary for the polymerase chain reaction (PCR). The flanking regions are designed specifically to minimise primer-dimer formation during amplification and to eliminate base pairing between the fixed regions. The randomised sequence in the oligonucleotide libraries can be obtained by using a mixture of activated monomer units, instead of a single species, during synthesis. The maximum theoretical size of the library is related to the number of randomised positions and the oligonucleotide diversity (y). A library of, for example, 40 randomised positions has a maximum theoretical diversity of y^N, and therefore contains $4^{40} = 1.2 \times 10^{24}$ different molecules. This diversity and complexity far outweighs that of commercial small organic molecules libraries (typically ~16,000 molecules), peptide libraries used in phage displays, and even the estimated amount of antibodies that a mouse can generate, which is believed to be between 10^9 and 10^{11} molecules.[102] The real power of the process lies in the diversity of the starting library. There are so many different molecules with differing tertiary structures contained within the library that it would be reasonable to assume that at least a few molecules can form the desired structures necessary for binding to the target.

The length of the randomised region should be large enough to ensure that the library contains the maximum number of molecules possible to manipulate in a standard molecular biology laboratory, in the order of 10^{15}, and assuming errors in workup this diversity may be estimated to reduce to 10^{13}-10^{14}. *N* needs only to be around 22-24 monomer units to achieve this, however, a further caveat is added as the DNA or RNA library must be large enough to fold into a complex tertiary structure capable of specific interaction with the target. Most libraries used tend to have *N* equal to or larger than 35nt. Due to limitations in the efficiency of oligonucleotide synthesis, starting with an aptamer library much larger than 35nt could cause incorrectly synthesised molecules to have an impact on the library quality. There is also a possibility that larger molecules may have two distinct folds complicating the method of *in vitro* selection, leading to the suggestion that a practical limit of around 80nt should be used.[103]

Whereas most aptamers, an example being the streptomycin-binding aptamer, are in the region of 30-46nt long, successful aptamers with sizes out with this suggested size limit have been found for some targets.[104] Indeed, without including the flanking regions, which may add another 50nt, aptamer sizes can differ radically. At one extreme the successful thrombin aptamer (see **Section 2.4.1**) is a 15mer, and at the other, the minimum binding region for an aptamer that binds serine protease in blood (protein C) was as long as 99nt.[105,106]

Aptamers in general have a molecular weight around 10kDa, much smaller than the antibody alternative (around 50-60kDa), which may prove advantageous in clinical uses.

2.3.2 The ssDNA SELEX cycle

There are numerous reviews available regarding the selection of aptamers by the SELEX process. The most complete include the works of James, Jayasena, Breaker and Famulok and the reader is directed to those for detailed information.[104, 107, 108, 109]

The ssDNA SELEX cycle can be broken down into 4 distinct steps.

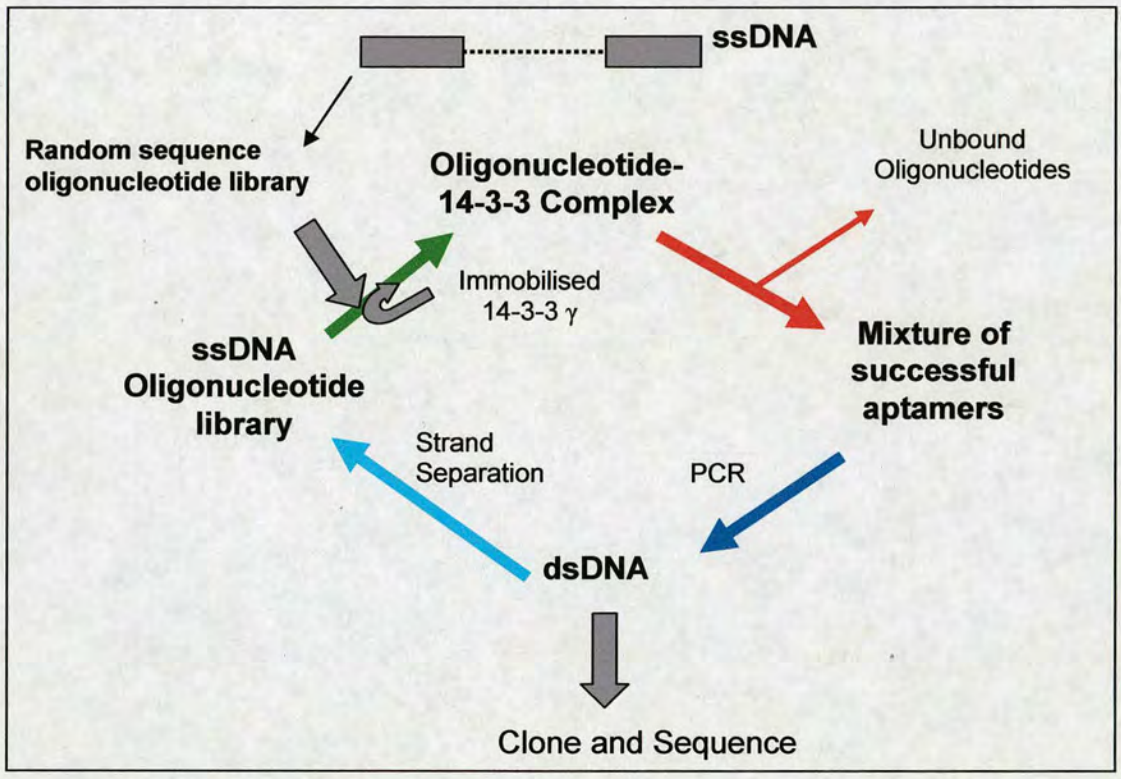

Figure 2.3: The ssDNA SELEX approach. The method can be broken down into 4 distinct steps; Step 1: Protein/Target incubation, Step 2: Partitioning/Eluting aptamers, Step 3: Amplification of binding candidates, and Step 4: Separation of dsDNA. Completion of Step 4 leads back to the start of a new cycle.

To start the screening process, a random sequence oligonucleotide library is incubated under pre-defined conditions with the target of interest. The conditions should be set depending on the diagnostic use of the aptamer to be used. The time of incubation, buffer, pH, temperature are among the variables which must be set by the investigator

before starting the process. The stringency of selection can also have an influence on the number of SELEX cycles required for aptamer identification but generally enrichment is commonly reached within 8-16 cycles (using more cycles is not unheard of).

The second step involves removing all those aptamers who do not bind and collecting those that do. Different techniques have been used for the SELEX partitioning step, although all methods have their own limitations and are not perfect at separating bound from unbound ligands. A common method for selecting aptamers against proteins involves using a nitrocellulose filter. Proteins, unlike DNA/RNA are retained well on nitrocellulose allowing unbound aptamers to be washed through and bound aptamers to be collected.[110] Some reports suggest that substantial amounts of oligonucleotides may be non-specifically trapped by the membrane causing problems with this method. Alternatively, immobilising the protein on a resin can be used for easy separation of the bound from unbound nucleic acids and allows procedures such as competitive elution which can be helpful in setting affinity and specificity parameters. Immobilisation also facilitates "counter-SELEX", an attractive strategy that improves recognition specificity. The problem with immobilisation is that it hinders the mixing process by reducing the mobility of the protein and producing steric hindrance to aptamer binding. Mixing the protein/aptamers in solution pre-immobilisation may help with this. Finally, two more recent published methods involve 1) the use of expensive robots in what is claimed to be an automated high throughput method of screening aptamers as pioneered by Cox and co-workers and 2) the use of capillary electrophoresis as a more direct and much quicker process of

selecting aptamers.[111,112] This method appears advantageous as it is easy to monitor and finds suitable candidates after just 1-2 cycles, saving much time.

When bound and unbound candidates are separated, the successful aptamers are led onto step 3, which involves amplification using the polymerase chain reaction (PCR), obtaining an enriched dsDNA library to be prepared for the next step. The definition of SELEX (systematic evolution of ligand by exponential enrichment) suggests that some form evolution will take place between in the aptamers between the starting library used and those aptamers collected at the end of the overall process. This evolution comes about by using error prone enzymes in the amplification, ensuring mutations occur during PCR. Each step of the SELEX cycle retains a small fraction of candidates with favourable properties. The mutations caused in the amplification generate additional diversity which could mean that the sequence of the best candidate at the end of many cycles was not present at the start of selection cycles.

Step 4 involves the separation of the dsDNA. This is generally done by using a 3' primer biotinylated at its 5' end, the dsDNA can be immobilised on a streptavidin resin as first reported by Espelund and co workers.[113] All that remains then is for the duplexes hydrogen bonds to be broken and the 5' strand to be collected. An alternative method used can be to use asymmetric PCR to obtain an excess of one of the strands as shown by Fukusaki *et al.*[114]

Upon optimisation, each cycle of the SELEX approach can take 2 days and when cloning and sequencing steps are added the whole unautomated approach can take up to 3 months to complete, faster than the amount of time to generate a cell line for a monoclonal antibody and its purification.

2.3.3 Modifications for an RNA SELEX

To start RNA SELEX, the initial DNA starting library is in vitro transcribed to get a corresponding RNA library. A promoter for an RNA polymerase is engineered within the 5' flanking region of the starting library to afford transcription (although unused throughout this study, a T7 RNA polymerase site was engineered into the aptamer starting library).

The library is subject to the necessary partitioning method and those RNA aptamers with the desired binding properties are collected. The successful RNA pool is amplified by RT-PCR and subject to further transcription before the enriched pool is applied to the target for a further round of selection. The transcription step replaces the strand separation step used in selecting ssDNA aptamers.

Often RNA libraries are chemically modified to enhance the nuclease resistance of the resulting aptamers (**see Section 2.2**). RNA aptamers are more common than the ssDNA counterparts, largely due to the belief that RNA can form a wider variety of structures than ssDNA. Interestingly, RNA and ssDNA aptamers both screened against thrombin interact at different sites on the protein.[115]

2.3.4 Considerations of the SELEX Approach

During SELEX, there is no guarantee that a successful aptamer may be obtained at then end of the selection process. The chances of finding a target binding sequence from the initial library seem to vary enormously depending on the target and exactly what the successful criteria is. It is often estimated that the chances of finding a target binding sequence is around 1 in 10^{11}-10^{12}, DNA or RNA binding targets appear to have a greater chance of success.[116] It is estimated that a library containing 40 random bases could have 1 x 10^{24} different sequences, suggesting that the library pool should contain sufficient aptamers to make it through to the following round. The early stages of selection should be used for library manipulation and not to reduce the diversity of the library far below its theoretical maximum.

The selection criteria used is also a fine balance between either too stringent or not stringent enough. By using wash steps that overly harsh, intermediate binding sequences that may have evolved beneficially for the library, could be wiped out. Washing in conditions that are too lenient would prevent the highest binding aptamers from being separated from those that are low affinity, and possibly prevent the efficient selection of those favourable aptamers.

The mutation necessary for the evolution of the aptamers is also a process that can be fraught with problems. The amount of mutation must be sufficient to ensure progress towards an evolved aptamer library, too few mutations will hinder the diversity of the sampled sequence space. On the contrary, if too many mutations occur, the library may completely overshoot the optimum sample space. Another PCR related problem may be that some molecules may be better at replication and as such it would be possible for less functionally effective molecules to be over-represented in the library used for the next stage of selection.

Aptamer libraries contain scope for structural pleiomorphism. If a specific aptamer can fold into more than one structure, and each structure has similar ΔG properties, problems could arise with selection issues. Although this could be a potential problem, using ssDNA aptamers instead of RNA limits the possible aptamer intra-structures available.

2.4 Aptamer Structures

As previously mentioned, many aptamers have had their structures solved, either by X-ray crystallography or more commonly by NMR. Two aptamer structures which received detailed study are discussed here and the reader is directed to the paper by Patel and co-workers for details on RNA aptamer structures and a further review by Hermann and Patel for a detailed discussion of further solved aptamer complexes.[117,71]

2.4.1 Thrombin aptamer

The thrombin aptamer was one the first known aptamers, it has been extensively studied and is often used as a control in the validation of novel aptamer analytical applications. The aptamer is a 15mer (d(GGTTGGTGTGGTTGG)) and forms two tightly stacked G-quartets with 3 loops of T-T base pairing between the two minor loops, thought to be stabilised by the addition of metal ions. The dissociation constant, K_d, has been determined to be between 1.4 and 6.2nM and has shown potent anticoagulant properties in vivo.[118] The G-octet is a common feature among DNA aptamers, an inhibitor of the integrase enzyme of HIV-1 also has a similar sequence and structure to that of the thrombin aptamer.

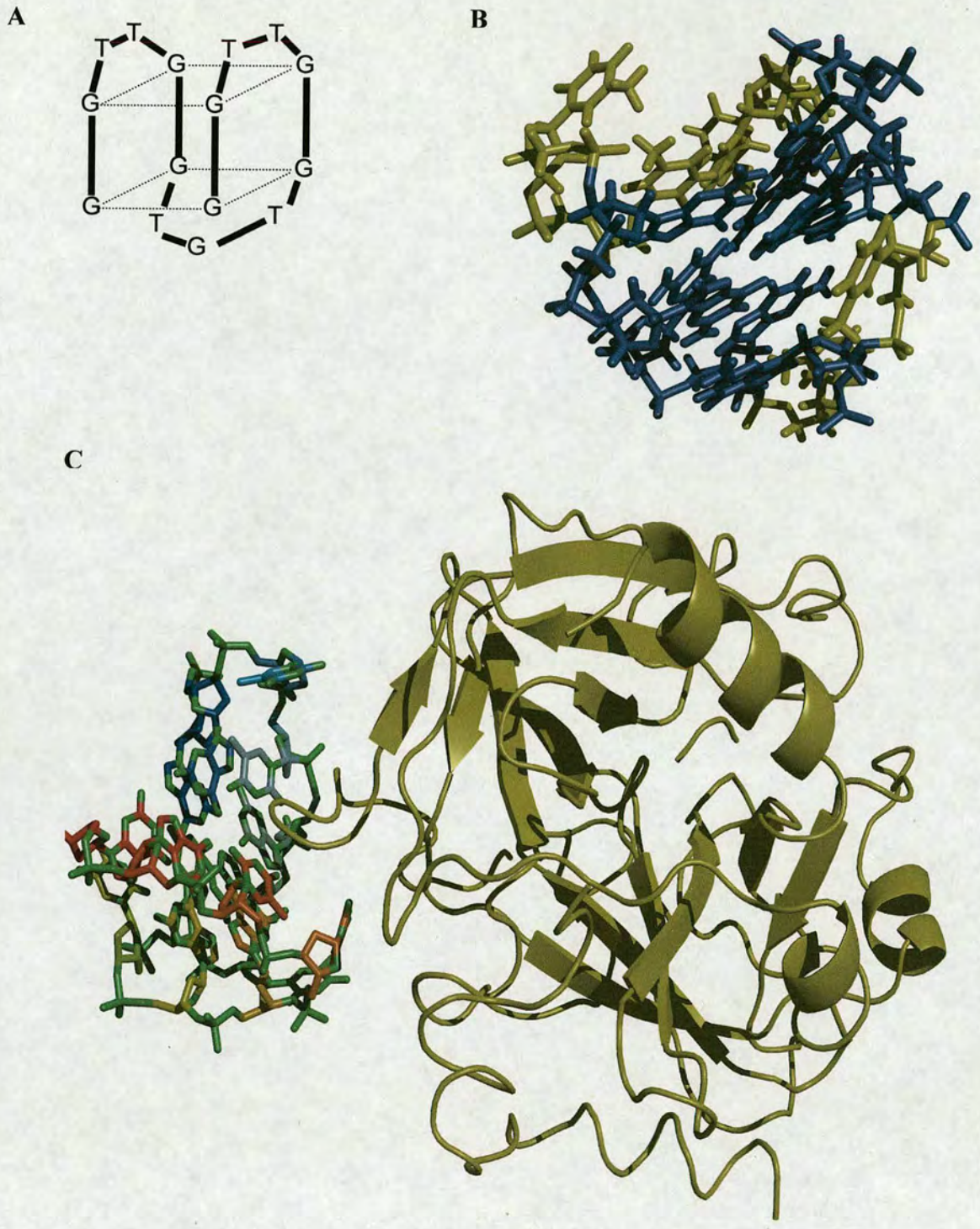

Figure 2.4: X-ray crystal structure of the thrombin binding aptamer **A** shows a diagrammatical representation of stacked g-quartet. **B** shows the NMR stacked thrombin aptamer, with G residues in blue and T in yellow. **C** shows the same aptamer inhibiting thrombin.

2.4.2 Crystal structure of the G-tetrad

The X-ray crystal structure of the G tetrad is shown below. The distances between each oligonucleotide are 1.8 to 2.0 Å.

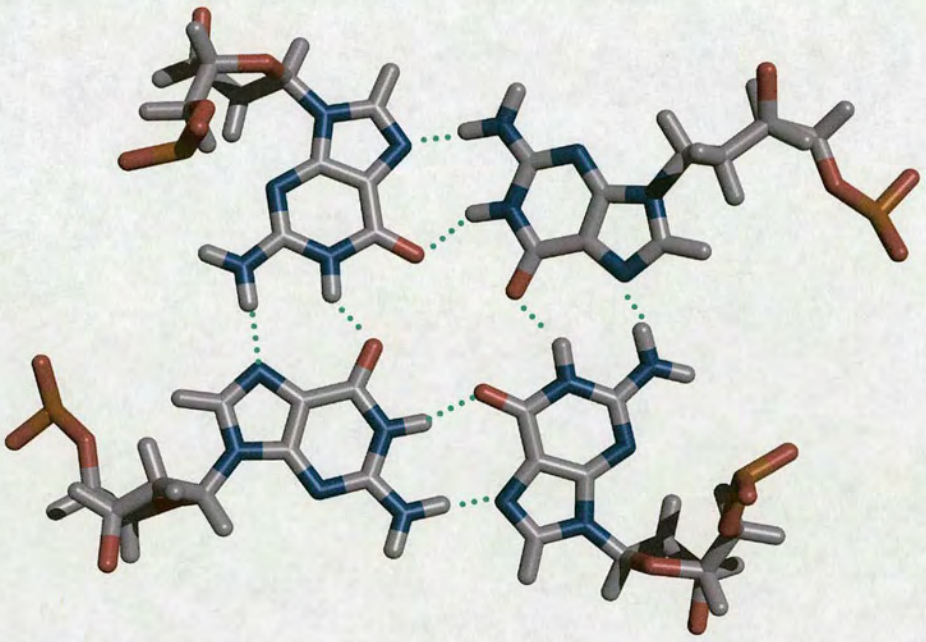

Figure 2.5: Crystal structure of the G-tetrad. The hydrogen bonds are highlighted in green.

2.4.3 HIV-1 RT Aptamer

Two different RNA aptamers (for HIV protease) have had their NMR structures solved, when bound to a 17 residue peptide derived from human immunodeficiency virus type 1 (HIV-1) Rev protein.[84] The Rev peptide which is generally unstructured in solution binds in an α-helical conformation to the RNAs. The peptide inserts into the RNA deep groove, widened through adaptive formation of non Watson-Crick purine-purine pairs and a U:A:U base triple.

A

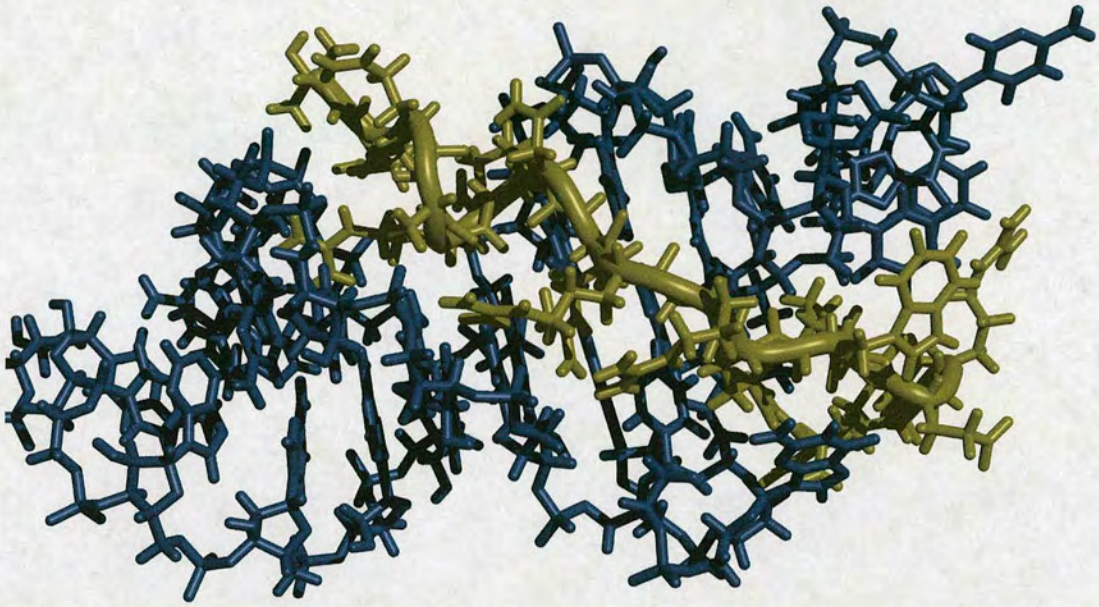

B

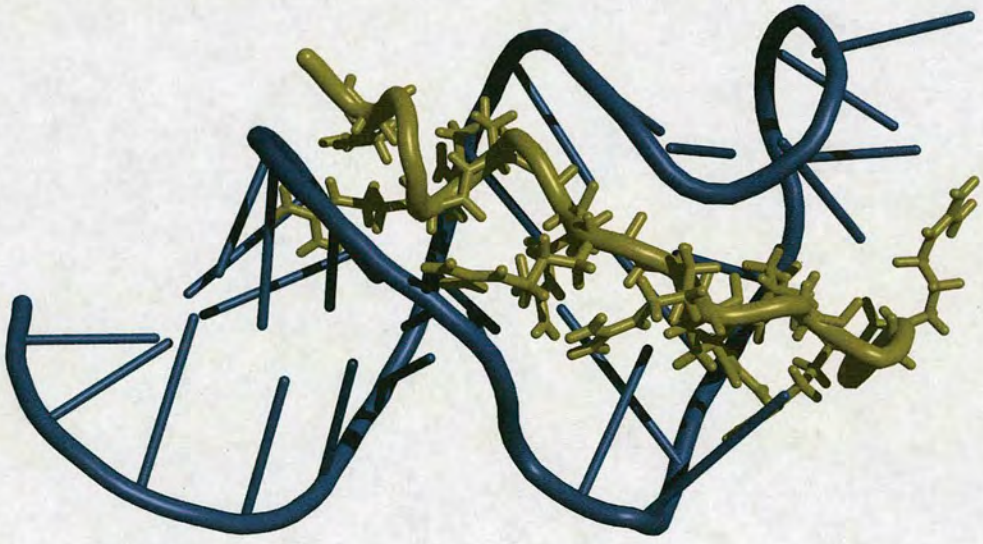

Figure 2.6: The NMR structure of the RNA aptamer interacting with HIV-1 RT. Figure **A** has highlighted the aptamer as a blue chain and shown the truncated enzyme in yellow. Figure **B** has the arginine residue side chains highlighted.

2.5 Aptamer Technology

2.5.1 Aptamers versus Antibodies

When considering the possible therapeutic and diagnostic values of aptamers, it is important to acknowledge the massive contribution that antibodies have made to these fields in the past 30 years, especially monoclonal antibodies.[119] The importance of antibodies cannot be understated, they provide standard diagnostic tests based on molecular recognition and remain invaluable in clinics worldwide. What has become apparent since the introduction of aptamers, is that they provide a real alternative to antibodies in many (not just niche) areas, and show signs of improving upon the current antibody technology already in place.[108]

Both classes of molecules, are biopolymers which can recognise targets with high affinity and specificity. They both bind with dissociation rates (K_d) in the low picomolar to low nanomolar range, however the binding of an aptamer appears to be a more specific interaction, with the potential ability to discriminate between closely related proteins sharing common sets of structural domains.

Aptamers, or more specifically DNA aptamers, are relatively stable compounds which can be heated or cooled (reversible denaturation) without damage to the sequence. Aptamers have a long term storage lifetime and can be transported at ambient temperatures. In contrast antibodies are temperature sensitive proteins with a limited shelf life and they can undergo reversible denaturation, often a costly and frustrating issue.

Aptamers are produced by total chemical synthesis and the reproducibility of this means that uniform activity is possible. Because aptamer selection is carried out in vitro, almost any molecule can be targeted, and the selection conditions can be tuned

for in vitro diagnostics. Antibody selection requires the use of a biological system, making it difficult to raise antibodies to molecules that have reduced immunogenic responses or molecules that are toxins, as well as limiting the physiologic conditions for optimising antibodies for diagnostics. The other problem with antibodies is that performance can vary batch to batch, meaning that immunoassays may need to be reoptimised with each new batch.

Other advantages of using aptamers include: (a) Aptamers, unlike antibodies, can be subjected to a wide range of chemical modifications; (b) No evidence of immunogenicity exists for aptamers and a method of isolating cross-reactive compounds has been developed for aptamers named toggle SELEX.[120]

2.5.2 Aptamers as Therapeutics

Aptamers have potential as therapeutic agents. Truncated aptamers are smaller than antibodies, ~ 15kDa compared to ~50kDa, and this may be beneficial for tissue penetration and shorter residence time in the blood. Another major advantage is that aptamer specific antidotes can be rationally developed to reverse the inhibitory activity of a drug, helping to provide safe, tightly controlled therapeutics.

The process of turning a therapeutic concept into a clinical application is remarkable achievement, and aptamers will soon be a class of molecules that have accomplished this feat. Fifteen years after the seminal work by Sullenger on the TAT/Tar nucleic acid sequence, new drug applications were filed on two aptamer compounds, Macugen and E2F decoy, both of which are non naturally occurring nucleic acid ligands. Macugen had now been approved by the US food and drug administration, although Corgentech recently announced that E2F failed phase III trials.[121]

Table 2.2 shows a selection of aptamers and their progress in clinical trial to date. The table, adapted from Nimjee *et al.* includes aptamers against a range of many different therapeutically relevant targets.[122]

Target	Oligo Type	Clinical Data	Selection (rounds)	For Treatment in	Reference
HIV-1 Tat	RNA		in nature	**Antiviral** HIV therapy	46
HIV-1 Tat	RNA		in vitro (11)	HIV therapy	123
HIV-2 Tat	RNA		in nature	HIV therapy	124
HIV-1 Rev response element	RNA	Phase I	in nature	HIV therapy	125
Hepatitis C NS3	RNA		in vitro (6)	Hepatitis C Virus (HCV)	126
Prion Protein PrP^{Sc}	RNA		in vitro (12)	**Transmissible spongiform encephalopathies (TSE's)**	127
α-thrombin	DNA	Phase I (2005)	in vitro (5)	**Anticoagulation**	128
Vascular endothelial growth factor (VEGF)	RNA	Drug Available, Macugen (FDA approved Dec (2004))	in vitro (12)	**Antiangiogenisis**, Age related macular degeneration (AMD)	129
Platelet-derived growth factor	DNA		in vitro (12)	**Anti-inflammatory**	130
Transcription Factor E2F	DNA/ RNA	Failed Phase III	in nature/in vitro (13)	**Antiproliferation**	131
Cytotoxic T cell antigen 4	RNA		in vitro (9)	**Immune Modulation**	132

Table 2.2: Current aptamers as therapeutics. Many more aptamers are currently undergoing early stage assays for clinical testing. Only a select few have been highlighted in this tale to show the range of targets/treatments where aptamer therapy may be of use.

2.5.3 Analytical Applications of Aptamers

In future aptamers may provide clinically relevant alternatives to antibodies in therapeutics, but at present the main interest in aptamers derives from their potential as ligands for diagnostic and related applications. They are currently in use or development for many different detection and/or capture assays. A few examples are discussed below.

2.5.3.1 Chiral Selection

The ability to study the different physiological behaviours of enantiomers of the same chiral molecule is of great interest to the pharmacological industry. The most suitable technique for separation of enantiomers is high performance liquid chromatography (HPLC) using various types of stationary phase chiral selectors (crown ethers, amino acids, etc). An alternative method would be to use a stereospecific aptamer that binds to only one enantiomer. This aptamer immobilised on a resin and used with HPLC can separate a racemic mixture, allowing analysis of the non-binding enantiomer (contained in the void volume) and the binding enantiomer (retained on the resin). This technique has been used to select the D isomer of arginine-vasopressin from the L isomer.[133] It has also been used to select tyrosine from numerous analogues.[134]

2.5.3.2. Affinity Chromatography

Protein purification by affinity chromatography is a well developed tool in protein chemistry, due to the speed of the process and the quality of the purified product. Classic examples include the use of nickel affinity resins to purify recombinant His-tagged proteins and antibody resins in the purification of fusion proteins. These techniques make possible the one step purification of proteins from whole cell lysates. There are numerous post selection modifications of aptamers possible, allowing many differing methods for aptamer immobilisation on resins. One such method involved the purification of L-selectin from unfractionated human serum by a ssDNA aptamer giving a 1500-fold enrichment with 83% recovery in the initial purification step.[135]

2.5.3.3. ELONA

ELISA's (enzyme-linked immunosorbent assay) were first described in 1971 and since then they have revolutionised clinical diagnostics in medicine.[136] They allow simple and rapid measurement of a variety of analytes with exceptional specificity and sensitivity. The most common ELISA used is the sandwich ELISA, involving two antibodies that bind simultaneously to the analyte. First, an immobilised antibody captures the protein and holds it near the surface of the microtitre plate, and then a secondary antibody, coupled directly to a specifically chosen enzyme will be used to bind to the protein. The analyte is now sandwiched between the two antibodies, and the enzyme coupled to the secondary antibody will provide a method for detection.

The ELONA (enzyme linked oligonucleotide assay) replaces one of the antibodies with an aptamer.[137] ELONA's have similar precision and accuracy to standard

sandwich ELISA's, but have the advantage that aptamers can be easily modified to include useful moieties which are easily detected. Modifications can simplify the process, improve the detection limit and error of the assay. ELONA's have been used in the detection of VEGF, (shown in **Table 2.2**) with accuracy, precision, and specificity well within the limits expected of a typical enzyme linked assay.

2.5.3.4 MALDI-MS

Matrix Assisted Laser desorption ionisation mass spectrometry (MALDI-MS), can be adapted to use aptamers as ligands for protein capture and analysis as described by Dick and McGown.[138] They used a thrombin-binding DNA aptamer modified matrix to selectively capture thrombin from human plasma, then released the protein for analysis. By simply washing the surface matrix under the correct conditions, the experiment can be repeated on the same spot using the same aptamer that had been previously loaded. A similar procedure has been used to selectively capture human insulin from extracts of pancreatic cells.[139]

2.5.3.5 Signalling Aptamers/Molecular Beacons

Molecular beacon aptamers are oligonucleotide sequences engineered to recognise a protein and to generate a fluorescent signal on binding, making them useful as signalling probes.[140] An aptamer with a fluorescent tag, when not bound to its target, forms a duplex with a complementary strand containing a fluorophore quencher. Addition of the target causes the aptamer to release its complementary

oligonucleotide, and bind preferentially to the target. In the process the fluorophore is released indicating binding. Conversely, an aptamer may contain both the fluorophore and quencher at opposite ends of the strand. In solution, the aptamer is minimally structured and the two signalling molecules are kept apart, meaning the aptamer is fluorescent. Addition of the substrate will cause the aptamer to form a stable 3-D structure, possibly bringing the quencher and fluorophore close enough to interact, and preventing the generation of the signal. An aptamer beacon has been produced by Hamaguchi and co-workers by modification of the existing thrombin binding aptamer.[141] Nucleotides complimentary to the 3' end of the aptamer were added to the 5' end of the DNA aptamer along with a fluorophore, a quencher was added to the 3' end. In the absence of thrombin, the aptamer forms a stem-loop structure but the addition of thrombin causes a conformational change leading to a parting of the fluorophore/quencher and the generation of a fluorescent signal.

2.4.3.6 Surface Plasmon Resonance

Unlabelled aptamers can be used to detect a target using SPR (surface plasmon resonance). In two examples using different targets using the BIAcore SPR system the target was immobilised on a gold film chip and challenged by aptamers in solution across the flow channel.[142] As the aptamer binds to the target, it causes a mass change on the gold film which leads to response signal. Conversely, having the aptamer immobilised to the chip and the target in the solution phase should also provide a measurable response. SPR has also been used to isolate the high affinity aptamers in a modification of the SELEX approach described by Misono *et al.*[143]

2.4.3.7 Aptamer-Modified Gold Nanoparticles

Metal nanoparticles possess strongly distance dependant optical properties and have extinction coefficients (of their surface plasmon absorption bands) over a 1000 times larger than those of organic dyes. Disperse gold nanoparticles appear red, but as the particles aggregate the colour changes to purple. GNP aggregation based sensors provide sensitivity and selectivity comparable to fluorescence based techniques. GNP's modified with an aptamer have been used to detect platelet derived growth factors (PDGF) in the low nanomolar range.[144] Addition of the target protein in a solution of modified GNP's will cause a visible change, measurable with UV-vis extinction spectra.

Chapter 3: Materials and General Experimental Methods

3.1 General Reagents

All chemicals and solvents were purchased from Sigma-Aldrich, Fischer, Pharmacia, Promega, Qiagen, Biorad, Invitrogen and New England Biolabs unless specified.

3.2 Equipment

PCR reactions were carried out in a Perkin Elmer DNA thermal Cycler or a Thermo Electron Corporation PCR Sprint Thermal Cycler. Electrophoresis carried out using a Biorad Protean minigel system (protein) or for pre cast protein gels an Invitrogen XCell *Surelock*™ Mini-Cell system. Electrophoresis of DNA was carried out using a GIBCO BRL H5 system. A Delaney BR401, Sorvall® RC-5B, and a DuPont Microspin 12 were used for centrifugation. A Savant SpeedVac® Plus SC110A gyrovap was used for drying DNA and protein precipitates. UV/Vis scans were conducted on an ATI Unicam UV/Vis spectrometer (UV4).

3.3 Sterilisation

Flame sterilisation was employed when sterile conditions were required, for example the inoculation of overnight cultures. Equipment and broth were sterilised using the autoclave (121°C for 15 mins at 15 psi). All inoculations were carried out under sterile conditions.

3.4 Solutions and Buffers

3.4.1 General

Ampicillin: a stock solution (100mg/ml) was prepared, filtered through a 0.2μm membrane to sterilise and stored at 4°C. A final concentration of 100μg/ml was used in various media.

Kannamycin: a stock solution (33mg/ml) was prepared, filtered through a 0.2μm membrane and stored at 4°C. A final concentration of 33μg/ml was used in various media.

Ethidium Bromide: a stock solution (10mg/ml) was made and used at a final concentration of 5μg/ml and stored in a dark bottle at 4°C.

IPTG: A stock solution of isopropyl-β-D-thiogalactopyranoside (100mM) was sterilised by filtration (0.2μm filter) and stored at 4°C.

1x NuPAGE® MOPS SDS running buffer: 20x NuPAGE® MOPS SDS running buffer (50ml, Invitrogen) was diluted with distilled waster (950ml).

1x NuPAGE® transfer buffer: 20x NuPAGE® Transfer buffer (50ml, Invitrogen) was diluted with methanol (100ml) and distilled water (850ml).

PBS: Phosphate Buffered Saline tablets (pH 7.4, Oxoid), were dissolved in distilled water (1 tablet/100ml) and sterilised by autoclaving.

PBST: Tween-20 was added to PBS to a final concentration of 0.05%v/v.

PBSM: $MgCl_2$ was added to PBS to a final concentration 1 mM.

PBSTM: Dried skimmed milk (Marvel) was added to PBST to a final concentration of 5%w/v.

SDS running buffer: Tris-HCl (25mM, pH 8.3), glycine (192mM), SDS (1%w/v).

SDS sample buffer: Tris-HCl (0.5M, pH 6.8, 1.0 ml), glycol (2.0 ml), SDS (10% w/v, 1.6 ml), 2-β-mercaptoethanol (0.4ml), bromophenol blue (0.05%, w/v, 2.0 ml).

Tris-Cl: Tris adjusted to the required pH with hydrochloric acid (pH 7.5).

TAE: Tris-Cl (40mM, pH 7.5), acetic acid (20mM), EDTA (1mM).

TE: Tris-Cl (10mM, pH 7.5), EDTA (1mM).

3.4.2 Protein Purification Buffers

Buffer A: Tris-Cl (50mM), Triton X-100 (0.05% w/v), Imidazole (20mM), and one Complete™ Proteinase Inhibitor Cocktail tablet (Roche) per 200ml, (pH 7.5).

Buffer B: Tris-Cl (50mM), Triton X-100 (0.05% w/v), NaCl (0.5M) and Imidazole (20mM), (pH 7.5).

Buffer C: Tris-Cl (50mM), Triton X-100 (0.05% w/v), Imidazole (250mM), (pH 7.5).

3.4.3 SELEX Buffers

SELEX buffer A: Tris-Cl (50mM), NaCl (150mM), (pH 7.5).

SELEX buffer B: Tris-Cl (50mM), NaCl (1M), (pH 7.5).

SELEX buffer C: Tris-Cl (50mM), Guanidinium Chloride (6M), (pH 7.5).

Strand Separation buffer:
Tris-Cl (50mM), NaOH (0.19M).

3.4.4 ELISA/ELONA Buffers

PBS Coating buffer 10x stock: PBS (50mM), NaCl (0.14M), KCl (2.7mM), KH_2PO_4 (1.5mM), Na_2HPO_4. $2H_2O$ (8.1mM), (pH 7.2).

Diluent/wash buffer 10x stock: NaCl (0.5M), $Na_2H_2PO_4.2H_20$ (2.5mM), $Na_2HPO_4.2H_20$ (7.5mM), Tween-20 (0.05% v/v).

Blocking Buffer: Coating Buffer (x1) with 5% (w/w) Casein.

The 10x stock solutions were diluted to 1x using distilled water (USF Elga water distiller used).

3.5 Media

3.5.1 *E.coli* Media

Agar plates: Bacto-agar (15g/l) was added to the specified media with the appropriate antibiotic to prepare agar plates.

Luria Bertani broth (LB): bacto-tryptone (10g), bacto-yeast extract (5g) and sodium chloride (10g) were dissolved in 1 litre of deionised water and the pH was adjusted to 7.5 using sodium hydroxide.[148]

2YT broth: bacto-tryptone (16g), bacto-yeast extract (10g) and sodium chloride (5g) were dissolved in 1 litre of deionised water and the pH was adjusted to 7.5 using sodium hydroxide.[148]

SOC broth: bacto-tryptone (20g), bacto-yeast extract (5g), sodium chloride (0.5g), magnesium chloride (5g) and glucose (3.2g) were dissolved in 1 litre of deionised water and the pH was adjusted to 7.5 using sodium hydroxide.[148]

S-Gal/LB/amp plates: a pack of S-Gal™/LB Agar Blend (Sigma C-4478) was dissolved in 500ml of deionised water and autoclaved. The solution was cooled to around 40°C and ampicillin was added before the plates were poured.

3.6 Bacterial Cell Lines

Strain	Genotype	Description/Applications
Top 10™ (Invitrogen)	F'mcrA D(mrr-hsdRMS-mcrBC) Φ80lacZΔM15 ΔlacX74 deoR recA1 araD139 Δ(ara-leu)7697 gal/U gal/K rpsL endA1 nupG	Used For transforming DNA ligations.
DH5α[145] (Invitrogen)	F'phi80d*lacZ* delta(*lacZYA-argF*)U169 *deoR recA1 endA1 hsdR17* (rk-, m k+) *phoA supE44* lambda-*thi-1 gyrA96 relA1*/F' *proAB*+ *lacIqZdeltaM15* Tn10(*tetr*)	Used for transforming DNA ligations and storage of plasmid stock
JM109 (Stratagene)	e14–(McrA–) *recA1 endA1 gyrA96 thi-1 hsdR17* (*r*K– *m*K+) *supE44 relA1* Δ(*lac-proAB*) [F′ *traD36 proAB lacIqZΔM15*].	Used for transforming DNA ligations and storage of plasmid stock
BL21(DE3) (Invitrogen)	F⁻ omp Thsds$_b$ (r_B^- m_B^-) gal dcm (DE3)	General purpose expression host.

Table 3.1 Cell Line Information

3.6.1 Storage of Bacterial Stocks

LB or 2YT medium containing the appropriate antibiotics were used for the short-term storage of transformed *E.coli*. Colonies of bacteria were stored on inverted parafilm sealed agar plates at 4°C for up to 28 days. For long-term storage, strains were frozen at -80°C in LB or 2YT containing 30% glycerol.

3.7 DNA Vectors and Plasmids

The plasmid used for the storage of 14-3-3 γ was the GST fusion plasmid pGEX 4T1 (Amersham biosciences). 14-3-3 γ was cloned into, and over-expressed in pQE-30 (N-terminal His-tag fusion, Qiagen). TA cloning vectors pGEM-T easy (Promega) and pCR2.1 (Invitrogen) were used to clone and sequence selected aptamers.

3.8 Oligonucleotide Primers

The following oligonucleotide primers were used. Endonuclease restriction sites in bold.

3.8.1 Sequencing Primers

pQE For	5'- GGAGAAATTAACTATGAGAGG-3'
pQE Rev	5'- GTTCTGAGGTCATTACTGG-3'
pGEX For	5'-GGGCTGGCAAGCCACGTTTGGTG-3'
pGEX Rev	5'-CGGGAGCTGCATGTGTCAGAGG-3'
pGEM For	5'- TAATACGACTCACTATAGGG-3'
pGEM Rev	5'-ATTTAGGTGACACTATAGA-3'
pCR2.1 For	5'-GTAAAACGACGGCCAG-3'
pCR2.1 Rev	5'-CAGGAAACAGCTATGAC-3'

The pQE 30, pGEX, pGEM and pCR2.1 primers were used to sequence pQE 30, pGEX 4T1, pGEM T easy and pCR2.1 plasmids, respectively.

3.8.2 Primers used for cloning 14-3-3 γ

RS1	5'- GATC**GGATCC**GTGGACCCCGAGCAACTGGT-3'
	BamH I
RS2	5'- GATC**GTCGAC**TTAGTTGTTGTTGCCTTCTC-3'
	Sal I

3.8.3 Primers used for SELEX

RS9978R	5'-AG**GG ATCC** GCCT GATT AGCG ATACT-3'
	Bam HI
RS9979R	5'-BBBC CC**CT GCAG** GTGA TTTT GCTC AAGC-3'
	Pst I
RS9981R	5'-CCC**C TGCA G**GTG ATTT TGCT CAAG C-3'
	Pst I

The B in RS9979R designates Biotin from biotin phosphoramidite, this primer along with RS9978R were used in SELEX PCR. RS9978R and RS9981R were used in cloning the aptamer library for sequencing purposes.

3.9 Transformation of *E .coli* competent cells with recombinant DNA

Competent cells were transformed according to the manufacturer's instructions. DNA (up to 50ng) was added to an aliquot of competent cells and gently mixed. This was left on ice for 30 minutes before the cells were heat shocked (42°C, 30s), then placed back on ice for 2 minutes. The cells had 80µl SOC medium added and were allowed to incubate at 37°C for 1 hr whilst agitating at 220 RPM. The cells were spread on selected agar plates and allowed to grow at 37°C for 16 hours.

3.9.1 Growing cells

Overnight cultures were grown up by inoculating in sterile conditions. A sterile pipette tip was used to pick a colony from a transformed agar plate and then added to a disposable centrifuge tube (50ml, Fisherbrand) that contained LB media (10 ml) with the appropriate antibiotics. The cells were grown at 37°C for 16 hours. For larger cultures the same procedure was scaled up by the necessary factor.

3.9.2 Preparation of Plasmid DNA (Mini Prep)

Cultures were grown by inoculating 2YT broth (10ml), containing the appropriate antibiotic, ampicillin (100µg/ml), in sterile conditions, with a single transformed colony and agitating at 37°C (220rpm, 18hr). The cells were harvested by centrifugation (13000rpm, 15min, 4°C) and the supernatant discarded. The plasmid DNA was extracted using either a QIAprep® Spin Miniprep Kit (Qiagen) or ChargeSwitch® NoSpin Plasmid Micro Kit (Invitrogen) following the manufacturers guide. The DNA was always eluted with 70µl TE.

3.9.3 Digestion of DNA with restriction endonucleases

The required amount of DNA (0.2-1.0µg) was treated with the appropriate amount of endonuclease and buffer and incubated for at least 3 hours at 37°C. Blue/Orange Loading Dye (Promega) was added and the sample was subjected to electrophoresis on 1% agarose gel. The gels were visualised under UV light.

3.9.4 Electrophoresis of DNA

The required amount of agarose (Sigma), typically 1g/100ml, was added to TAE buffer and heated at 100°C until completely dissolved. The solution was allowed to cool to 55°C, followed by the addition of ethidium bromide (final concentration of 0.5μg/ml). The gel was poured into a casting cassette and allowed to set at room temperature. DNA was loaded and the gel was ran at 100 V until the adequate separation was achieved.

3.9.5 Purification of DNA

DNA was purified from agarose using a QIAquick® Gel Extraction Kit (Qiagen) following the manufacturer's instructions.

DNA was also purified directly from PCR using either QIAquick® PCR Purification Kit (Qiagen) or the ChargeSwitch® PCR Clean-Up Kit (Invitrogen).

3.9.6 Amplification of DNA

Typically each reaction contained 2 Ready-to-Go™ Taq Polymerase beads (Amersham Biosciences), 50pmoles of each primer and 100μg of the template DNA. The reaction volume was made up to 50μl with deionised water. Reactions were subjected to a 5 minute 95°C preheating step followed by up to 30 cycles of 95°C for 1 min, 54°C for 1 min and 72°C for 2 mins. Reactions were terminated with a 10 minute 72°C extension step. 5μl of the PCR mix was then checked on an agarose gel allowing the remainder to be purified.

Alternatively, high fidelity amplification was carried out using a different enzyme. The same concentrations of primers and template was used along with 5µl Pfu Turbo buffer (10X), 1.25µl 10mM dNTPs, 1µl (2.5 units) Pfu Turbo polymerase (Stratagene) and the reaction volume was made up to 50µl with deionised water.

The annealing temperature was varied depending which primers were to be used. For aptamer amplification the cycle was as follows: 95°C (1 min), 60°C (1 min) and 72°C (1.5 min).

3.9.7 Cloning of PCR Products

Direct Cloning- PCR products were directly cloned into either vector pCR 2.1-TOPO using the TOPO TA® Cloning Kit (Invitrogen) or into vector pGEM® T-Easy using the pGEM® T-Easy Cloning Kit (Promega) following the manufacturers guidelines. The relevant restriction sites had been engineered into the PCR primers allowing efficient endonuclease digest.

Indirect Cloning- Purified PCR products were digested with the relevant enzymes for at least three hours and then ethanol precipitated. The required plasmid was cut with the enzymes, ethanol precipitated and then subjected to shrimp alkaline phosphatase (Sigma-Aldrich) following the manufacturers instructions. After another ethanol precipitation, the insert and plasmid were mixed in a 2:1 ratio and mixed with high concentration T4 DNA ligase (New England Biolabs) in no more than 10µl following the manufacturers protocol. This was allowed to incubate for 16 hours at 21°C before a sample (4µl) was added to a high efficiency, competent bacterial cell line and transformed following the manufacturers instructions.

3.9.8 PCR screen

Colonies were picked from a plate, and then touched against another agar plate at a known grid position. The remaining colonies on the pipette tip were resuspended in 50µl of water. The cell resuspension was boiled for five minutes and the solution centrifuged (13K) for two minutes. A sample (5µl) was taken and used as a template in a PCR reaction to amplify the required gene using the appropriate primers. The resulting reaction was run on an agarose gel and visualised using UV light.

3.9.9 DNA sequencing

Sequencing reactions were carried out on an Electron Corporation PCR Sprint Thermal Cycler. Each sequencing reaction typically contained DNA template (5 pmoles, 4µl), primer (3.14 pmoles, 1µl), BigDye Version 4.1 (2µl; PE Biosystems, UK) and ddH_2O (2µl). The reaction was cycled 30 times at 95°C for 30 sec, 45°C for 15 sec and 60°C for 4 min. Automated DNA sequencing was performed on an ABI prism 377 DNA sequencer using the Sanger dideoxy chain termination method.[146] Sequence data was analysed using Contig-Express within the Vector NTI Advance™ V9 software package (Invitrogen).

3.9.10 DNA precipitation/ Ethanol precipitation

DNA was precipitated with an equal volume of 3M sodium acetate (pH 5.3): ethanol (0.1:2 v/v), which was mixed well with the DNA solution and kept at -80°C (1 hour). The solution was then centrifuged (13K, 30mins, 4°C) and the supernatant carefully discarded, so as to avoid agitating the pellet. The precipitated DNA was then washed with ice cold 70% ethanol (100µl), centrifuged (13K, 5mins, RT) and again the

supernatant was carefully discarded. The DNA pellet was dried under vacuum allowing resuspension in chosen buffer.

3.9.11 DNA concentration analysis

DNA (1µl) was diluted to 100µl with distilled water and the concentration was measured using an Eppindorf Biophotometer (OD_{260} x 50mg/ml x dilution factor = DNA concentration (ng/ml), OD_{260} 1 = 50 ng/ml).[147]

3.9.12 Crush and Soak

Using a clean, sterile scalpel the band of interest was excised from the gel and transferred to a sterile 1.5 ml centrifuge tube (eppendorf). A disposable pipette tip was used to crush the excised band against the side of the tube, before 0.4ml of 'elution buffer' was added (0.5M ammonium acetate, 10mM magnesium acetate, 1mM EDTA pH 8.0 and 1.0% SDS) allowing incubation at 37°C for 1 hour. The solution was centrifuged at 13K, 1 min, 4°C before careful removal of the supernatant using a drawn out Pasteur pipette. 0.9ml ice cold ethanol was added to the excised band and the solution then gently agitated at 4°C for 30 mins before centrifugation (13K, 30mins, 4°C) allowing careful removal of the supernatant. The pellet was resuspended in 200µl TE pH 7.6, then 25µl 3M Na Acetate pH 5.2 and 450µl ethanol were added. The solution was incubated for 30 mins at 4°C before another centrifugation step (13K, 30mins, 4°C) and again the supernatant was carefully removed. The pellet was rinsed with 100µl 70% ethanol, spun at 13K, 5 mins, the supernatant was removed and the pellet was resuspended in 60µl TE.

3.10 Recombinant Protein Expression and Purification

3.10.1 Protein Expression in *E.coli* host

3.10.1.1 Mini Induction

2YT broth (1ml), containing ampicillin (100µg/ml), was inoculated with a single colony and agitated at 37°C (250rpm) until an OD_{600} between 0.6 and 0.8 was reached. A control (0.5ml) was taken and the remainder was induced with IPTG (1mM) and agitated at 37°C (250rpm, 3hr). The supernatant was harvested by centrifugation (13 000, RT, 10min). The supernatant was discarded and the cell pellet was resuspended in SDS sample buffer (50µl) and distilled water (50µl), boiled (10min), then loaded (20µl) onto a SDS-Page gel (12%) and subjected to electrophoresis.

3.10.1.2 Large Scale Preparation (2L)

2YT broth (300ml), containing ampicillin (100µg/ml), was inoculated with a single colony of $(His)_6$14-3-3γ and agitated at 37°C (250rpm, 18hr). The medium was distributed evenly between 2YT broth (4 x 500ml in 2L flasks) containing ampicillin (100µg/ml) until an OD_{600} between 0.6 and 0.8 was reached. A control (0.5ml) was taken and the remainder was induced with IPTG (1mM) and agitated at 37°C (250rpm, 3hr). The cell pellet was harvested by centrifugation (5K, 15min, 4°C). The supernatant was discarded and the cell pellet was stored at -20°C until the protein was purified according to its requirements.

3.10.1.3 Purification of 14-3-3γ

Cells over-expressing 14-3-3γ were resuspended in buffer A (20ml) containing a single Complete™ Proteinase Inhibitor Cocktail tablet (Roche) and allowed to mix gently for 1 hour at 4°C. The cells were disrupted by sonication (10 pulses of 20 seconds with 20 second intervals) at 4°C and the cell debris was removed by centrifugation (15 000 rpm, 20 min, 4°C). The supernatant was passed through a 0.45μM membrane before the addition of excess nickel nitrilotriacetic acid (Ni-NTA) superflow beads (Qiagen). Following the bead manufacturers protocol, the beads were washed with 10 column volumes of Buffer B and eluted with Buffer C. Uninduced, induced, supernatant, wash and elution fractions were electrophoretically separated on a SDS-PAGE gel. Eluted 14-3-3γ was dialysed (3 times in 2L of solution) against phosphate buffer pH 7.5 using SnakeSkin membrane (MW 15 kDa, Pierce) and stored at 4°C.

3.10.1.4 Polyacrylamide gel electrophoresis (PAGE)

SDS-PAGE was used to analyse proteins on the basis of their molecular mass. The technique used was the discontinuous buffer system of Laemmeli.[148] Alternatively, proteins were analysed on precast 12% Bis-Tris Nu-PAGE® gels (Invitrogen) according to manufacture's instructions.

To analyse overexpression, a sample cell pellet was resuspended in 20μl 1 x SDS sample buffer per 0.1 unit of OD_{600} measured pre centrifugation (for example, an OD of 0.8 would mean that a 1ml pellet would be resuspended in 160μl of 1 x SDS sample buffer). The samples were denatured by boiling for 10 minutes and a sample for each (20μl) was loaded onto the gel.

Gels were visualised using Coomassie blue or GelCode Blue Stain reagent (Pierce).

3.10.1.5 Protein Concentration Determination

The protein concentration was determined according to Bradford using bovine Serum Albumin as a reference (BioRad Protein Assay, BioRAD).[149]

3.10.1.6 Mass Spectrometry

3.10.1.6.1 Electrospray Mass Spectrometry

Electrospray mass spectrometry was performed on a micromass Platform quadrupole mass spectrometer equipped with an electrospray ion source. The cone voltage was set to 70V and the temperature to 65°C. A Waters 2690 HPLC unit with a Waters 486 Tunable Absorbance Detector was connected to the mass spectrometer. Protein samples were separated on a Jupiter 5μg C-5 300A column at a constant TFA concentration of 0.01% using a linear gradient of 10-100% acetonitrile in water over 40 min with a flow rate of 0.05 ml/min. The total ion count of all ions in the range m/z 500 to 2000 and the UV chromatogram at 280nm were recorded for the reverse-phase HPLC separation. The mass spectrometer was scanned at intervals of 0.1s, the scans accumulated, the spectra combined and the average molecular mass determined using the MaxEnt and Transform algorithims of the MassLynx software. Robert Smith and Dave Clarke helped with this service.

3.10.1.6.2 Protease digestion and peptide mass mapping

The peptide mass mapping for digested gel bands were conducted using a MALDI-TOF MS (Tof-Spec 2E, Micromass). The excised band was digested with trypsin (100 μg/ml) and chymotrypsin (100 μg/ml), performed at 37 °C in chymotrypsin digestion buffer (50mM Tris-HCl, 10mM $MgCl_2$, 50mM KCl, pH 8.0), and allowed to proceed for four hours, before termination by addition of 0.05% TFA. For analysis of the reduced proteolytic digest 1 μl of the peptide mixture was removed and reduced with 100 mM TCEP. For MALDI-MS analysis oxidized and reduced peptide digests were desalted and concentrated using C18 ZipTips (Millipore Corp.). 1 μl of analyte and 1 μl of matrix solution (a saturated solution of α-cyano-4-hydroxycinnamic acid in 50% acetonitrile with 0.1% TFA) were mixed, left to air-dry on a MALDI plate and MALDI-MS results were obtained in the positive mode. Andy Cronshaw helped with this service.

3.10.1.7 CD spectrometry

Protein samples were in assay buffer (10 mM sodium phosphate, pH 7.5) throughout. CD measurements were made in the far UV (190-260 nm) region on a Jasco spectropolarimeter at protein concentrations of *ca.* 15-20 μM.

3.11 SELEX

3.11.1 Preparation of aptamer library

The DNA was prepared using solid phase synthesis on an ABI Expedite™ 8909 Nucleic Acid Synthesis System.

Phosphoramidites (Sigma-Aldrich) were dissolved in anhydrous acetonitrile to a standard concentration (0.067M). The 5'-DMTr group of the 5'-terminal base was removed with 3% trichloroacetic acid in dichloromethane. The next phosphoramidite in the sequence was activated by reaction with 0.45M tetrazole and reacted with the free 5'-OH of the previous phosphoramidite. Coupling was 30 seconds per base. Acetic anhydride and N-methylimidazole were used to cap free hydroxyl groups left unreacted. The phosphite triester was oxidised to the stable pentavalent phosphotriester by the use of 0.1M iodine in THF/pyridine/water thus completing a single cycle.

The aptamer library is as follows:

5'-CCGAAGCTTAATACGACTCACTATAGGGATCCGCCTGATTAGCG

ATACT-[40N]-ACTTGAGCAAAATCACCTGCAGGGG-3'.

The 40 random bases were produced from a single pot containing an equimolar concentration of the four available phosphoramidite bases.

After complete synthesis the aptamer library was cleaved from the support with concentrated ammoniuim hydroxide at room temperature (16hr). The pool was purified by HPLC and stored lyophilised.

Aptamer generation carried out with the help of Professor Tom Brown and Dr Dorkus Brown (University of Southampton, Chemistry Department).

3.11.2 γ-^{32}P labelling DNA

All work was carried out in a controlled radiation room, behind a Perspex shield. 500pmoles of the aptamer library (20μl) had γ^{32}P-ATP (30μci, 3μl), ligase buffer (10X, 5μl), 20 units T4 PNK (2μl) and water (19μl) added. This was incubated at 37°C for 15 mins before the addition of ATP (100mM, 1μl). The solution was incubated for a further 45 minutes at 37°C, before running on gel.

The 12% acrylamide/7M Urea gel was prepared gel was prepared following the protocol in Maniatis[145]. A loading buffer was prepared with 0.05% bromophenol blue and 0.05% xylene cyanol made up in 500μl H_2O, which then had formamide (500μl) added. 50μl of this buffer was added to the 50μl labelled DNA and ran on the gel. The bromophenol blue runs with an approximate mass of 15 oligonucleotides and the xylene cyanol with a mass of around 40 oligonucleotides. After the bromophenol blue band ran off, the gel was removed from the tank and stored overnight at –20°C wrapped in saran wrap.

The following day the gel was carefully removed from the cassette, and moved into a suitable autoradiography cassette. The gel was then subject to exposures of 20s, 40s and 2min, and each film was developed. Dark bands were visible showing the migration of the labelled aptamer library. The relevant band was removed following the "crush and soak" method (**Section 3.9.12**) and diluted in 50μl of buffer.

3.11.2 ssDNA/Protein Selection

The 14-3-3 γ stock solution was maintained at a concentration 14.2mg/ml. 8µl of this stock (0.1mg, 2.15 x 10^{15} molecules) had 20µl of the ^{32}P γ-radiolabelled aptamer library added (1.5 x 10^{14} molecules). 22µl of sterile TE was added to the solution and then this was allowed to agitate gently at 4°C for 16 hours on a blood rotator.

Ni^{2+}-Sepharose beads (Amersham Biosciences) were washed according to the manufacturers instructions. 10µl of the bead solution (capacity to bind 0.4mg His-tagged protein, 4X excess) was washed into 50µl sterile TE solution. This added to the aptamer-protein solution and allowed to gently agitate for a further hour at 4°C.

The solution was spun at 6.5K for 2 mins and the supernatant was carefully removed and collected as fraction A0. 50µl of 'SELEX Buffer A' was added to the beads and this was allowed to agitate for 5 mins on the blood rotator. Again, the solution was spun at 6.5K for 2 mins and the supernatant was collected as fraction A1. The wash/spin procedure was repeated a further 3 times with 'SELEX Buffer A' (fractions A2-A4). 50µl of 'wash buffer B' was added and the wash/spin procedure was repeated a further 4 times (fractions B1-B4). 50µl of 'SELEX Buffer C' was added to the beads and this was allowed to agitate for 1 hour at 37°C before the supernatant was collected. This was repeated with a further 50µl 'elution buffer C' for 30 mins, and the fraction was pooled with the previously collected sample, labelled C1. Sample C1 contains the denatured ssDNA to be used in further rounds.

Aliquots of all fractions had their radiography counts per minute (CPM) read using a TRI-CARB 2100TR scintillation counter (Perkin-Elmer).

3.11.3 Preparation for PCR

The ssDNA was eluted in a high concentration guanidinium chloride solution which would inhibit PCR. The ssDNA was desalted using a Supelco supelclean LC-18 SPE 3ml tube, prepared following the manufacturers instructions using a peristaltic pump. To fraction C1, 500µl of sterile H_20 was added. This solution was then added to the desalting column, and washed with 10ml of sterile water, ensuring there was enough solution to keep the beads immersed. The column was removed from the pump and placed into a clamp. Acetonitrile/DCM (75:25) (600µl) was added to the beads and allowed to pass through by gravity. This was collected in 2 x 300µl fractions. The organic solution was evaporated using a gyrovac (30 mins, 42°C), and the pellets were resuspended in 2 x 20µl sterile TE fractions, before being pooled together.

3.11.4 α-^{32}P dCTP labelling DNA

All work was carried out in a controlled radiation room, behind a Perspex shield. Redivue deoxycytidine 5' [α-^{32}P]- triphosphate, triethylammonium salt was used to label DNA (Amersham Biosciences, AA0075).

A sample of the aptamer library (20µl) had primers 00979R (5.3µl, 500 pmoles) and 00978R (8.6µl, 500 pmoles) added, along with 5'[α-^{32}P]dCTP (1µl, 10µCi), water (15µl) and two ready-to-go taq™ polymerase beads added. The solution was amplified by PCR; 95°C for 5mins then 12-18 cycles (95°C-30s, 54°C-20s, 72°C-60s), and ran on an agarose gel for visualisation and purification using the QiaQuick gel purification system.

3.11.5 Separating the dsDNA

0.5ml Streptavidin magnetic beads (New England Biolabs) were prepared following the manufacturers instructions. The equilibrated streptavidin magnetic beads were added to the PCR pure product and allowed to gently agitate on a blood rotator for 1 hour. The beads were washed 6 times with 0.5ml wash buffer according to the manufacturer's instructions, then dsDNA was separated by the addition of 2 washes of dsDNA strand separation buffer (300µl), 15 min incubations at room temperature. The supernatant contained the starting library for the next round of selection, while the 3' biotinylated strand remained immobilised to the streptavidin beads.

The library was eluted in a buffer that would have been inhibitive for the next round of selection. To prepare the ssDNA, it was ethanol precipitated (**Section 3.9.10**). ssDNA was resuspended in 50µl PBSM and the final concentration was calculated using the extinction coefficient at Abs. 260nm (OD^{260} x 33mg/ml x dilution factor = ssDNA concentration (ng/ml), OD^{260} 1 = 33 ng/ml).

3.12 Aptamer Determination

3.12.1 Surface Plasmon Resonance Analysis

Surface plasmon resonance analysis of aptamers was carried out on a BiacoreX (Biacore, Sweden) using an NTA chip (Biacore, Sweden). The running buffer used was PBSM and the washing buffer used in between injections was glycine (10mM, pH 2.0). The temperature was maintained at 25°C, and unless stated elsewhere, the

flow rate was kept at 20µl/min. All aptamer samples were heated to 95°C for two minutes and cooled on ice before application.

The NTA chip contains a matrix of carboxymethylated dextran pre-immobilized with nitrilotriacetic acid (NTA). The NTA surface was charged with Ni^{2+} by the addition of $NiSO_4$ (0.25M, 5 minutes), followed by chelation of recombinant $(His)_6$14-3-3γ (1mg/ml, 5µl/min 10 minutes). Aptamer responses were recorded by addition of aptamer (10µM (unless otherwise stated), 3 minutes).

3.12.2 Aptamer Affinity Purification

500µl of sample (either MBH or Ovine CSF spiked with 14-3-3 (10µl, 14.2 mg/ml)) had 10µl of 100µM biotinylated aptamer added and was mixed with gentle agitation for 2 hours at room temperature. 50µl of magnetic streptavidin beads (Roche) were washed from their ethanol solution into 50µl wash buffer (Tris-Cl (50mM, pH 7.5), NaCl (150mM)). The beads were added to the protein aptamer solution and allowed to gently agitate (1hr, RT). The solution was applied to a magnet and the supernatant was removed and collected. The beads were washed 5 times with 100µl wash buffer, and the resultant beads were collected and resuspended in 50µl wash buffer. For analysis, 40µl from; flow through, each wash fraction and the collected beads had 3X SDS sample buffer added (20µl) before heating at 95°C for 5 minutes. The samples were spun at 13K for 2 mins and 40µl from each was loaded onto two 4-12% Bis-Tris gel (Invitrogen), 20µl per gel. One gel was used to stain with GelCode blue, the other followed the procedure for a standard Western Blot.

3.12.3 ELISA

Doubling dilutions of $(His)_6$14-3-3 γ were applied in triplicate to an Immulon 4HBX 96-well plate (Thermo-Electron Corporation). All wash steps were carried out on a MRW strip washer (Dynex technologies) using the set wash programme (six 200µl/well wash cycles with 30 second soak periods between washes) using ELISA wash buffer.

An Immulon plate was coated with K-19 antibody (Santa-cruz biotechnology (100µl in 10ml of coating buffer, 100µl per well), 1 hour at 37°C then at 4°C overnight. The plate was washed as directed then blocked by the addition of casein (5% w/v) in coating buffer (1hr, 4°C) 100µl per well, before another wash cycle, followed by the addition of the 14-3-3 protein. The 14-3-3 stock (14.2mg/ml) had 60µl removed and was diluted down to 4mg/ml with diluent buffer. 2µl was added to 398µl diluent buffer and heated to 55°C for ten minutes. This solution (fraction 1) had 3 x 50µl aliquots applied to the plate and 200µl was added to 200µl diluent buffer (doubling dilution) to make fraction 2 which had 3 x 50µl fractions added to the plate and had 200µl added to 200µl diluent buffer to make fraction 3 and henceforth. When all protein fractions are applied to the plate, the plate was incubated at 37°C for 1 hour before a further wash step. K-19 anti-14-3-3 antibody (rabbit polyclonal IgG) diluted 1:1000 was added to each well (50µl), incubated for 1 hour, before a further washing step followed by addition of goat anti-rabbit HRP conjugate antibody, diluted (1:10 000) (50µl), which was allowed to incubate for 1 hour. The plate was subjected to a further washing step before addition of 3,3,5,5 Tetramethylbenzidine(TMB) substrate, which was incubated for 15 minutes, before the reaction was quenched with the

addition of 0.18M H_2SO_4(100µl). The absorbance at 450nm measured on a Wallac victor II spectrophotometer.

3.12.4 Enzyme Linked Oligonucleotide Assay (ELONA)

Identical concentrations (0.25mg/ml) of $(His)_6$14-3-3 γ were applied to a 96 well Immulon-4HBX plate (Thermo Electron Corporation) and the aptamers used were applied in triplicate with doubling dilutions. Identical wash steps were carried out as per the ELISA procedure.

The plate was coated with K-19 antibody (100µl in 10ml coating buffer) for 1 hour at 37°C then stored at 4°C overnight. After washing, the plate was blocked by the addition of casein (5% w/v) in ELISA coating buffer (1hr, 4°C) and was subjected to a further washing step before addition of the 14-3-3 protein. 176µl of 14-3-3 (14.2mg/ml) was added to 10ml of wash buffer and 100µl was added to each well followed by incubation at 37°C for 1 hour before a further wash step. The biotinylated aptamer (400µl, 100µM) was heated to 95°C, cooled to room temperature and subjected to doubling dilutions in diluent buffer, following the same procedure as ELISA. 50µl of each aptamer concentration was applied in triplicate to the plate and incubated for 2 hours at 37°C before unbound aptamers were washed off. Streptavidin horseradish peroxidase was then applied to each well (1:10 000, 100µl) incubated for 30min at 21°C before washing. TMB (100µl) was added to each well and left at room temperature for 15 mins before the reaction was quenched with the

addition of 0.18M H_2SO_4(100µl). The absorbance of each well was checked at 450nm on a Wallac victor II spectrophotometer.

3.12.5 14-3-3 isoform analysis by ELONA

An Immulon-4HBX plate pre-coated with K-19 (100µl in 10ml Coating Buffer) and blocked with casein (5% w/v in blocking buffer) had 14-3-3 isoforms loaded. Each isoform (0.5mg/ml) was heated to 60°C for 5 minutes before addition to the plate twice in triplicate (50µl per well) (two aptamers were getting analysed thus A:1-3 for one aptamer and A:4-6 for another aptamer for that 14-3-3 isoform). After a 1 hour incubation period (37°C) and subsequent wash, aptamer S16-8 or S16-2 was added (10µM, 50µl), pre heated to 95°C for 5 minutes and cooled on ice, and incubated for 2 hours at 37°C (S16-2 was added to wells A-H, 1-3 and aptamer S16-8 A-H, 1-6). The plate was subjected to a further wash step before the addition of streptavidin horseradish peroxidase, applied to each well (1:10 000, 100µl) and incubated for 30min at 21°C before washing. TMB (100µl) was added to each well and left at room temperature for 15 mins before the reaction was quenched with the addition of 0.18M H_2SO_4(100µl). The absorbance was checked at 450nm on a Wallac victor II spectrophotometer.

3.12.6 Protein Blot analysis with S16-8

Each recombinantly expressed 14-3-3 isoform (4µg) was made up into 40µl of 1X SDS Sample buffer. The samples were boiled for 5 mins before addition to two Bis-

Tris 4-12% Gels (20µl per gel). The protein samples were separated electrophoretically, one gel was stained with gel code, and the other transferred to PVDF membrane (Amersham) following the western blotting protocol. The membrane was blocked using casein (5% w/v in PBST, 16hr, 4°C) before washing steps similar to the western procedure. The western procedure was copied except instead of the primary antibody, biotinylated S16-8 was used (diluted to 100µM in 10ml PBST) and the secondary antibody was streptavidin-HRP (1:10 000 in PBST).

3.12.7 Gel Filtration Analysis

Analysis carried out on a Pharmacia AKTA purifier (GMI) using gel filtration column 16/60 Superdex^{TM} 75 (Dextran-agarose column, 120ml, Amersham Biosciences).

The column had a flow rate of 1.2 ml/min using running buffer: Tris-HCl (pH 7.5), NaCl (50mM) and Triton X 100 (0.05% v/v). Absorbance was recorded at 220nm, 260nm and 280nm.

The controls of 14-3-3 γ alone (25µl 14.2 mg/ml, diluted in 975µl running buffer) and S16-8 alone (25µl, 100µM, diluted in 975µl running buffer) were recorded.

S16-8 (25µl, 100µM) was added to $(His)_6$14-3-3 γ (25µl, 14.2mg/ml) and diluted to 1ml using running buffer. The solution was agitated on a blood rotator (1hr, room temperature) before addition to the column.

3.12.8 Aptamer sequence alignment

Aptamers were aligned using either Align X in the Vector NTI 9 suite or ClustalW. Both programs use a ClustalW alignment algorithm.

3.12.9 Aptamer phylogenetic tree

A phylogenetic tree was automatically generated upon preparing a sequence alignment with Align X in the Vector NTI 9 suite. The tree was generated using the sequence distance method and the Neighbour Joining Algorithm.[166]

Chapter 4: Results and Discussion

4.1 Cloning, Expression and Purification of 14-3-3 γ

The expression and purification of 14-3-3 proteins has been carried out in a number of earlier studies. High expression has been achieved using 14-3-3 fusion proteins.[150]

At the start of this study, a library of all the human 14-3-3 genes and some other mammalian 14-3-3 genes cloned into a range of different expression vectors, was made available by Professor Alastair Aitkin (Division of Biomedical & Clinical Laboratory Sciences, University of Edinburgh). Of the seven human isoforms, six were available as GST fusions, and epsilon, was available as a maltose binding protein fusion. Baxter and co-workers have previously shown that 14-3-3 isoforms β, ε, γ, η are all detected in the CSF of patients with sporadic CJD.[60] However the γ isoform is most abundant in the disease state and so it seemed logical to select an aptamer for this isoform.

In the previous studies, the mammalian 14-3-3 γ gene had been cloned into a GST expression vector, pGEX-4T1 (Figure 4.3); affording the fusion plasmid pGEX-4T1/14-3-3γ. GST, glutathione-S-transferase, is a soluble enzyme that catalyses the conjugation of reduced glutathione in a detoxification pathway in cells. GST gene fusions have been extensively used to co-express target proteins. These fusions confer useful properties: (a) they tend to be well expressed, thus many hard to express proteins cloned downstream from the GST gene are often better expressed as a GST fusions; (b) they frequently confer solubility to otherwise insoluble targets; (c) GST provides an excellent carrier protein for crystallisation and (d) the GST domain provides a useful ligand for the immobilisation (GST affinity chromatography) of the fusion protein, and for detection of the fusion protein using anti-GST antibodies.[151]

However for aptamer selection the GST 14-3-3 γ fusion would be an unsuitable substrate, GST is expressed with a mass of 28 kDa, thus trying to select aptamers to 14-3-3 γ (also 28kDa) when fused to GST would inevitably lead to many aptamers specific for the GST sequence. Although in principle, counter-selection steps could be used to eliminate GST specific aptamer enrichment, it would involve extra steps in the SELEX procedure and perhaps eliminate good 14-3-3γ binding aptamers from the library. In addition, a proportion of the 14-3-3 γ protein surface area would be sterically hindered by the positioning of the GST protein, preventing aptamer access and thus reducing the number of potential binding sites. There would also be a small possibility that some aptamers could interact at the GST/14-3-3 γ interface leading to false results when the SELEX process was complete: such aptamers might work well on an assay with the 14-3-3/GST fusion, but not with the wild type 14-3-3.

4.1.1 Cloning 14-3-3 γ

ATGGTGGACC	CCGAGCAACT	GGTGCAGAAA	GCCCGGCTGG	CCGAGCAGGC
GGAGGGCTAC	GACGACATGG	CCGCGGCCAT	GAAGAACGTG	ACAGAGCTGA
ATGATCCACT	GTCGATGAGG	AACGAAACCT	TCTGTCTGTG	GCCTACAAGA
ACGTTGTGGG	GGCACGCCGC	TCTTCCTGGA	GGGTCATCAG	TAGTATTGAG
CAGAAGACGT	CTGCAGACGG	CAATGAGAAG	ATTGAGATGG	TCCGTGCGTA
CCGGGAGAAG	GTAGAGAAGG	AGTTGGAGGC	TGTGTGCCAG	GATGTGCTGA
GCCTGGTGGA	TAACTACCTG	TACAAGAATT	GCAGCGAGAC	CCAGTACGAG
CGCAAAGATT	TGTACCTGAA	GATGAAAGGG	GACTACTACC	GCTACCTGGC
TGAAGTGGCC	ACCGGAGAGA	AAAGGGGCGA	CGTGGTGGAG	TCCTCCGAGA
AGGCCTACAG	CGAACGCGAG	ATCAGCAAAG	AGCACATGCA	GCCCACCCAC
CCCATCCGAT	TAGGTCTGGC	TCTTAACTAC	TCCGTCTTCT	ACTATGAGAT
CCAGAACGCC	CCAGAGCAAG	CGTGCCACTT	GGCAAGACCG	AGTTCGAGGA
GGCCATCGCC	GAGCTTGACA	CCCTCAACGA	GGAGTCCTAC	AAGGACTCCA
CGCTCATCAT	GCAGCTCCTC	CGCGACAACC	TCACGCTCTG	GACGAGCGAC
CAGCAGGACG	ACCACGATGG	GGAGAAGGCA	ACAACAACTA	A

Figure 4.1: 14-3-3 γ gene. The gene containing 742 bases

MVDREQLVQKA RLAEQAERYD DMAAAMKNVT ELNEPLSNEE RNLLSVAYKN
VVGARRSSWR VISSIEQKTS ADGNEKKIEM VRAYREKIEK ELEAVCQDVL SLLDNYLIKN
CSETQYESKV FYLKMKGDYY RYLAEVATGE KRATVVESSE KAYSEAHEIS KEHMQPTHPI
RLGLALNYSV FYYEIQNAPE QACHLAKTAF DDAIAELDTL NEDSYKDSTL IMQLLRDNLT
LWTSDQQDDD GGEGNN

Figure 4.2: 14-3-3 γ amino acid sequence. The protein contains 247 amino acids. Information available at UniProtKB/Swiss-Prot entry P61981.[152]

The 14-3-3 γ gene was cloned from the GST fusion plasmid however tagging the 14-3-3 γ protein with a smaller fusion is attractive for several reasons. Tagged proteins can be attached to resin, facilitating protein purification. It also seemed an attractive idea to use a resin bound protein for this SELEX approach. The 'His' tag system, where a base sequence encoding five or six histidine residues is expressed at the 5'- or 3'- end of an ORF is one of the most commonly used tagging systems in current use. The fact that His tags facilitate purification and are relatively small and thus generally do not interfere with protein folding appears to recommend their use in this type of experiment.

As described in Chapter 2, many partitioning methods have been used for SELEX including; filter absorption, non-denaturing gel electrophoresis, immunoprecipitation and centrifugation (in the case of entire cells).[153] Target immobilisation on chromatography beads has also been used and this allows counter selection elution steps to further improve the specificity of the nucleic acid/ligand interaction. Target immobilisation was used successfully by Bock and co-workers in selecting aptamers to the classic thrombin aptamer.[105]

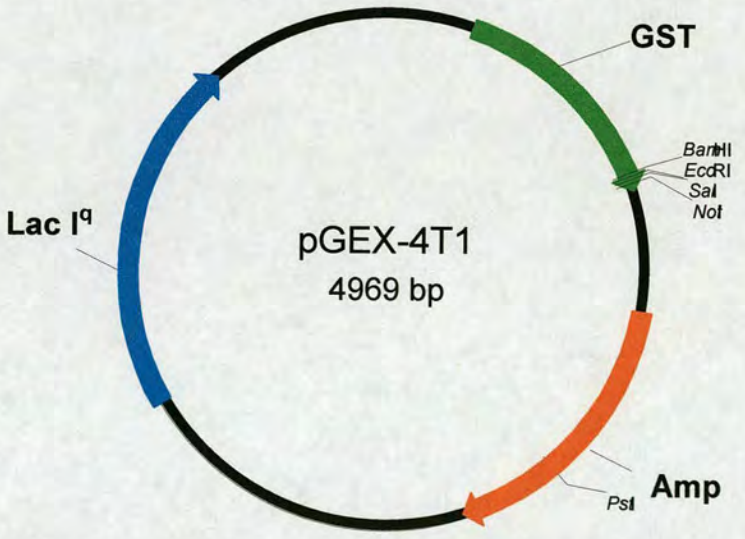

Figure 4.3: Plasmid pGEX 4T1. The ampicillin resistance gene (Amp) is present on the construct and the 14-3-3 gene was cloned between the *BamH* I and *Sal* I restriction sites.

The 14-3-3 γ gene was amplified from the pGEX-4T1/14-3-3 γ template by PCR using the forward primer "RS01" (incorporating a *Bam HI* restriction site), and reverse primer "RS02" (engineered with a *Sal I* site). The PCR product was then ligated into the N-terminus His tag expression vector pQE-30 (**Figure 4.4**) using the *Bam HI* and *Sal I* restriction sites. The resulting plasmid was named pQE30/14-3-3γ and DNA sequencing of the insert from the forward sequencing ('type III/IV') primer for pQE vectors confirmed that the gene had been faithfully transcribed by PCR.

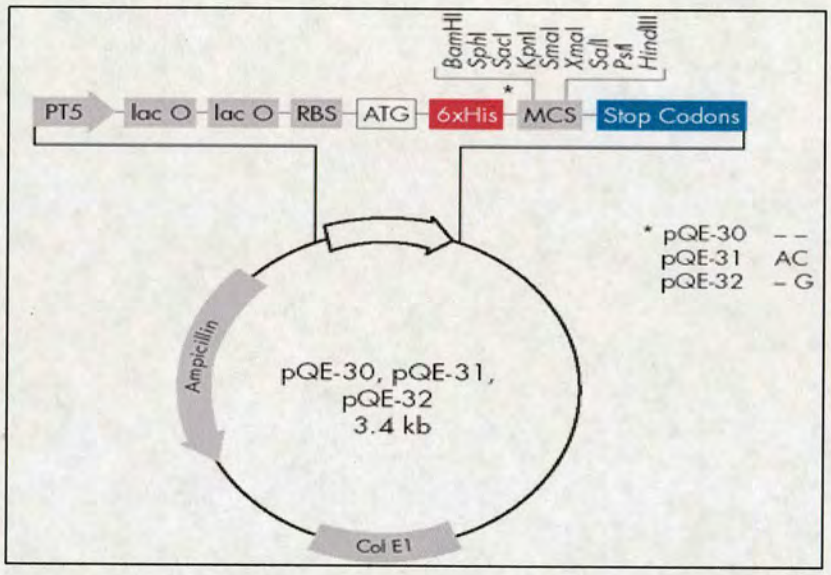

Figure 4.4: Plasmid pQE-30. The plasmid was digested at the *Bam* HI and *Sal* I sites allowing the 14-3-3 γ gene to be inserted in the MCS. Plasmids pQE-31 and pQE-32 contain additional amino acids between the 6 x His sequence and the MCS, used to ensure the gene is inserted 'in-frame'.

Trial expression was performed in various *E. coli* cells (DE3 lysogens). Optimum protein expression was obtained using the BL21 (DE3) strain, induced with isopropyl-1-thio-β-D-galactopyranoside at 37°C.

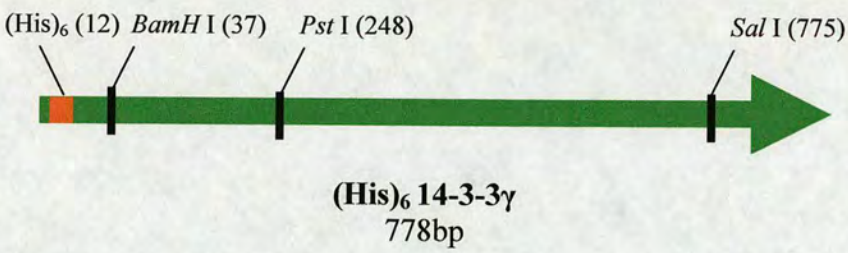

Figure 4.5: Schematic Representation of cloned pQE30/14-3-3γ gene. The endonuclease restriction sites present in the cloning region of pQE30 are highlighted.

4.1.2 14-3-3 γ Purification

The pQE30/14-3-3γ cell lysate was fractionated by IMAC (immobilised metal affinity chromatography) using a nickel-NTA resin. The protein was eluted using 250 mM imidazole, and was immediately diluted 1:1 with 50mM PBS and dialysed against this buffer. SDS-PAGE analysis indicated that the 14-3-3 γ purity was ≥ 90%. The final yield of 14-3-3 γ was typically around 14 mg/L of cell culture.

M**RGSHHHHHH GS**VDREQLVQ KARLAEQAEG YDDMAAAMKN

VTELNEPLSN EERNLLSVAY KNVVGARRSS WRVISSIEQK TSADGNEKIE

MVRAYREKVE KELEAVCQDV LSLVDNYLYK NCSETQYERK

DLYLKMKGDY YRYLAEVATG EKRGDVVESS EKAYSEREIS KEHMQPTHPI

RLGLALNYSV FYYEIQNAPE QACHLAKTEF EDAIAELDTL NEESYKDSTL

IMQLLRDNLT LWTSDQQDDH DGGEGNNN

Figure 4.6: pQE30/14-3-3γ amino acid sequence. The sequence contains an additional eleven amino acids (shown in bold) including the 6 x His residues, to the wild type 14-3-3 γ sequence.

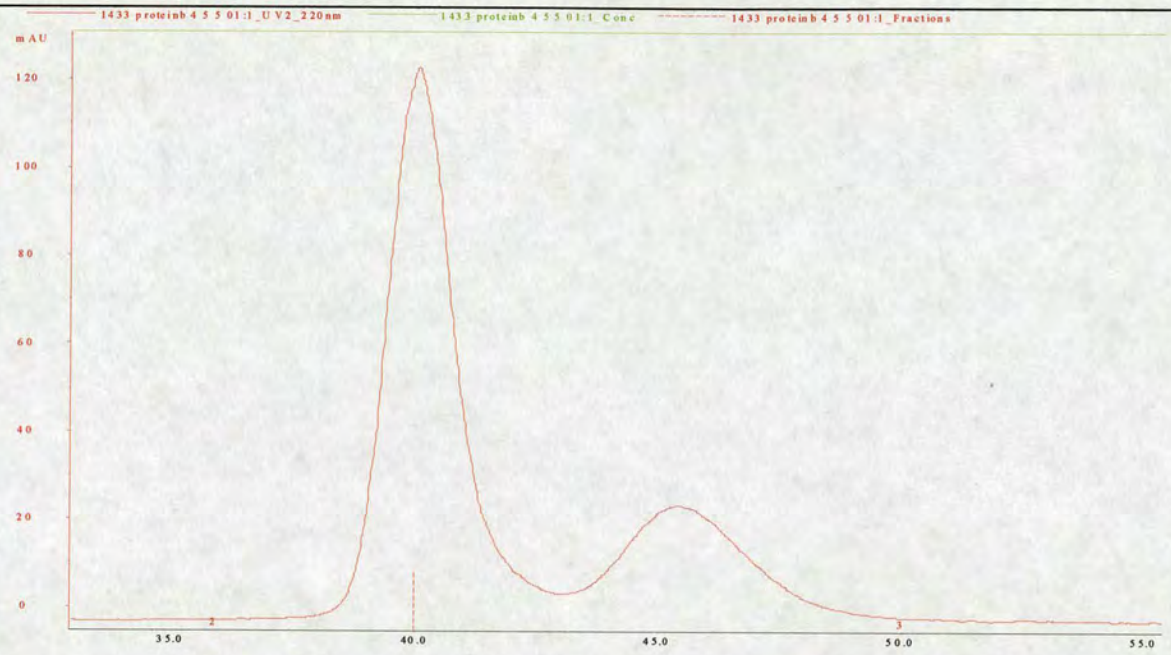

Figure 4.7: Chromatogram of 14-3-3 IMAC. The chromatogram shows two peaks for 14-3-3γ. Both peaks were identified on SDS-Page to confirm the estimated purity of the expressed protein suggesting that they correspond to the monomeric and dimeric forms.

4.1.3 Characterisation of Purified $(His)_6$ 14-3-3 γ

Prior to starting lengthy, time consuming SELEX selection of aptamers it was important to ensure that the overexpressed protein was correctly folded.

The collected peak fractions were run on an SDS-Page to confirm the identity of a species with similar molecular weight to 14-3-3 protein (**Figure 4.8**). A further SDS-Page gel was transferred to nitrocellulose for antibody probing. Rabbit produced K-19 (also known as SC629; Santa Cruz shown in **Table 1.3**) was used as the primary antibody with biotinylated goat anti-rabbit HRP (horse radish peroxidase) the secondary. Treatment of the membrane with TMB allowed imaging.

The western blot clearly shows that the expressed protein, is recognised by the anti 14-3-3 antibody; K-19. The K-19 antibody is labelled as an anti-β 14-3-3 antibody,

however as mentioned previously, the antibody which has an N terminal epitope, is not isoform specific allowing use in detection of the γ isoform. The early epitope is not a problem with detecting the protein as the proteins are denatured as part of the process of running the SDS-Page gel.

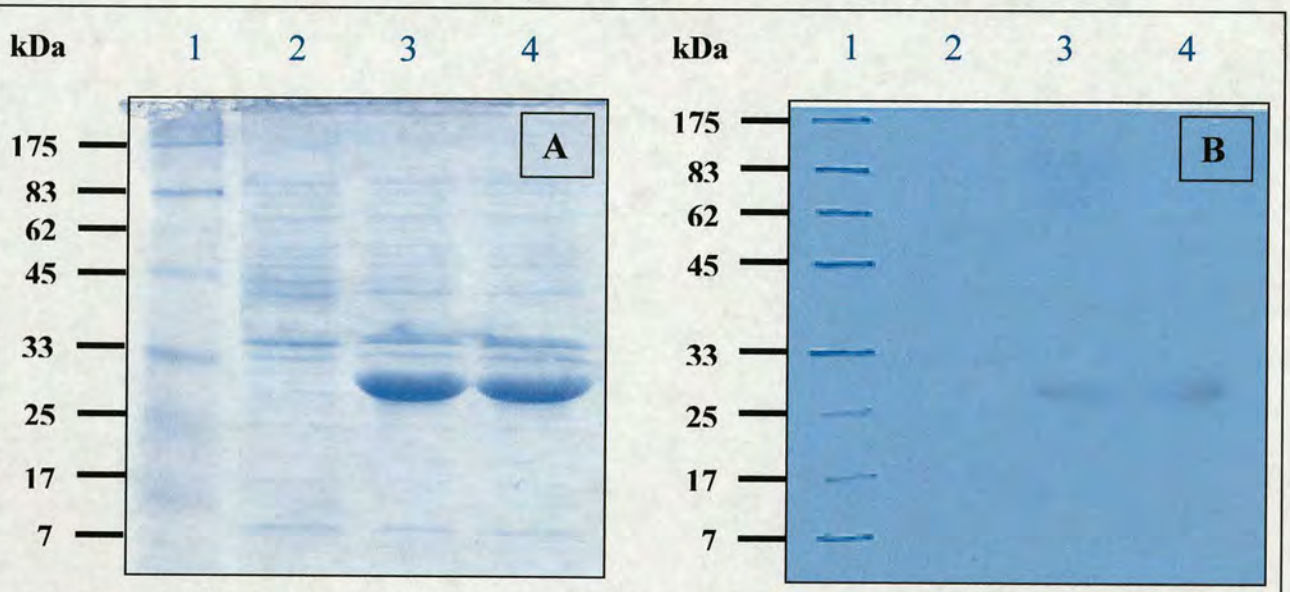

Figure 4.8: SDS-Page and Western blot of 14-3-3γ. **A** shows SDS-PAGE carried out under denaturing conditions. *Lane 1*, marker P7708, *Lane 2* Control pQE30/14-3-3γ uninduced, *Lane 3* Induced pQE30/14-3-3γ clone 1 and *Lane 4* Induced pQE30/14-3-3γ clone 2. **B** a 1 minute exposure of an identical gel transferred to nitrocellulose and Western blotted using anti 14-3-3 antibodies.

4.1.4 Mass Spectrometry of 14-3-3 γ

Electrospray MS revealed the presence of one species with a molecular weight 29639.8 ± 2.34 (**Figure 4.9**), corresponding to full length 14-3-3 γ with 6 histidine residues attached (29936.13 Da). A further experiment was set, a tryptic digest of the protein sample followed by MALDI-MS confirmed that the digested protein was 14-3-3, peptide fingerprinting used the Mascot search engine (www.matrixscience.com). The MALDI-TOF spectrum is not shown, however the digested peptides used in fingerprinting are as follows:

816 – (LAEQAER) 903 – (VISSIEQK) 1080 – (YLAEVATGEK) 1189 – (DSTLIMQLLR) 1277 – (EHMQPTHPIR) 1644 – (NVTELNEPLSNEER) 2167 – (TAFDDAIAELDTLNEDSYK)

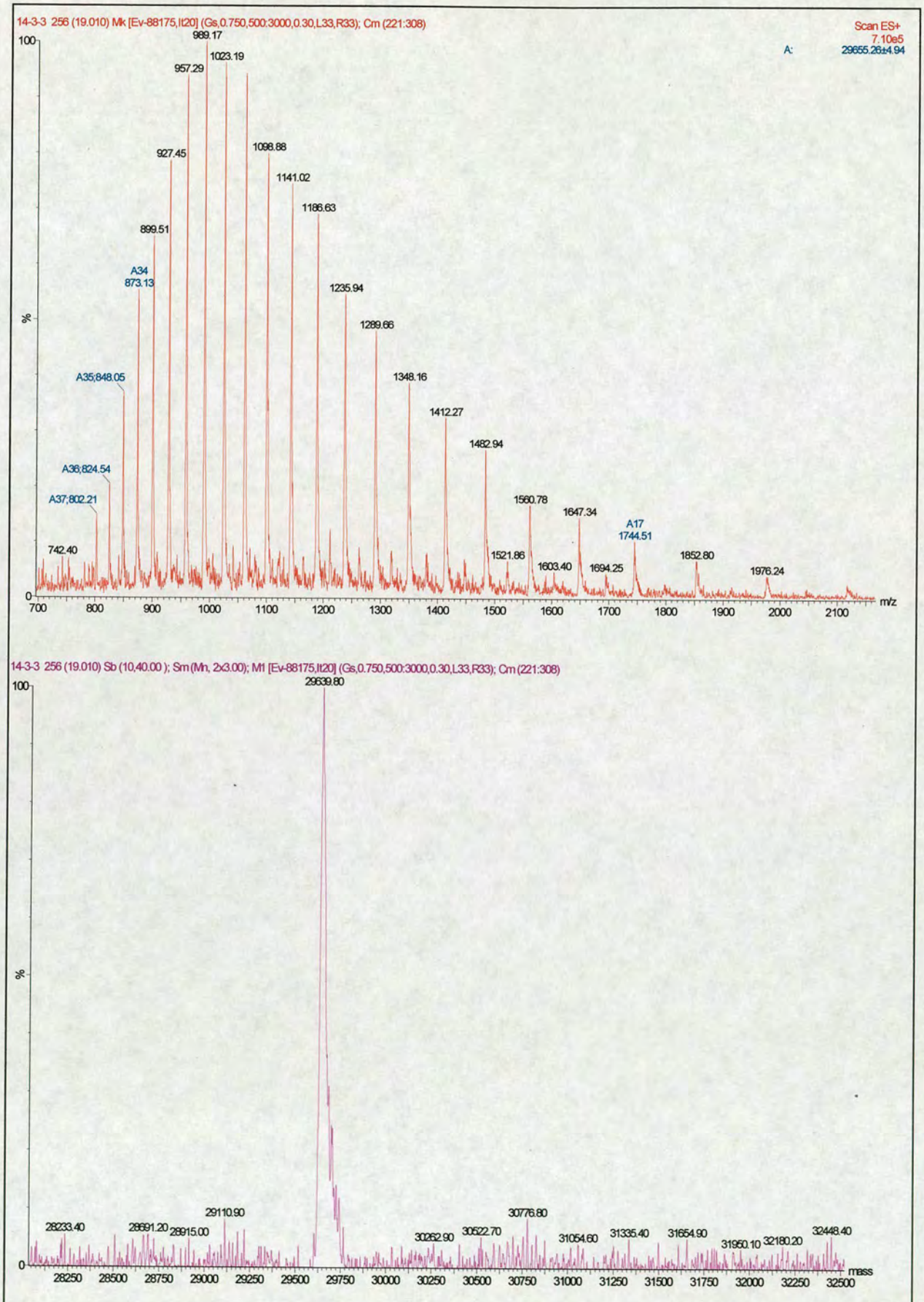

Figure 4.9: LC-MS of (His)$_6$14-3-3γ. 14-3-3 analysed by electrospray mass spectrometry. The calculated molecular weight (29639 Da) corresponds to full length recombinant (His)$_6$14-3-3γ.

4.1.5 Circular Dichroism of 14-3-3 γ

Circular dichroism (CD) was used to estimate the secondary structure of the expressed recombinant $(His)_6$ 14-3-3 γ. Far UV region (180-240 nm) CD analyses the peptide bond adsorption; features such as α-helixes and β-sheets give rise to patterns of characteristic shape and magnitude of CD spectrum. For more information on circular dichroism the reader is advised to read the review by Kelly and Price.[154]

The family of 14-3-3 proteins are highly α-helical molecules (see **Chapter 1**). The observed spectrum for $(His)_6$14-3-3 γ was typical of a protein that is predominantly α-helical, characterised by a far UV scan that has a trough between 200 and 230nm. Analysis of the spectrum using the programme DICHROWEB showed that recombinant protein was 70% α-helical and 4% β-sheet, similar to the results obtained by Robinson *et al.* in their analysis of the secondary structure of other 14-3-3 proetein isoforms.[156, 157]

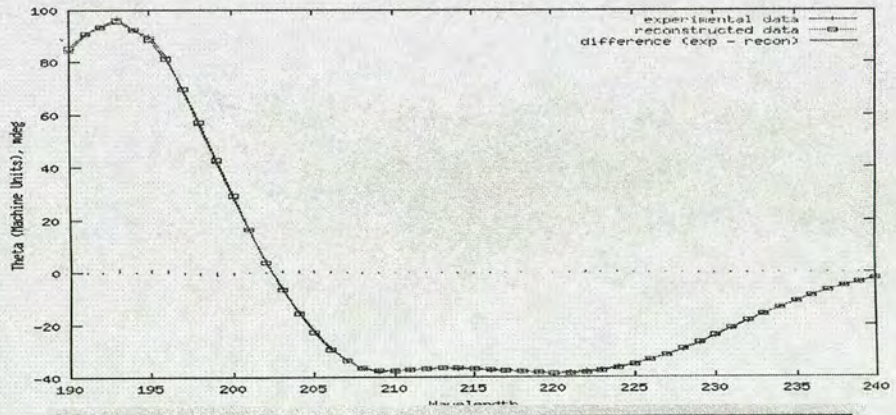

Helix1	Helix2	Strand1	Strand2	Turns	Unordered	Total
0.50	0.20	0.02	0.02	0.07	0.18	0.99

Figure 4.10: Circular Dichroism of 14-3-3 γ. CD results processed by DICHROWEB[155], suggest that recombinant 14-3-3 γ is 70 % α-helical and 4 % β-sheet.[156]

4.2 Recognition of 14-3-3 γ by antibodies

As further confirmation that the conformation adopted by the bacterial recombinant $(His)_6$ 14-3-3 γ was identical to that of the mammalian protein, the interaction of the un-denatured protein with several commercially available antibodies was evaluated.

4.2.1 Surface Plasmon Resonance

Surface Plasmon Resonance was used to study the real time interactions of His-tagged 14-3-3 γ with commercially available antibodies on a Biacore® *X* system. 14-3-3 γ was immobilised via the N-terminal hexa-histidine residues to a Ni-NTA chip and the interaction with four different anti-14-3-3 antibodies examined. Antibodies; K-19, C-16 (also known SC629 and SC731, both Santa Cruz), KK 1106 (PAN antibody) and SLAK, were used. C-16 is the only one of these which is 14-3-3 γ specific.

In Biacore systems, the surface plasmon resonance (SPR) phenomenon occurs when polarised light, strikes an electrically conducting gold layer at the interface between media of different refractive index: the glass of a sensor surface (high refractive index) and a buffer (low refractive index).[157] The polarized light is directed toward the glass face of the sensor surface, reflected light is detected within a Biacore system. The SPR signal can be explained by the electromagnetic coupling of the incident light with the surface plasmon of the gold layer. The plasmon is influenced by a layer just a few nm over across the gold-solution interface, causing a reduction in the intensity of the reflected light, producing a sensorgram. The signal is directly proportional to the size of the ligand molecule immobilised.

Each SPR chip contains two flow cells; fc1 is for reference and fc2 for measurement. Initially the protein is loaded onto both flow cells, before an antibody solution is

passed through only fc2. When the antibody binds the protein there is a change of mass and indirectly, the mass change between fc2 and fc1 gives a response difference shown on a sensorgram. A high mass antibody molecule, will give a greater response than that of a low mass antibody molecule, therefore to get a clear picture, both the molecular mass and concentration of antibody solution must be known.

All the antibodies used had measurable association with the recombinantly expressed protein. The association curves were reproducible, under specific washing conditions and were concentration dependent. The SLAK antibody was most sensitive (1:2000 dilution, 350RU), or at least gave the largest response difference under very dilute conditions. KK 1106 (PAN) antibody gave a response at higher concentrations, however the response curves were unusual (1:40 dilution, 100RU). K-19 gave intermediate responses and appeared to be the best binder albeit at relatively high concentrations (1:20, 100RU); C-16 was only effective at high concentrations (1:5, 100RU).

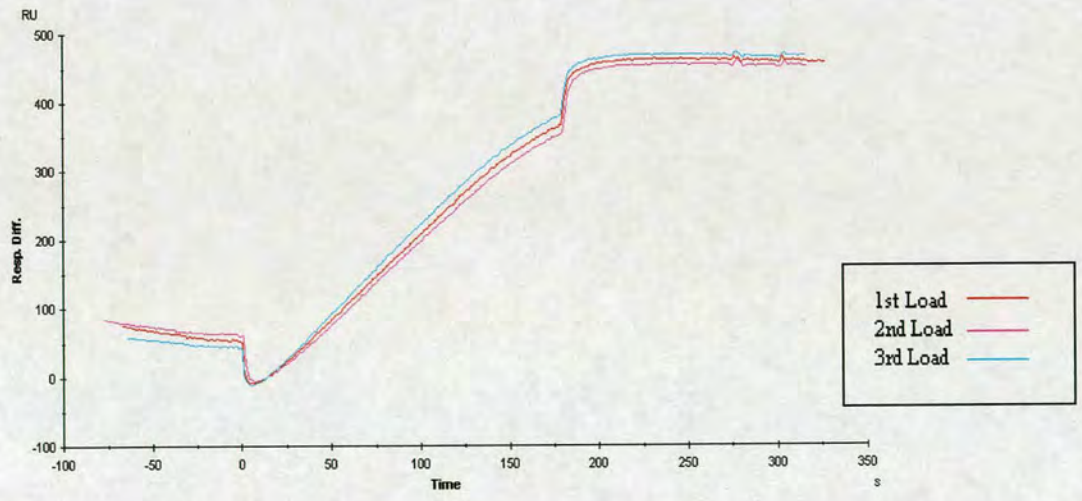

Figure 4.11: Chromatogram of repeatable results using antibody KK 1106. 3 30µl injections with flow rate 10µl/min are shown. Glycine buffer (10mM, pH 2.0) used in washing steps.

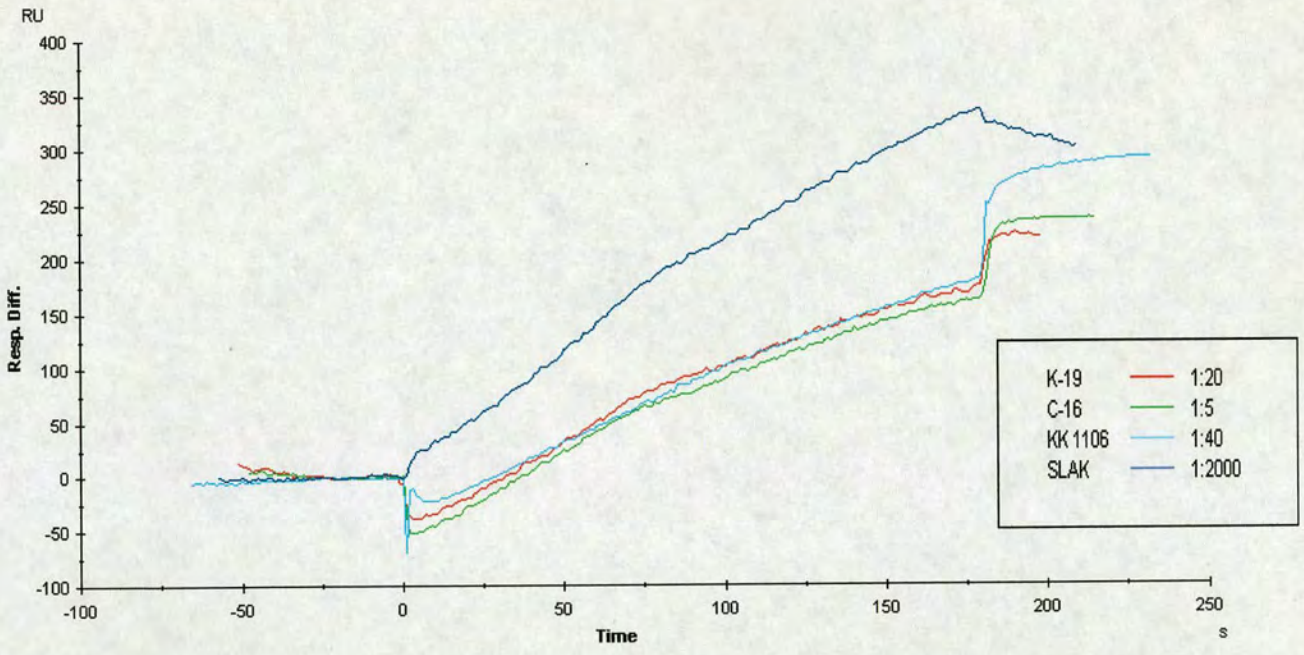

Figure 4.12: Comparison of the four anti 14-3-3 antibodies by SPR. All had 30µl injections, with a flow rate of 10µl/min.

Figure 4.12 provides compares four of the available anti 14-3-3 antibodies and provides a basis for possible comparison of a successful aptamers against the best antibody alternatives. The heavily diluted SLAK antibody gave the greatest response difference. Diluting SLAK any lower than 1:2000 led to inconsistent responses.

Since the recombinantly expressed 14-3-3 γ had the correct DNA sequence, had a secondary structure (by CD) consistent with that of published 14-3-3 isoforms to date and interacted with expected antibodies, it seemed likely that the protein was correctly expressed and folded.

4.3 SELEX

4.3.1 The SELEX Approach

In Chapter 2 I describe the outlining principles of the SELEX process, a technique that appears, at first sight, to be technically simple. It should be noted however, that in the 13 years following the discovery of aptamers and this technique of selection, only around 40 protein-aptamer studies were published. Given the potential of aptamers in protein detection and diagnostics, this indicates that the selection process available is not technically simple to perform. Indeed aptamer selection has only recently become routine using high throughput methods as shown by Cox *et al.* using automated selection techniques.[111]

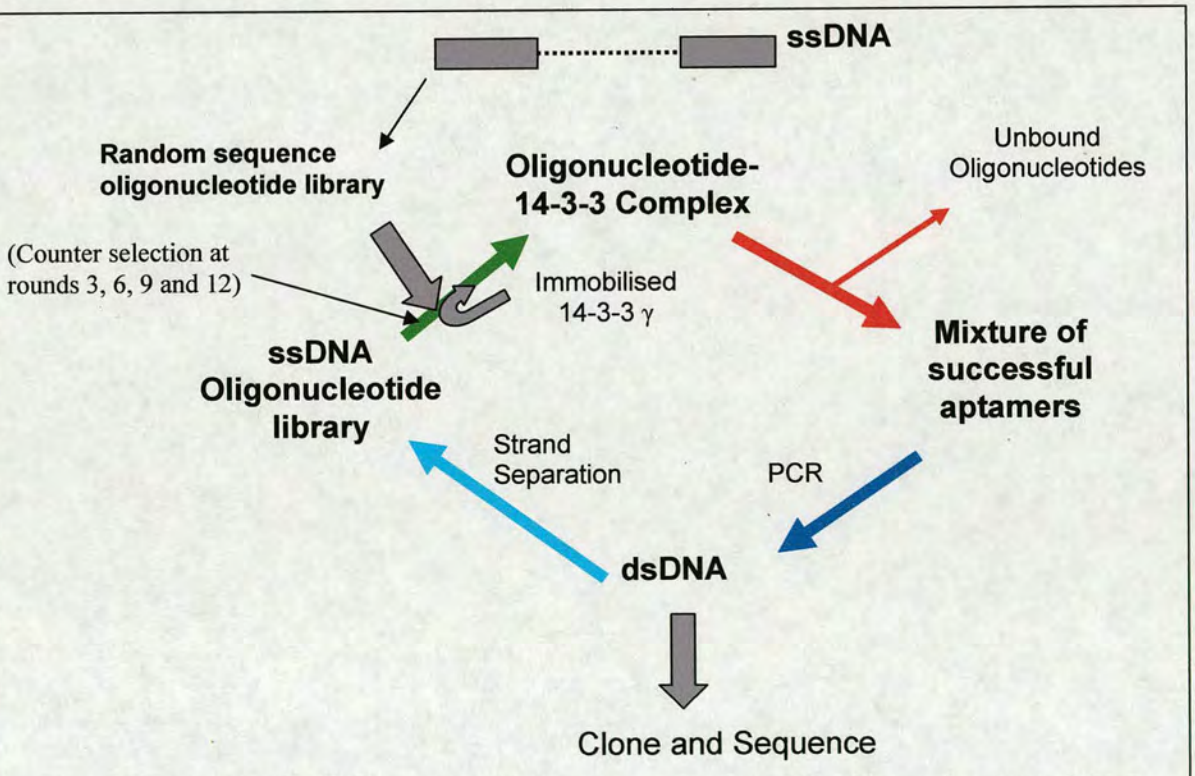

Figure 4.13: The SELEX cycle with counter selection. The Figure is adapted from Figure 2.3, the counter selection steps have been added to the diagram for clarity.

An alternative approach was taken in the study presented here, adapted from the method used by Murphy *et al.* Murphy and co-workers selected DNA aptamers to thyroid transcription factor 1 (TTF1), the protein was expressed as a his-tag fusion and was immobilised on Ni-NTA magnetic beads, a magnet was used to separate those aptamers bound to the protein and those still free in the solution.[158]

Attaching the target protein to an insoluble resin by his-tagging affords a SELEX procedure performed without the use of robotics and gives a procedure that appears robust and susceptible for any protein capable of immobilising on a resin.

The starting library and primers were similar to the library used by Green *et al.* in selecting aptamers to vascular endothelial growth factor.[159] The library **"RS997R"** was prepared using the solid phase phosphoramidite method first described by Sinha *et al.*[160]

5'-CCGAAGCTTAATACGACTCACTATAGGGATCCGCCTGATTAGCG

ATACT-[40N]-ACTTGAGCAAAATCACCTGCAGGGG-3'.

Figure 4.14: RS997R; Aptamer Staring library. The synthesised pool contains a completely randomised 40 base cassette – [40N], flanked by known primer annealing regions containing restriction sites, *BamH* I and *Pst* I.

An equal mixture of the four phosphoramidites was used to generate the random positions. Here it should be noted that there is some argument about the ratio necessary for *completely* random incorporation, Szostak has suggested an ACGT ratio of 1.5:1.5:1:1 and this has been disputed by James.[104] The different ratios required to achieve complete randomness is a feature of the synthetic chemistry involved, minor differences between laboratories would be expected. For that reason an equal mixture of the bases was used in the random cassette.

The PCR primers used were **"RS9978R"** 5'-AGGG ATCC GCCT GATT AGCG ATACT-3', the biotinylated reverse primer **"RS9979R"** 5'-BBBC CCCT GCAG GTGA TTTT GCTC AAGC-3' where B designates Biotin from biotin phosphoramidite and **"RS9981R"** 5'-CCCC TGCA GGTG ATTT TGCT CAAG C-3', the unbiotinylated reverse primer used in cloning and sequencing. The primers were designed with restriction sites, *Bam* HI in the 5' primer and *Pst* I in the 3' primer. The incorporation of these sites was based on the contingency that they could be used for excision and cloning in the event of problems with TA cloning.

The Green library template was used as there seemed little point in redesigning new flanking regions when previous art has shown this to be a successful starting library. As discussed earlier, starting libraries must be carefully designed to minimise the risk of the starting pool having intra-molecular structures. The 5' flanking region provided scope for RNA aptamers instead of ssDNA aptamers by containing a T7 promoter sequence for in vitro transcription. A contentious point of using the library/primers of Green *et al.* is that their 3' primer contains 3 biotin molecules (for use in strand separation). Strand separation is generally carried out using biotin to immobilise the dsDNA on a streptavidin resin before disruption of the hydrogen bond and collection of the free strand (although asymmetric PCR can be used). Generally a single biotin molecule appears sufficient to carry out this step successfully, so using 3 biotin molecules may seem over excessive, although Green might argue that using 3 biotins still enabled a successful SELEX process.

The ssDNA library was purified on an 8% polyacrylamide/7 M Urea gel. The band was visualised under UV light, excised from the gel, eluted by the crush and soak method (**Section 3.9.12**), ethanol-precipitated and pelleted by centrifugation. The pellet was resuspended in phosphate-buffered saline supplemented with 1mM $MgCl_2$.

The first selection had approximately 500pmoles of 5' γ-^{32}P end-labelled (for the radio-labelling technique see 3.1.17), purified on a 12% acrylamide/7M Urea gel, visualised by autoradiography and the radioactive band was eluted and resuspended in total 50µl TE. The concentration of DNA µg/µl was estimated using UV absorbance at 260nm and the specific activity recorded in dpm/µg. 20µl of the radiolabelled DNA stock (around 200pmoles) was heated to 95°C for 5 minutes, chilled on ice for 1 minute before addition to 8µl 14-3-3 γ (2nmoles). In the early cycles of SELEX, a molar excess of protein molecules over DNA molecules was used, ensuring that any aptamers that have a chance of binding should have the opportunity. In the first cycle, a 10X molar excess of protein over ssDNA. This ratio of target to aptamer is in line with the recommendations made by Irvine *et al.* who examined the effects of different target:DNA ratios in some detail.[161]

The solution containing the protein and radiolabelled DNA was allowed to equilibrate with gentle agitation overnight at 4°C, followed by 30 minute incubation at room temperature. Ni-NTA beads previously equilibrated with SELEX buffer A, were added to the mixture and allowed to gently agitate at room temperature for 1 hour. The 1.5ml microcentrifuge tube containing the solution was gently spun to collect the beads and the supernatant carefully removed. The beads were subjected to further washing steps before the bound DNA was eluted and transferred to PCR tubes.

After completion of each cycle during the early rounds of SELEX, the radioactivity in each wash fraction was measured by scintillation counting. The results are shown in Figure 4.15 for rounds two through to four. The early results show that there appeared to be an enrichment up until the 4th cycle as each elution fraction (C1) contained more radioactive counts than the previous cycle. However, care must be taken in interpreting this as a positive result, the counts recorded were relatively low,

not significantly above that of the control. Further rounds of SELEX gave less impressive scintillation counts and less apparent enrichment (see **Table 4.1**).

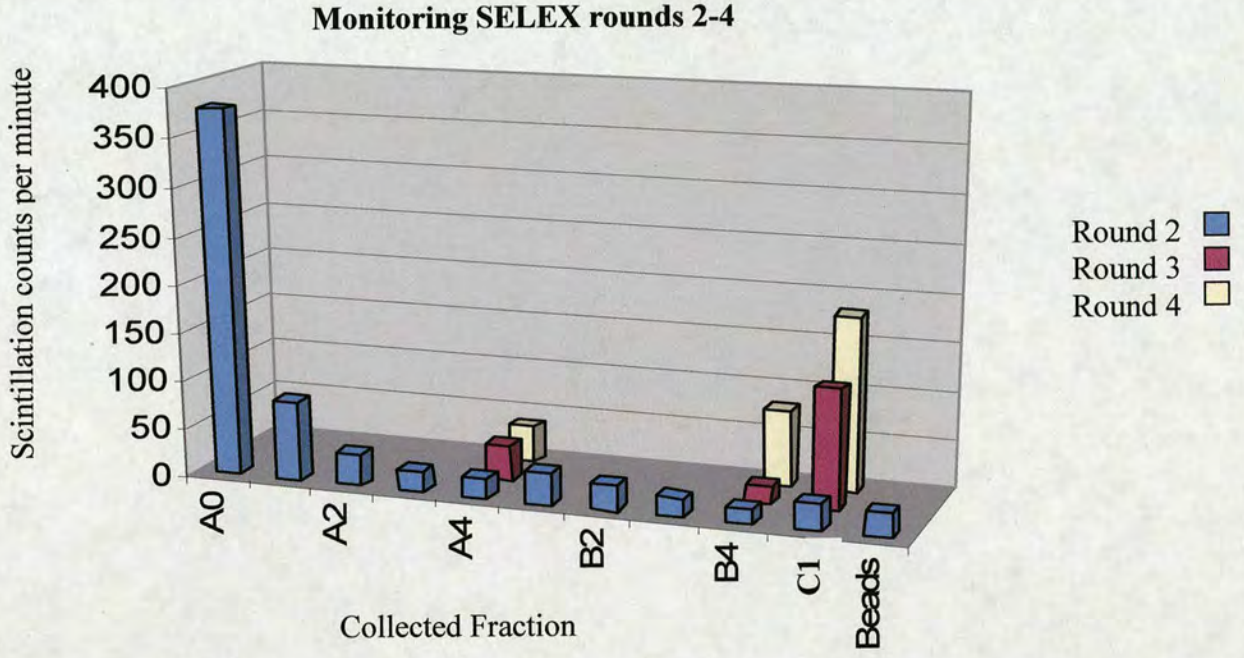

Figure 4.15: Scintillation results for SELEX rounds 2-4. Supernatant fraction A0, wash fractions A1-A4, B1-B4 and the eluted fraction C1 are shown against the counts per minute for three rounds.

4.3.2 SELEX Counter Selection

An important step during the SELEX process is that of counter selection, eased by target immobilisation. Counter selection was used to remove aptamers that bind Ni-NTA beads after rounds 3, 6, 9 and 12. A 50µl aliquot of a10% slurry of Ni-NTA beads, pre-equilibrated into PBS-T, was added to the ssDNA in PBS-T and incubated with mild agitation for 20 minutes. The beads were discarded and those aptamers contained in the supernatant were collected and used in the next round of selection. Similar counter selection steps were taken in cycles 5 and 10 against His-tagged ferric binding protein C, removing any aptamers that bind the hexahistidine residues.

Counter selection provides an opportunity to improve specificity of ligand binding. Counter selection steps against other 14-3-3 isoforms should ensure that successful aptamers were 14-3-3 γ specific.

4.3.3 Development of the Radiolabelling technique

In their studies on selecting aptamers to VEGF, Green *et al.* incorporated a new radiolabel by having the 5' primer γ-^{32}P end-labelled after each selection round thus affording a labelled pool of ssDNA after each PCR step. End-labelling DNA is time consuming and involves separation using an acrylamide/urea gel, requiring patience, skill and using hazardous chemicals that it would be better to avoid. An alternative method was developed in which the labelling of DNA was carried out during the PCR step. [α-^{32}P]-dCTP was added, to the PCR cocktail, affording radiolabelled cytosine to be incorporated into the aptamer pool during amplification, thus generating radiolabelled ssDNA. This procedure has the potential of saving time without compromising the integrity of the SELEX procedure.

Cycle	A4	B4	C1
1	20	16*	28
2	39	20*	125
3	37	79*	181
4	63	40	33
5	22	22	28
6	87	24	61
7	36	25	78
8	44	28	93
9	33	20	28
10	20	18	37
11	22	19	28
12	68	36	48
13	18	23	20
14	27	28	20
15	39	22	33
16	39	28	43

Table 4.1: SELEX scintillation results. The Cycle number is shown along with the counts per minute from fractions A4 (wash 4, low salt), B4 (wash 4, high salt) and C1 (eluted aptamer fraction). Fractions B4 for cycles 1, 2 and 3 used low salt buffer (*), as the conditions were deliberately gentle in the early stages. Care must be taken in interpreting these results as they are not significantly above the control.

The results shown in Table 4.1 led to a revision of the planned SELEX procedure. It had been hoped that there would be an almost exponential enrichment of aptamers, shown by a continuous increase in the counts in the supernatant fraction C1. What actually happened was that the counts in this fraction remained almost constant throughout. Some of the apparent trends can be accounted for by the experimental protocol; the counts increase gradually from cycle 1 to 3 but then decline at cycle 4 before gradually increasing again through to cycle 8. This may be accounted for by cycles 1 to 3 using only low salt buffer in the washing steps, whereas cycle 4 onwards introduced a further high salt washing step leading to more stringent selection. The

recovered aptamer counts increase gradually again from 4 to cycle 8, after which no apparent trend was clear. The experimental volume/procedure used in cycles 4 to 8 were identical, trying to enrich the library without tampering with conditions. By cycle 8, the recovered aptamer radioactivity in the supernatant was apparently again on the increase which was taken as an opportunity to introduce further stringency steps, and change the ratio of aptamer to protein. Up until cycle 8, the protein/aptamer ratio always had the protein molecules in a 10 molar excess but at this point things changed.

During the SELEX protocol, it became clear that measuring the radioactivity in the supernatant was not giving useful results and those that were obtained may not have been entirely related to the concentration of ssDNA contained within the eluted pool. A factor could be that during the PCR, where the radioisotope was incorporated, only the cytosine residue was labelled and although perhaps this might be a small effect, the evolution may have been pushed towards cytosine deficient probes.

The results obtained from radioactive monitoring indicate that the particular method used, in this case, does not give a good indication of the fraction of aptamers making it through each selection round.

It is noteworthy that Murphy *et al.* chose not to monitor cycle by cycle but instead to clone a sample after 5, 10 and 15 cycles and check to see if SELEX was driving the library towards a consensus sequence. They found no enrichment after 5, modest enrichment after 10, and they stopped enrichment after 15 cycles. Many SELEX experiments have followed a similar idea of intermittent in vitro monitoring rather than step by step.

The SELEX method used was continued and from cycles 9 onwards, the concentration of ssDNA was also recorded pre and post selection by checking the absorbance value at 260nm, the method favoured by Murphy *et al.*

Cycle	Pre ssDNA nmoles	Post ssDNA nmoles	% Retained
9	16.8	0.00204	0.0121429
10	12.4	0.00272	0.0219355
11	4.91	0.00302	0.0615071
12	1.68	0.001	0.0595238
13	0.585	0.0123	2.1025641
14	0.065	0.009	13.846154

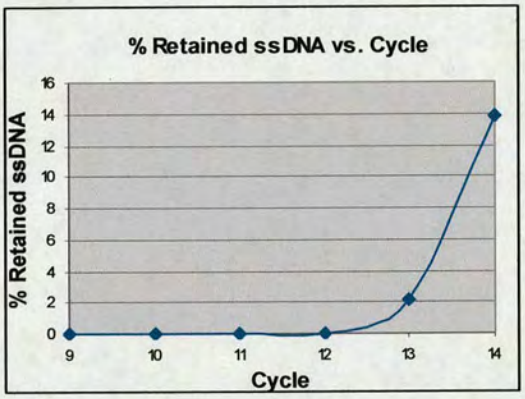

Table 4.2 and Figure 4.16: Absorbance results for SELEX cycles. The absorbance was calculated for ssDNA pre and post selection to allow calculation of the % of ssDNA retained after the washing steps.

It is noteworthy that Vianini and co-workers report similar results to those obtained here in their process of selecting DNA aptamers to L-tyrosinamide.[162] They recorded the percentage of DNA recovered at the end of each cycle and found that as the cycles were manipulated, the percentage recovered were directly affected, similar to the results shown in **Table 4.1**.

4.3.4 Clone Analysis

After eleven rounds, post PCR dsDNA was cloned and sequenced to analyse for a possible consensus motif. The dsDNA obtained at the end of cycle 11 was subjected to PCR with primers "RS9979R" and "RS9981R". The DNA was purified and an aliquot of the aptamer pool dsDNA was ligated into pGEM T Easy vector, a TA cloning vector. The resultant plasmids were used to generate *E.coli* clones which were spread on S-Gal plates. Thirty-four positive colonies were picked, grown overnight and their DNA was extracted and digested with *Pst* I and *Nco* I. The restriction results are shown in **Figure 4.18**.

Of the 34 clones, 14 contained an insert with the approximate size of an aptamer from the library (114 bp's). Each of these was sequenced using the pGEM forward and reverse primers. The sequence alignment of ten aptamers, those with readable data are shown in **Figure 4.19**.

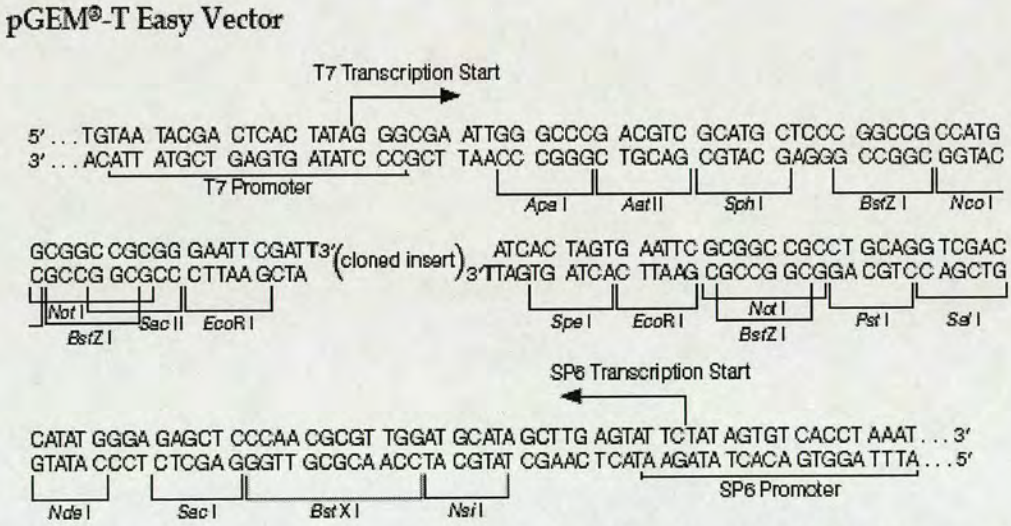

Figure 4.17: The promoter and multiple cloning site of pGEM-T Easy Vector. The dsDNA from PCR had A' overhangs allowing ligation into the T overhang region. Analysis used the *Nco* I and *Pst* I restriction sites.

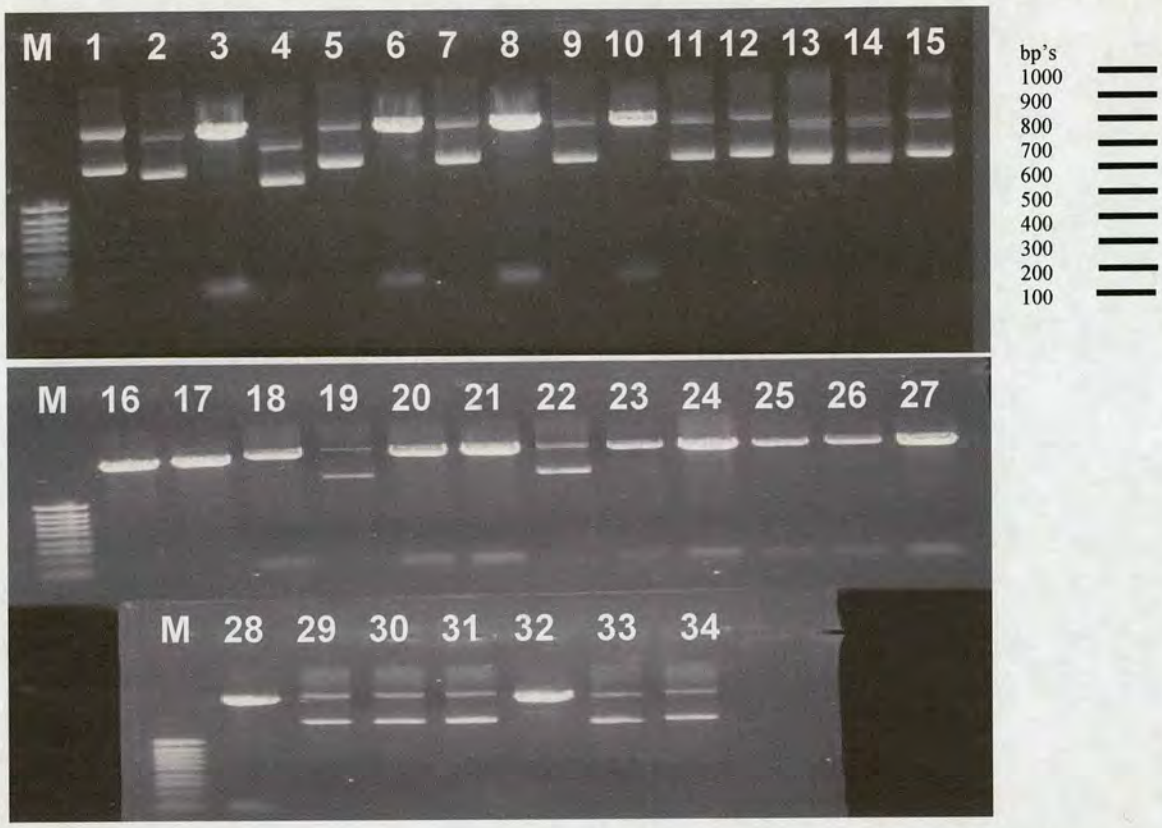

Figure 4.18: Digested cycle 11 clones. An aliquot of dsDNA was used after the completion of cycle 11 for SELEX analysis by ligating into a cloning plasmid then transformed allowing screening of plasmids. 34 clones were picked, 14 of the plasmids contain inserts around 120bp's, used for DNA sequencing. The marker is shown on the right (not to scale).

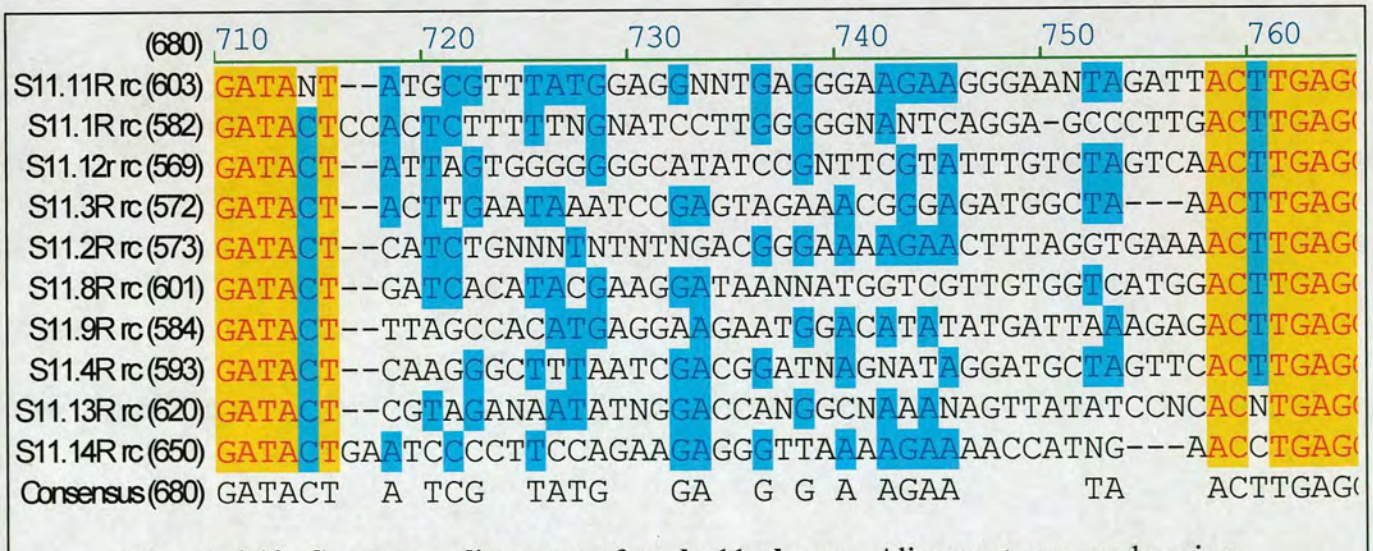

Figure 4.19: Sequence alignment of cycle 11 clones. Alignment was made using the ClustalW algorithm, little conservation appears amongst the clones. The data contains a number of undefined residues. [163]

As the PCR products could be inserted into the vector in either direction, sequencing of flanking regions around the 40 base randomised regions provided information of the aptamer direction, useful for alignment. The data presented from the cycle 11 consensus in **Figure 4.19**, allowed a clone to be produced using what ClustalW interpreted to be a consensus pattern. The sequencing data contained many unidentified residues; however enough information was contained to test for enrichment. As discussed in **Chapter 2**, aptamers containing G-quartets are relatively common motifs from ssDNA SELEX, and indeed a couple of the clones sequenced contained G-rich sequences. However, taking the whole library into consideration, there was nothing to suggest that, guanine was being favoured over any other base in the selection process. It should be noted that successful T-rich libraries have also been produced so not having a G rich library is not necessarily indicative of a bad result.[115]

At this stage I elected to evaluate one of the sequences using SPR. The interaction of a cycle 11 aptamer with $(His)_6$14-3-3γ was examined using the starting library 00977R as a control. SPR had already been used to evaluate antibodies against 14-3-3, thus substituting the antibody for an aptamer would provide a quick method for analysis. The clone S11.11 contained the majority of the consensus motifs within, thus the consensus aptamer S11 was based largely on this particular clone.

The sequence to be cloned for SPR analysis, named S11 is shown in **Figure 4.20**. The clone is similar to sequence S11.11, with unknown residues replaced by the consensus base.

GATACTATGCGTTTATGGAGGATTGAGGGAAGAAGGGAACTAGATTAC

Figure 4.20: Aptamer S11. The residues highlighted in red are those from the consensus motif, the green residues are the bases copied from the cloning vector and blue residues are engineered bases that were not contained within the original sequence S11.11.

The ssDNAs anticipated structure was computed using mfold software provided by Zuker and Turner.[164] The folded DNA structure (Appendix I) of the cycle 11 aptamer was encouraging as the clone appeared to have the potential to adopt a definite tertiary structure. Successful aptamers have, in general, a strong folded structure similar to tRNA, and as such this clone was synthetically produced.

S11 was compared against the starting library (00977R) using SPR (shown in Figure 4.21). The analysis of this clone used a BiacoreX containing a Ni-NTA chip loaded with expressed recombinant 14-3-3 γ [7]. This result suggests that by the end of cycle 11, the aptamers selected, or at least the apparent consensus sequence represented by S11, shows an improved affinity towards the 14-3-3 γ which was an encouraging result as it showed that the selection was being driven towards aptamers that bind to the expressed 14-3-3 γ. The cycle 11 clone has a definite early association as can be seen in the increase in response units from around 0 to 125 RU. The starting library shows no association to the 14-3-3 γ chip. The initial spike is related to the two samples being in different buffers.

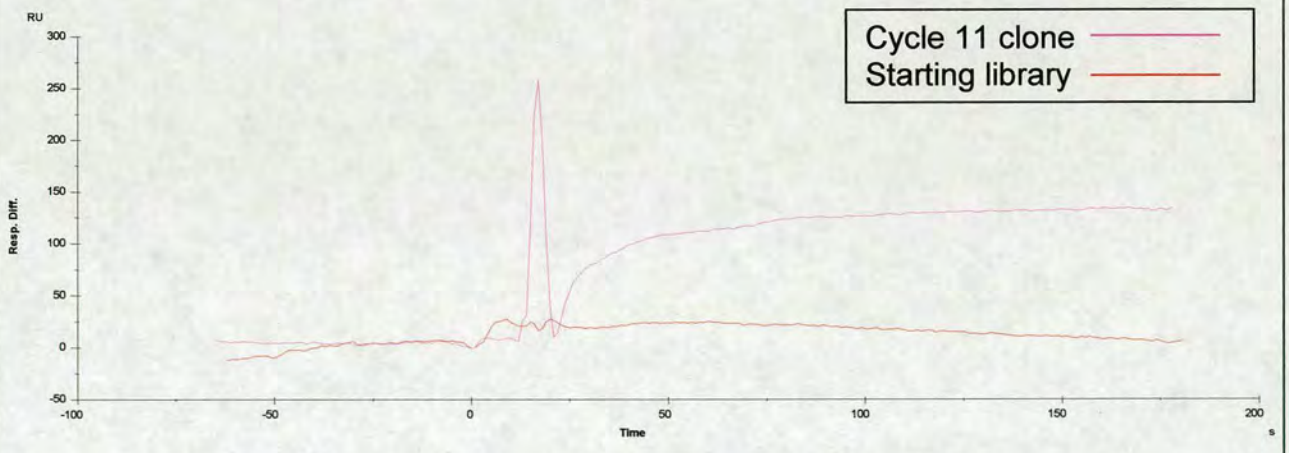

Figure 4.21: Comparison of the cycle 11 SELEX (S11) clone against the aptamer starting library.

[7] The flow rate was set to 10µl per minute and a 3 minute, 10µM load was injected with either the starting library or with the cycle 11 clone (both had been heated to 95°C then cooled on ice pre-load).

With this result in hand, the decision was made to continue the SELEX approach until 16 rounds had been completed. However after 16 rounds, there was no significant change in the amount of eluted radioactivity or of the concentration of ssDNA in the eluted fraction to suggest that SELEX should be halted at this point. If the results had suggested that at least 75% of the pool loaded was contained in the eluted fraction, this would have indicated saturated enrichment of the aptamer pool.

The library pool used for sequencing was continued forward from cycle 11, not just those aptamers who had been cloned at that period. That is to say that the apparent consensus clone (S11) even though showed promise, was not included in the further rounds and all the clones that had successfully completed the previous 10 rounds (or were evolved from clones that had) were given the opportunity to complete the SELEX process.

At the end of the process, after the final PCR (using the non-biotinylated 3' primer), 124 "positive" clones were picked and grown overnight for further plasmid extraction/digest. Of the 124 clones, 112 contained an appropriate insert and were sequenced. Ninety two of these gave readable data. The sequence alignment is shown in **Figure 4.22**.

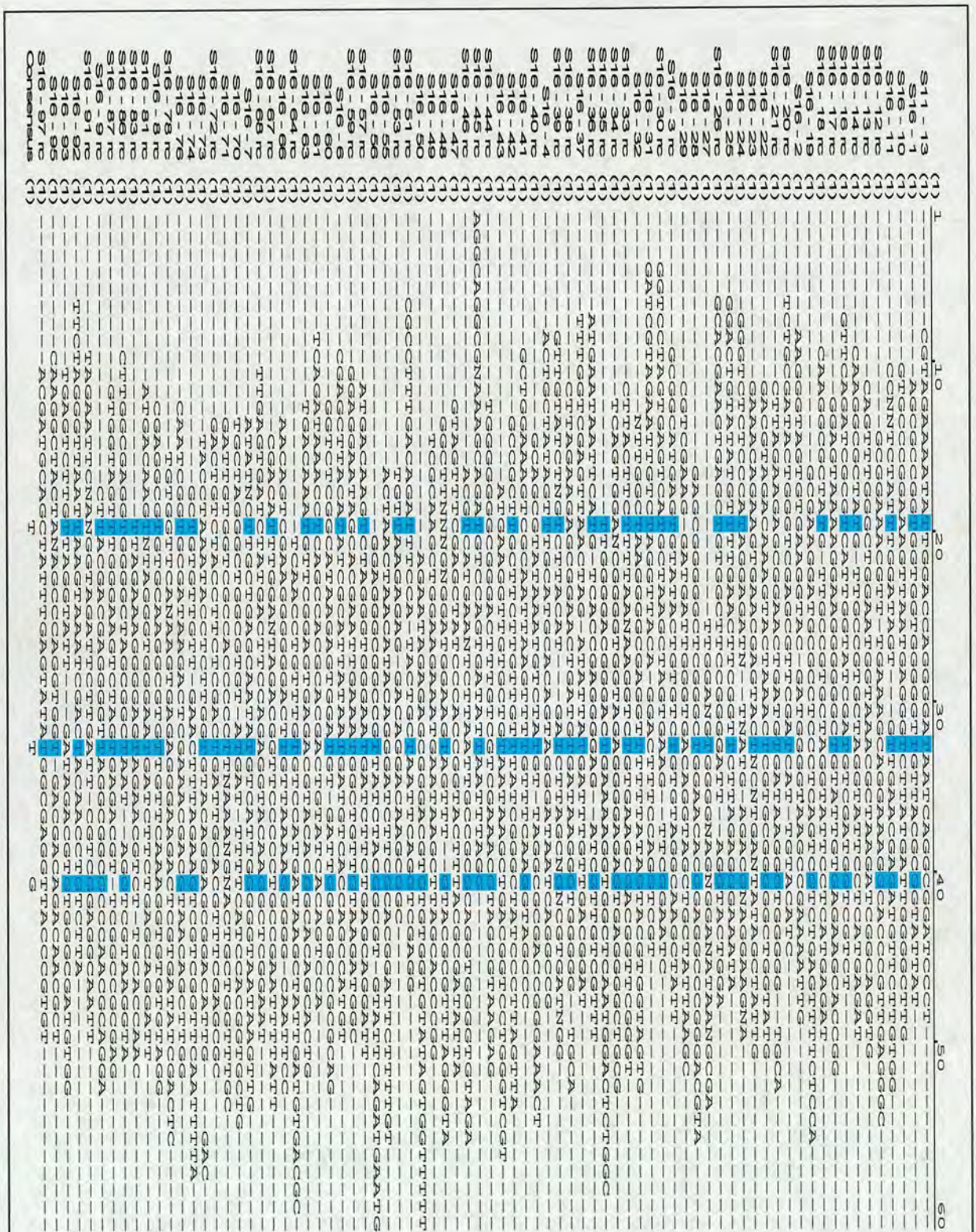

Figure 4.22: The sequence alignment of cycle 16 clones. Of 112 clones, 92 returned with readable data. The sequence alignment performed by ClustalW.

Clone (S16-)	A	C	G	T	N	No. Bases
1	4	5	17	11		37
2	13	3	16	8		40
3	8	6	13	13		40
4	11	8	11	10		40
6	12	10	7	12		41
7	11	4	11	14	1	41
8	7	5	18	11		41
9	8	10	14	4		36
10	8	5	15	11		39
11	7	5	11	15	2	40
12	12	8	15	5		40
13	10	6	15	9		40
14	8	9	11	12		40
16	6	8	12	14		40
17	12	4	18	6		40
18	8	9	11	12		40
19	6	13	10	11		40
20	7	9	10	12		38
21	11	4	17	8		40
22	11	7	14	8		40
23	14	5	9	9	3	40
24	11	6	12	7	4	40
25	11	4	11	15		41
26	8	7	16	9		40
27	7	1	12	4	5	29
28	7	10	20	3		40
29	10	6	14	10		40
30	10	7	12	11		40
31	9	7	11	13		40
32	7	3	15	14	1	40
33	8	7	11	14	1	41
34	7	4	23	7		41
35	9	7	16	8		40
36	10	6	11	13		40
37	10	3	10	17		40
38	11	4	17	8		40
39	6	6	10	14	4	40
40	11	8	12	9		40
41	10	7	10	12		39

Clone (S16-)	A	C	G	T	N	No. Bases
42	4	10	9	18		41
43	8	6	14	12		40
44	8	6	18	8		40
45	13	5	12	9	1	40
46	9	7	13	10	1	40
47	9	10	8	13		40
48	7	3	15	12	4	41
49	13	8	10	6		37
50	9	2	16	13		40
51	9	10	9	12		40
55	11	9	7	13		40
56	8	7	15	10		40
57	11	5	13	11		40
59	13	4	14	9		40
60	7	7	18	8		40
61	13	14	6	7		40
63	12	9	12	7		40
64	9	8	9	14		40
66	12	6	14	8		40
67	7	10	8	14	1	40
68	11	7	11	11		40
70	5	8	13	14		40
71	6	11	10	11	3	41
72	6	12	9	13		40
73	11	9	10	10		40
74	8	5	10	17		40
76	13	9	11	7		40
78	11	6	13	10	1	41
81	11	4	13	11	1	40
83	11	6	9	6		32
86	8	6	17	9		40
87	7	6	17	10		40
91	10	5	10	13	2	40
92	13	7	6	14		40
93	7	3	16	13		39
95	12	11	11	5	1	40
97	9	7	12	10		38
	707	514	956	801	39	3014
	23.7%	**17.3%**	**32.1%**	**26.9%**		

Table 4.3: Clones 1 to 97 with their ratio of nucleotides determined.

Guanine is most abundant nucleotide, almost twice as common as cytosine in the final pool. The DNA sequencing was largely successful with very few unknown bases. This may be an anomaly however many ssDNA aptamers published to date contain G-quartets so perhaps the evolved pool may be this way for a reason.

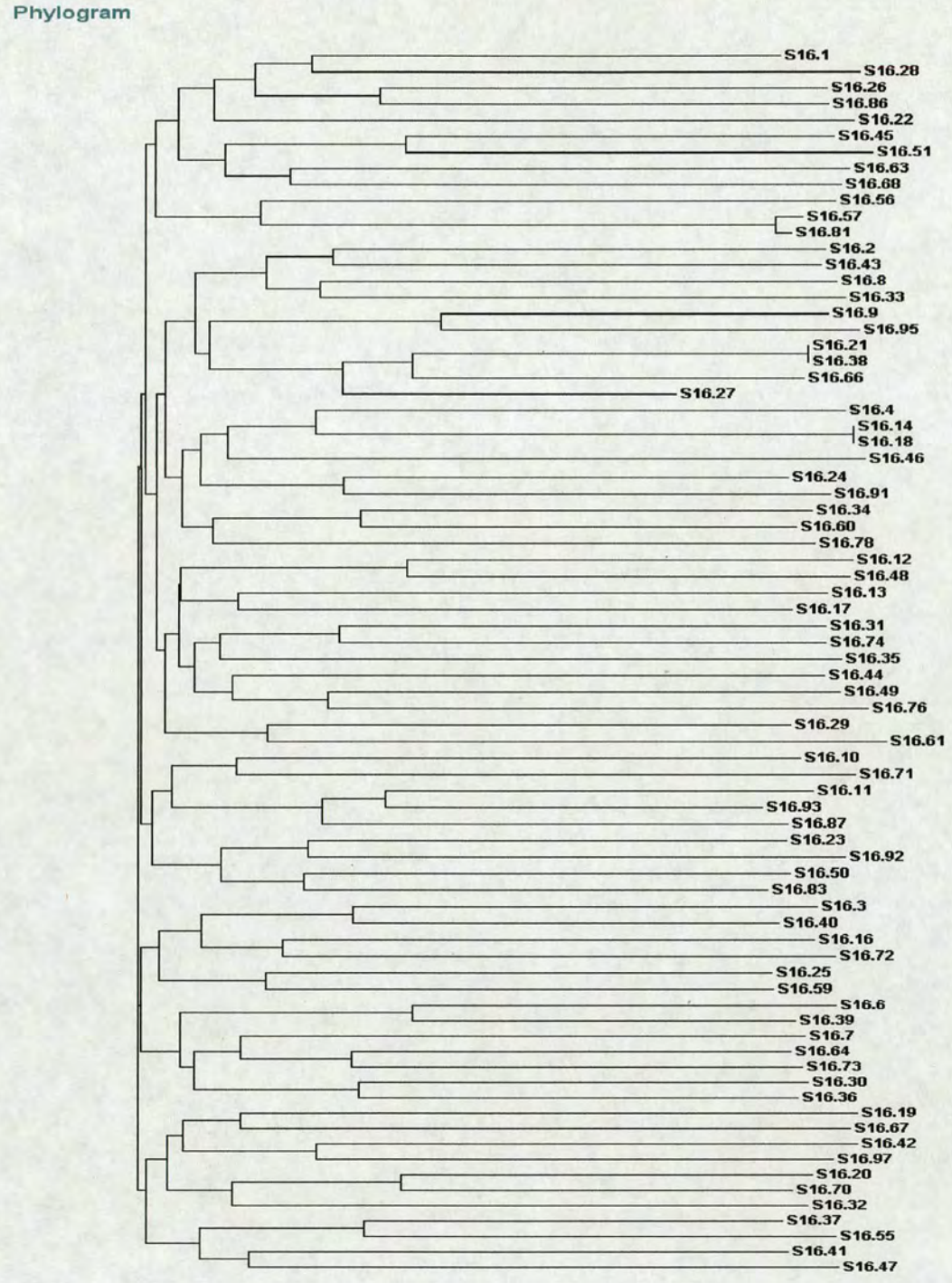

Figure 4.23: Phylogenetic tree of Aptamer sequences. The phylogenetic tree was built using the sequence distance method and the Neighbor Joining tree reconstruction algorithim, and displayed using Align X available on Vector NTI suite 9.[165] Branch lengths are proportional to the amount of inferred evolutionary change.

The sequence data obtained from the 92 clones indicated that the library was not being driven to a convergent sequence or even to a series of aptamer families. A comparison of the cycle 11 clones and those of cycle 16 would suggest that the library was perhaps even more divergent after further cycles. These facts, together with the indications of binding from the radioactive experiment were a cause for concern. However I had the opportunity to discuss the matter with Sergey Krylov, a visiting speaker at the University of Edinburgh. Krylov pointed out that many of his own results had led towards families of aptamers rather than towards specific motifs or G-quartet enrichment [private communication]. It was improbable that aptamers with no association with 14-3-3 managed to make it so many rounds of selection, when there were thorough and relatively harsh (1M NaCl) washing steps, along with counter selection steps that should eliminate any probes that bind the Ni-NTA or microcentrifuge tubes.

The data presented in **Table 4.3**, shows what was once a completely random library (which should have roughly 25% of each nucleotide) was now a weighted library where cytosine residues (17.3%) had become less common, predominantly at the expense of guanine (32.1%). Comparing **Table 4.3** and **Figure 4.22** suggested that perhaps all sequences should not be aligned together and breaking the sequences down further into phylogenic groups, from **Figure 4.23** might lead to more encouraging results. The T-rich tubulin specific aptamers described by Fukusaki *et al.* contain little sequence alignment.[114] They broke their sequenced into four families, T rich, G rich, G/T rich and other, neither family has a high degree of sequence analogy but they still managed to screen for an aptamer with a dissociation constant in the order of 10μM. In addition, Sayer *et al.* selected 12 aptamers to the

HIV-1 SU glycoprotein, gp120, all with an affinity in the order of 100nM, most of which share little sequence convergence.[166]

A decision had to be made at this point; whether to continue the SELEX process or to attempt to pick out a 14-3-3 γ aptamer from the 92 member library. The fact that there was little sequence convergence militated against the first option. To analyse how cycle 16 aptamers associated with 14-3-3 γ, different experimental techniques were available. Surface plasmon resonance, ELONA and affinity purification could all be used to determine the most suitable aptamer across all applications.

To carry out binding assays three points would have to be covered: (1) the clones would have to be synthetically produced; (2) truncation: including the flanking regions, aptamers would be around 65 bases long, making perhaps unnecessarily costly probes, thus where to truncate the aptamer would be important and (3) a tag would be necessary for ELONA and affinity purification.

For a trial of cycle 16 aptamers, aptamer S16.1 had its invariant region synthetically produced untagged, for analysis by SPR. As a cycle 11 consensus clone had been previously synthesised, the first experiment that was set up was to see if there was enrichment during the final five cycles.

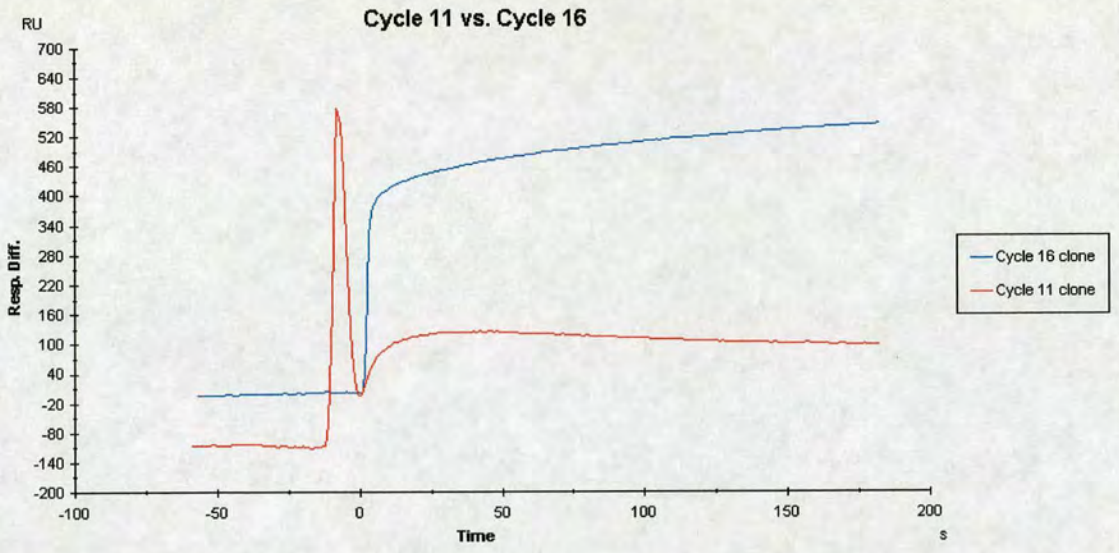

Figure 4.24; Comparison of the cycle 11 consensus clone (S11) versus S16.1. Again the consensus S11 clone gives a response around 150 RU whereas the cycle 16 clone shows an initial association of 400 RU, increasing to 550 RU over 180 seconds.

Figure 4.24 shows a positive result, however this does not necessarily reflect an enrichment. S16-1 is not related to the cycle 11 clone through enrichment, it was a completely different clone that was being analysed. The definitive result coming from Figure 4.24 is that there is a definite association event happening when both aptamers are passed down the Biacore, containing the immobilised 14-3-3γ. The next logical step would be to see if the response is concentration dependant. S16-1 (16 cycle-clone 1), was diluted to range of concentrations and equal volume aliquots were passed across the flowcells. Results are shown in Figure 4.25.

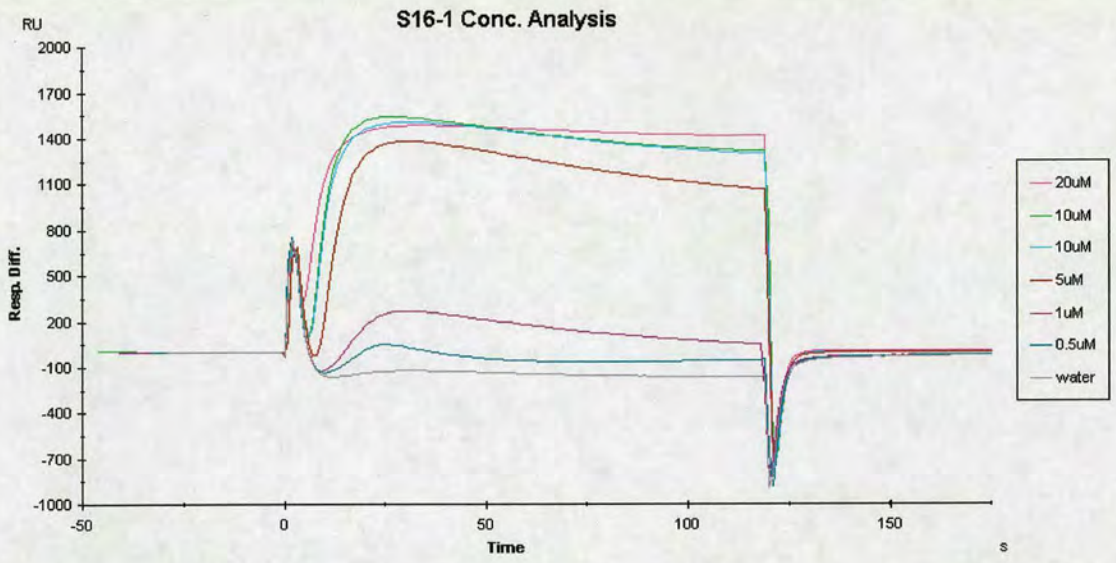

Figure 4.25: Cycle 16 Clone 1 concentration analysis. Clone 1 (S16-1), was analysed using 5 different concentrations to see if the response was concentration dependant. The 10μM sample was carried out in duplicate to show that that the results were repeatable. The clone gave concentration dependant responses against the 14-3-3 γ.

Figure 4.25 shows that SPR of different concentrations of S16.1 leads to approximately concentration dependant curves. The 10μM clone was carried out in duplicate to prove that results were repeatable. The figure leaves some outstanding questions regarding the k_{on}/k_{off} of clone S16-1. All clones have an initial association event, followed by a gradual decline in the response difference. This would suggest that this particular aptamer "recognises" 14-3-3 γ however is not showing any strength of binding to the 14-3-3 protein. Again spikes in the curves are related to the difference in buffer between the running buffer used and the aptamer solution.

With the two previous figures in mind, trial aptamer S16-1 gave encouraging results using SPR thus the decision was made to synthesis more of the sequenced cycle 16 aptamers for further analysis.

With so many different sequences contained within the library, and no conserved motif, the next difficulty was to find which of the clones had the apparent best affinity to 14-3-3 γ. The decision was made to produce twenty of the 92 sequenced clones for further analysis.

There is a problem associated with using truncating aptamers. It was decided to truncate to the randomized 40 region, a decision that could prevent aptamers folding into the relevant 3-D structure, an unavoidable risk due to cost. 40 bases provided scope for tertiary structure, the theophylline aptamer contains 15 nucleotides, so 40 provided enough room for the relevant structure to form.

The truncated aptamers were 5' biotinylated, the tag is necessary for further experiments, however there is the problem that the modification may cause steric hindrance to the epitope. The modification is unlikely to enhance the binding but it is a real possibility that the bulky biotin group could block it.

A cost and time problem was posed with regards to which of the 92 clones should be further analysed for 14-3-3 association. The first 20 clones were produced for analysis by SPR, and those that gave promising results were synthesised with a modification for further analysis by ELONA (enzyme linked oligonucleotide assay).

If more time had been available then instead of simply truncating all aptamers to the initial randomized 40 bases.

4.4 Cycle 16 Clone Analysis by Surface Plasmon Resonance

All experiments were carried out using a Ni-NTA chip that had been preloaded with 14-3-3γ[8].

An experiment was devised to analyse the impact of the biotin tag on the SPR result. Clone S16.1, produced with and without a biotin tag attached, had 10μM, 60μl injections were compared. Untagged S16.1 gave a large response difference, around 3000 RU, the biotinylated gave a much less encouraging response, with negative RU.

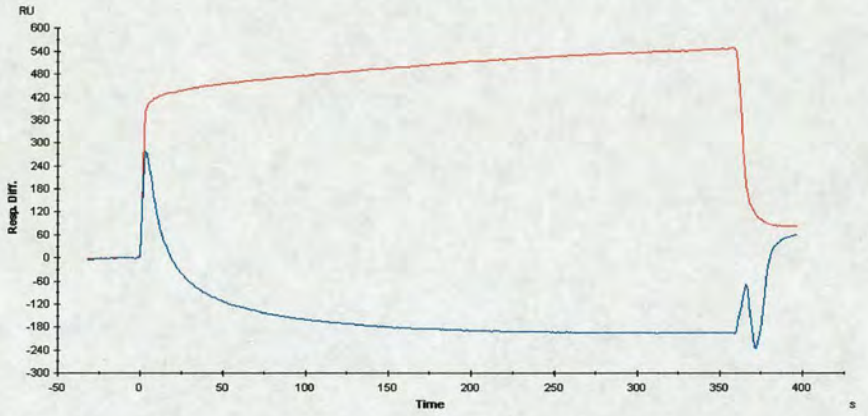

Figure 4.26: S16-1, Biotinylated comparison. The unbiotinylated S16-1 (red) and biotinylated S16-1 (blue) response compared using SPR, both ran at 10μl, 60μl injections.

Figure 4.26 shows that biotinylation of the clone S16-1 significantly alters the SPR response. Unbiotinylated S16-1 shows a definite recognition event with weak binding, biotinylated S16-1 gives no association event. Although this may have appeared disappointing, it was inevitable that biotinylation of some probes would lead to poor results using a specific assay.

[8] The running buffer used was PBSM, the washing buffer used in between injections was glycine (as had been successful in the previous antibody study). The temperature was maintained at 25°C, and unless otherwise stated, the flow rate was kept at 10μl/min. All aptamer samples were heated to 95°C for two minutes and cooled on ice before application. The concentration of the aptamer solution will be shown.

More of the biotinylated cycle 16 aptamers were analysed by SPR, as shown in Figure 4.27.

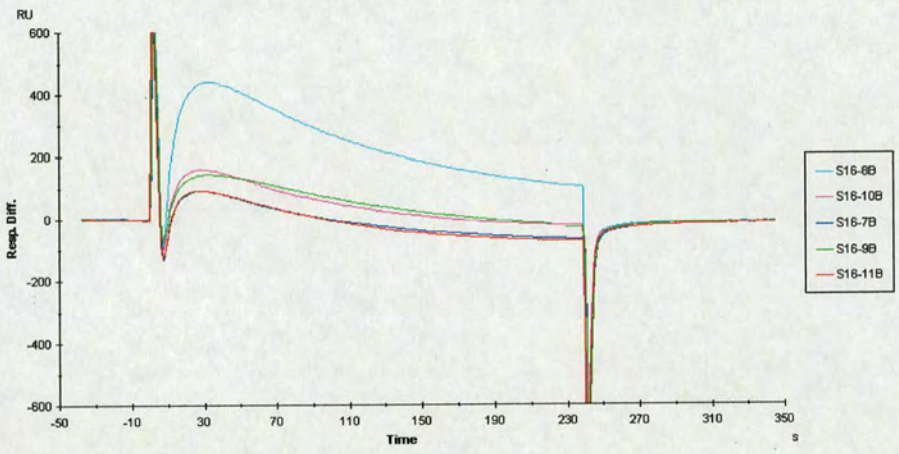

Figure 4.27; SPR of biotinylated aptamers. The result of passing five of the biotinylated aptamer sequences across the 14-3-3 loaded Ni-NTA chip is shown. Each aptamer is shown in the legend.

Biotinylated cycle 16 aptamers were providing poor responses using SPR. From Figure 4.27, each aptamer has some sort of immediate association, however the curve suggests that there is no binding event and the aptamers are quickly washed from the immobilised protein.

4.5 Aptamer characterisation using Enzyme Linked Assay

4.5.1 ELISA

The enzyme linked immunosorbent assay was developed in 1971 for the simple and rapid measurement of a variety of analytes with exceptional specificity and sensitivity.[136] ELISA's are commonly used in a sandwich assay format, requiring the use of 2 antibodies or binding proteins that bind the analyte at the same time. The capture antibody is immobilised on a surface, the detection antibody is coupled to an enzyme compatible with the desired method of detection. The term sandwich assay is relevant because the analyte is sandwiched between the two antibodies in the system. ELISA is one of the most frequently used techniques for affinity analysis using antigen-antibody interactions, although it is not suitable for kinetic analysis.

Before attempting the interaction of an aptamer with 14-3-3 γ using a sandwich assay (ELONA, see below), an ELISA using 14-3-3 and antibodies was set up to prepare a protein standard curve (shown in Figure 4.28). Recombinantly expressed 14-3-3 γ was subjected to serial doubling dilutions from a 4000μg/ml standard using unspiked buffer as a background control, 100μl added to each well. Following this incubation, the plate was washed with a 96 well plate washer using a wash buffer. The wash program directed six 200μl/well wash cycles with 30 second soak periods between washes. During the soak period the plate was agitated. K-19 anti-14-3-3 antibody (rabbit polyclonal IgG) diluted 1:1000, 50μl was added to each well, incubated for 1 hour, before a further washing step followed by addition of 50μl goat anti-rabbit HRP conjugate antibody, diluted (1:10 000), which was allowed to incubate for 1 hour. The plate was subjected to a further washing step before addition of 3,3,5,5

Tetramethylbenzidine (TMB) substrate, incubated for 15 minutes, and the reaction was quenched with the addition H_2SO_4 and the absorbance at 450nm measured.

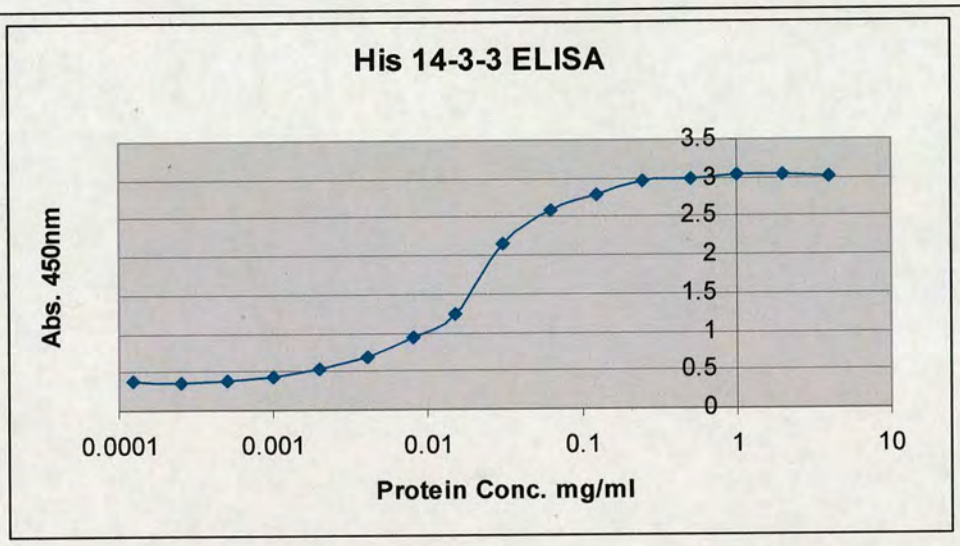

Figure 4.28: The 14-3-3γ ELISA standard curve. Curve prepared using doubling dilutions of 14-3-3 γ in triplicate. K19 antibody used in analysis.

4.5.2 ELONA

The enzyme linked oligonucleotide assay (ELONA), first described by Drolet *et al.* is a rapid assay that can give the relative binding abilities of the aptamers to protein, based on the sandwich ELISA.[137] The precision, specificity and accuracy of Drolets method are similar to those of a typical enzyme linked assay (ELISA). Typically the ELONA assay has a theoretical minimum detection limit of 25pg/ml (protein to be detected). ELONA has been used for a number of aptamer targets including cytokines,[167] ricin toxin,[168] kinetoplastid membrane protein-11 (KMP-11),[169] TTF1,[144] and C595,[170] (an anti-MUC1 monoclonal antibody).

The 14-3-3γ assay was set us as a typical sandwich enzyme linked assay. The anti 14-3-3 antibody K-19 was used as the microtitre plate bound capture reagent to

immobilise 14-3-3 γ in a 96 well plate. Addition of the biotinylated aptamer was followed by addition of a streptavidin fusion with horse radish peroxidase (HRP). The amount of bound HRP was then assayed colorimetrically by addition of *o*-phenylenediamine dihydrochloride (Drolet's work used a fluorescein labelled aptamer and Alkaline phosphatase (AP) conjugated anti-fluorescein FAb fragments). The ELONA was carried out in triplicate using doubling dilutions of the aptamer. The protein concentration was maintained at 0.5mg/ml.

Using ELONA we could screen all synthetically produced biotinylated aptamers, allowing comparison of their apparent association. From the protein standard curve in Figure 4.28, the minimum dilution of 14-3-3 necessary for maximum response was 0.5 mg/ml. A 96-well plate was coated with capture antibody K-19 and subsequently 50µl of $(His)_6$14-3-3 γ (0.5mg/ml) was added. The biotinylated aptamer was added[9] and incubated at 37°C for 2 hours followed by addition of a streptavidin-HRP conjugate enzyme. Similar to the ELISA, the amount of bound HRP was then assayed.

Clone S16-	Abs (450nm)
1	1.75
2	1.03
3	0.74
4	0.73
8	1.89
9	0.51
12	0.61
13	0.4
16	0.59
26	0.42

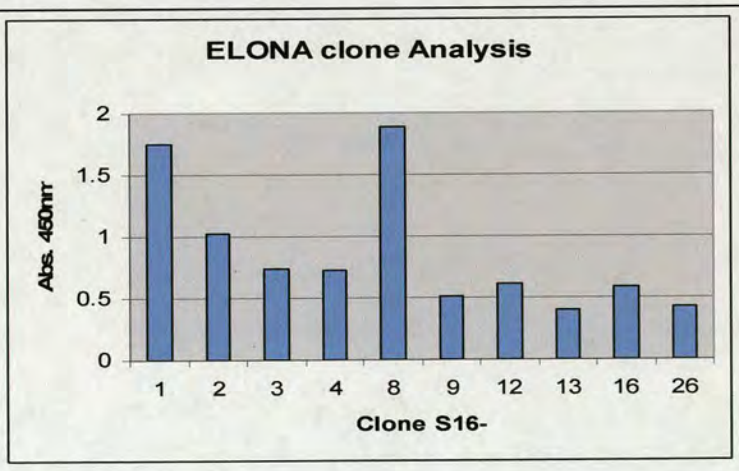

Figure 4.29: Analysis of 10 different SELEX clones by ELONA. All samples were at a concentration of 20µM. 50µl of each was added to each well. Experiments were conducted in triplicate.

[9] All aptamers heated to 95°C for 5 minutes and cooled on ice before addition. 50µl of 10µM biotinylated aptamer stock. Experiments were carried out in triplicate.

Clones S16-1 and S16-8 appear to have the greatest responses using this ELONA method. Ten clones are not represented in Figure 4.29 because they had an affinity lower than the set threshold.

Following from the results obtained in Figure 4.29, the three best ELONA aptamers, (S16-1, S16-2 and S16-8) were used to characterise quantitatively immunocomplex formation. K-19 capture antibody coated to the 96-well plate was used to immobilise $(His)_6$14-3-3γ allowing a saturation curve to be obtained. The relative saturation, *i*, is displayed as a function of the aptamer concentration. To determine the K_d of the interaction between aptamer and protein, a linearization method was followed.[171] Following the work of Liliom and that of Orosz the K_d^{app} were calculated.[172] The K_d^{app}, the apparent dissociation constant of the immunocomplex, can be obtained from the reciprocal slope of the plot $1/(1-i)$ vs. Apt_{tot}/i where Apt_{tot} is the total concentration of aptamer.

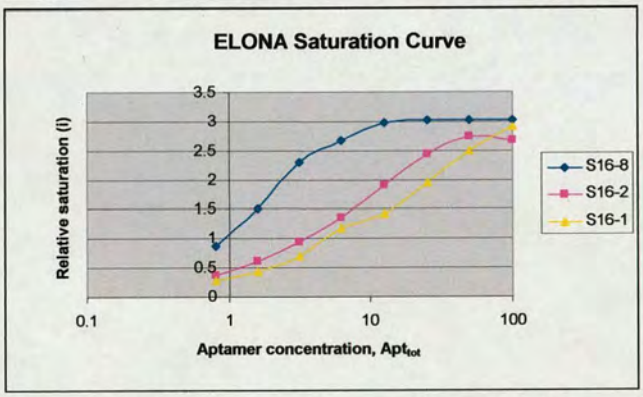

Figure 4.30: ELONA saturation curve. The relative saturation against the aptamer concentration is shown.

Aptamer	K_d^{app} μM
S16-1	15.6
S16-2	5.4
S16-8	0.56

Table 4.4: The K_d^{app} of selected cycle 16 aptamers. The three most promising ELONA aptamers were selected for further analysis, their saturation curves allowed calculation of the apparent K_d.

4.5.3 14-3-3 Isoform analysis using ELONA

Following on from the work where the best $(His)_6$14-3-3γ aptamers were selected and their K_d calculated, the two aptamers showing with the lowest K_d, S16-8 and S16-2, were used for further analysis to compare the aptamer response with respect to the different 14-3-3 isoforms. Antibody K-19 was coated onto a 96 well plate and used to capture 14-3-3 proteins, all proteins were loaded at a concentration of 100μM. The aptamers were used to complete the 14-3-3 "sandwich" allowing detection, the aptamer concentrations were fixed at 10μM.

Isoform	S16-8	S16-2
His Gamma	2.472	0.441
GST Gamma	2.047	0.441
Zeta	1.886	0.47
Beta	2.091	0.409
Sigma	1.902	0.384
Tau	1.925	0.396
Eta	2.184	0.511
Fraction 4	2.267	0.436

Isoform	S16-8 %His Gamma
GST Gamma	82.8
Zeta	76.3
Beta	84.6
Sigma	76.9
Tau	77.9
Eta	86.9
Fraction 4	91.7

Figure 4.31: Comparison of the different 14-3-3 isoforms by ELONA. The S16.8 clone gives a significantly greater response to all the isoforms than the S16-2 clone.

Aptamer S16-8 consistently gives a higher response than the S16-2 clone. It gives the greatest response against his tagged 14-3-3 γ but it also interacts with other isoforms in the 14-3-3 family.

To ensure that the secondary antibody was not responsible for the results, a further control experiment was set up to analyse this. A 96 well Immulon 4HBX 96 well plate was coated with K-19 capture antibody overnight. The plate was then blocked with 5% BSA and washed thoroughly before addition of the protein samples (4μg protein added to each well). The plates were washed, aptamer S16-8 (50μl, 100pM) was added to wells 1-3/A-H, and all other wells had buffer added. After 1 hour

incubation, the secondary antibody was added to all the wells and ELONA procedure carried out.

	1	2	3	4	5	6	7	8	9	10	11	12
A	His 14-3-3 γ			His 14-3-3 γ			**S16-8 Aptamer No Protein**					
B	GST 14-3-3 σ			GST 14-3-3 σ								
C	GST 14-3-3 ζ			GST 14-3-3 ζ								
D	GST 14-3-3 τ			GST 14-3-3 τ						**No Aptamer No Protein**		
E	GST 14-3-3 σ			GST 14-3-3 σ								
F	GST 14-3-3 β			GST 14-3-3 β								
G	GST 14-3-3 γ			GST 14-3-3 γ								
H	GST 14-3-3 η			GST 14-3-3 η								
	+ Aptamer S16-8			**No Aptamer**								

	1	2	3	4	5	6	7	8	9	10	11	12
A	**0.093**			**0.051**			**0.053**					
B	**0.061**			**0.048**								
C	**0.061**			**0.050**								
D	**0.068**			**0.051**								
E	**0.064**			**0.050**						**0.050**		
F	**0.066**			**0.048**								
G	**0.066**			**0.048**								
H	**0.072**			**0.053**								

Figure 4.32: Comparison of 14-3-3 isoforms with aptamer S16-8 in sandwich enzyme assay. 14-3-3 γ gives the greatest response however all isoforms give measurable responses above background.

The results from Figure 4.32 indicate that aptamer S16-8 is detecting all 14-3-3 isoforms and it is not the secondary antibody responsible for results, nor is S16-8 forming a complex with the 96-well plate. This means that the previous ELONA studies can be regarded as being solely due to the interaction of aptamer and protein. Similar to the ELONA study against all 14-3-3 isoforms, the $(His)_6$14-3-3γ shows the greatest response using this method of protein detection.

S16-8 was the best aptamer using the ELONA method. Other techniques were used to determine if S16-8 was as robust using alternate assays. The interaction of different 14-3-3 isoforms with S16-8 was analysed further.

4.6 Protein Blot Analysis with Aptamer S16-8

The interaction of S16-8 with all seven human 14-3-3 isoforms was also analysed by protein blot analysis. Protein samples, all 2μg, were prepared for SDS page by boiling in Llamealli sample buffer then separated electrophoretically on a 4-12% Bis-Tris gel. One gel was stained with GelCode blue, the second had its proteins transferred to a PVDF membrane, and was subsequently blocked overnight at 4°C with 5% BSA. The membrane was probed with biotinylated S16-8 diluted to 100μM, in 10ml of PBS-T, before treatment with streptavidin-HRP (1:10 000) in PBS-T. The membrane was thoroughly washed before addition of ECL plus (Amersham Biosciences) western blotting detection system and imaging on a Hyperfilm™ MP film. The results are shown in **Figure 4.33**.

S16-8 bound to all 14-3-3 isoforms, but not to the His-tagged GST used as a control was not illuminated by this method of detection. The surface plots[10] can be used to determine the ratios of peaks to each other. The Western blotted surface plot suffers from high background although data can still be obtained. The most significant point may be that there is no peak is shown for His-tagged GST protein in the western surface plot. The Western image suffers from high background levels, even though the membrane was blocked thoroughly with BSA.

[10] Surface plots carried out using ImageJ 1.36[10]

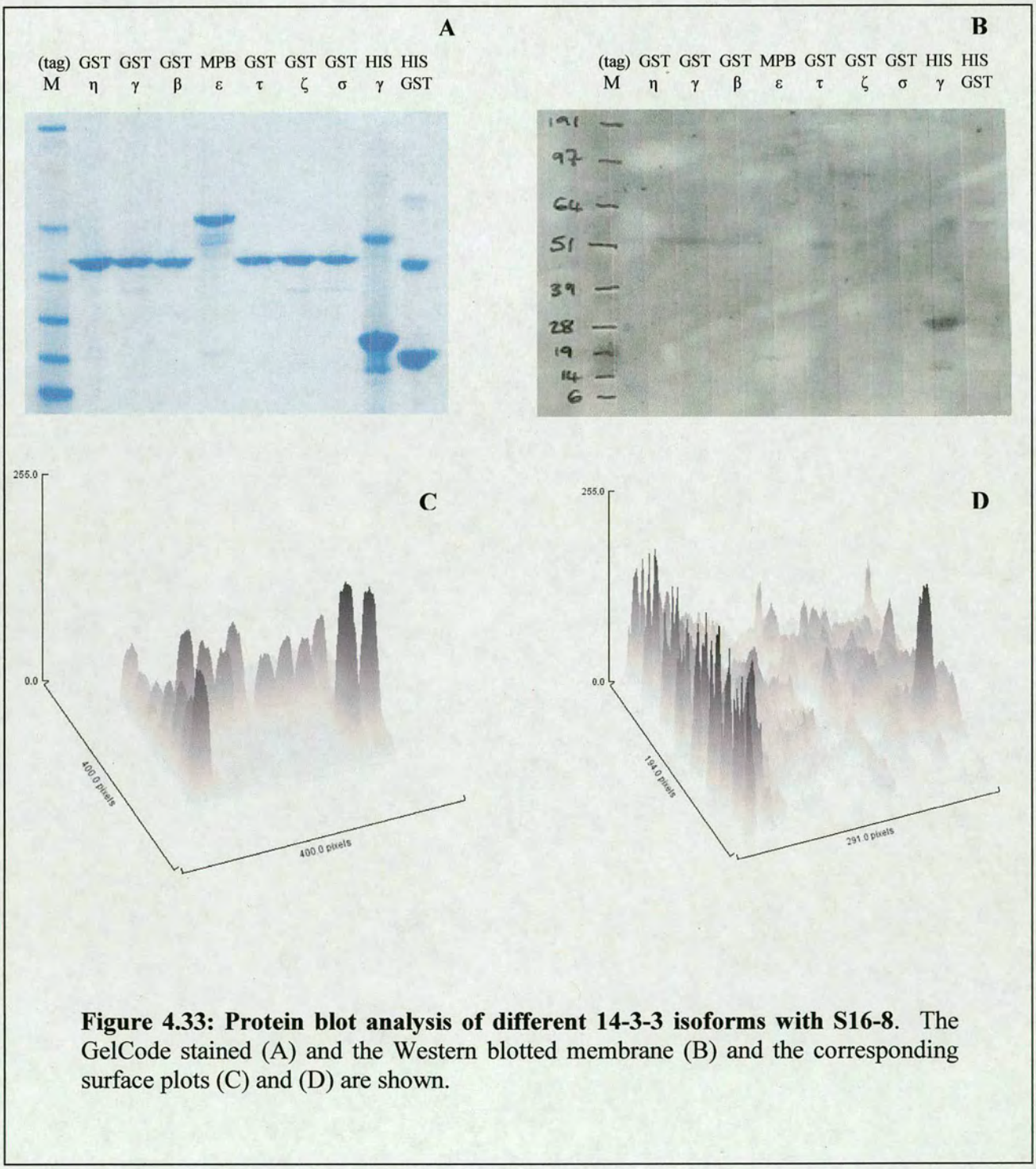

Figure 4.33: Protein blot analysis of different 14-3-3 isoforms with S16-8. The GelCode stained (A) and the Western blotted membrane (B) and the corresponding surface plots (C) and (D) are shown.

4.7 Gel Filtration Analysis

Gel filtration analysis of the interaction of $(His)_6$14-3-3γ with S16-8 could provide data regarding the binding of the two species. Analysis of spectra could provide details regarding if the aptamer binds to each monomer unit in the dimer or just one.

Recombinant 14-3-3 γ added to aptamer S16-8 was passed down a gel filtration column (16 60 Superdex^{TM} 75 (Amersham Biosciences)) to analyse for a binding species.

For controls, 25µl of 14-3-3 (14.2 mg/ml) added to 975µl Tris HCl pH 7.5, NaCl (0.15M) (running buffer), (**A**) and passed down column, the other control had 25µl of 100µM S16-8 made to 1 ml with running buffer (**B**), passed through the same column. To analyse for binding between the two species, 25µl protein, incubated with 25µl 100µM S16-8, was made to 1 ml with running buffer (**C**). The solution was incubated with gentle agitation overnight and ran on the same gel filtration column, using the same programme as both controls. Results displayed in Figure 4.34.

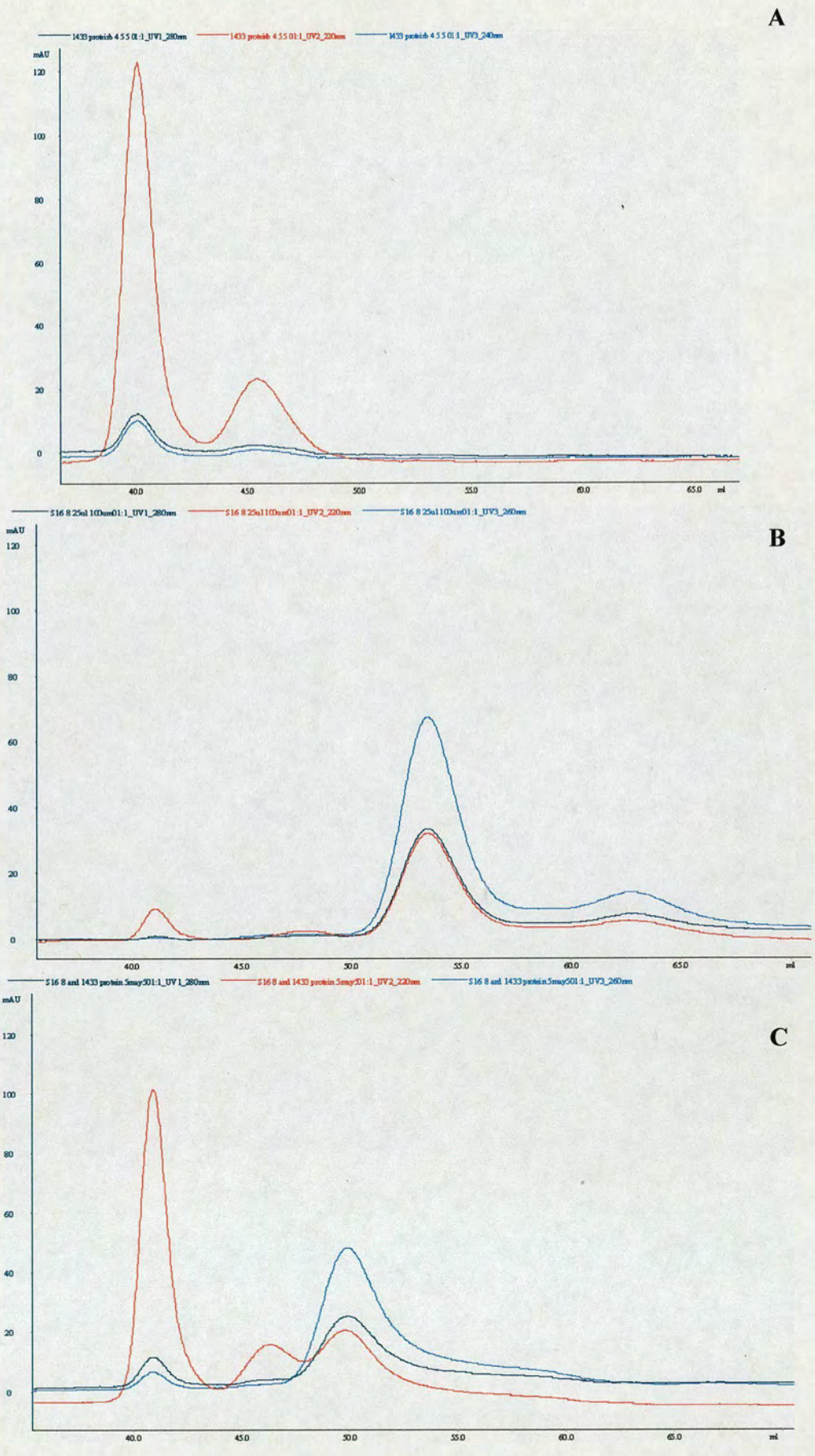

Figure 4.34: Gel Filtration analysis of 14-3-3 and aptamer S16-8. Chromatograms A and B show controls for the experiment, A has the 14-3-3 protein alone passed through column and B aptamer S16-8 alone. Chromatogram C shows the result of the ssDNA-protein mix passed using same method.

The chromatograms observed in Figure 4.34 did not provide the results that were hoped for. The protein peaks in the 14-3-3 control were eluted at 40 ml for the dimer and 46 ml for the monomer unit. It was hoped that after addition of the aptamer to 14-3-3, the peaks would shift suggesting the addition of a ~12kDA unit (the mass of the aptamer). Analysis of the protein/aptamer led to the conclusion that the protein peaks had shifted but to smaller peaks. The peak previously observed at 58kDa (representing the dimer unit) had shifted to representing a smaller mass particle. The monomer peak was also shifted in the direction to represent a smaller mass particle. The result of the chromatograms, comparing the timing of the peaks, suggest that the 3 peaks shown in image C relate to the monomer and dimer units of 14-3-3 (from A) and of free S16-8 aptamer (from B) and not, as had been hoped, from a binding species.

To try to understand this result, textbooks explaining the gel filtration technique have been studied, although no comparison of this result have been found to date. The result observed for the protein/aptamer shift remains unanswered and requires further analysis.

4.8 Affinity Purification

To analyse the interaction between proteins and their specific antibodies, immunoprecipitation, a form of affinity purification can be used to rapidly separate proteins from plasma and whole cell lysates.

The method can be adapted to use an aptamer to purify a protein instead of the antibody. Aptamer affinity purification has is used in a number of systems including the StreptoTag system, a neat method for isolating RNA binding proteins, and aiding purification of 48S, a translation initiation complex.[173,174]

To analyse 14-3-3 interaction, 10µl of biotinylated 10µM S16-8 (heated to 95°C for 2 mins then cooled on ice for 5 minutes) was added to 50µl of homogenised mouse brain, and the resultant solution was agitated gently for 1 hour at room temperature. Subsequently, magnetic streptavidin beads were added and the unbound protein was washed from the immobilised aptamer. The immobilised fraction and the wash fractions were collected, denatured by boiling in Llaemmeli buffer, then resolved on a 4-12% Bis-Tris gel (Invitrogen), and either stained with GelCode Blue (Pierce), or transferred to PVDF for use in Western blotting.

A similar experiment was set to check if the aptamer could associate with 14-3-3 in CSF, 10µl of 10µM biotinylated S16-8 was added to 100µl of Ovine CSF pre-spiked with recombinantly expressed 14-3-3 γ. Again the gel was either stained with GelCode blue or transferred for Western blotting.

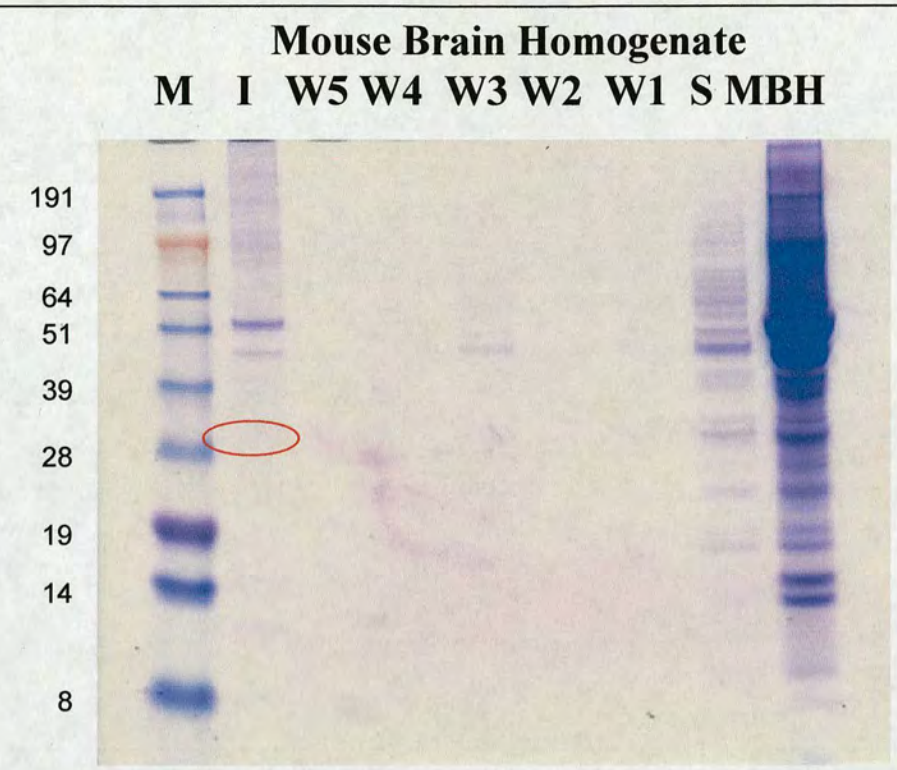

Figure 4.35: The Mouse Brain Homogenate immunoprecipitation reaction. MBH (mouse brain homogenate), S(supernatant), wash fractions 1 to 5 (W1 to W5) are shown along with the aptamer/immunoprecipitated fraction I. The marker (M) is shown on the left. The red circle highlights a barely visible band for 14-3-3. Gel stained with GelCode Blue.

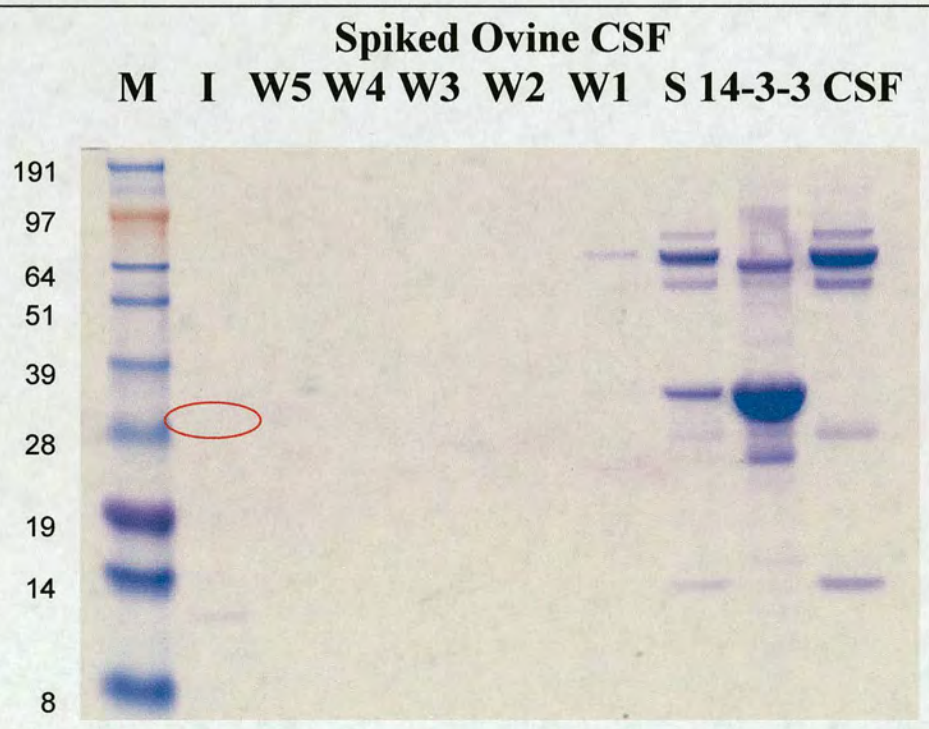

Figure 4.36: Ovine cerebrospinal fluid spiked with 14-3-3 immunoprecipitation. Lanes as follows: Unspiked ovine CSF -(CSF), recombinant $(His)_6$14-3-3γ -14-3-3, the spiked CSF supernatant (S), wash fractions W1 to W5) along with the aptamer/immunoprecipitated fraction- I. Gel stained with GelCode Blue.

The Western blot of the spiked ovine CSF purification and the purified mouse brain homogenate are shown in Figure 4.37. The anti 14-3-3 antibody K-19 was used for detection.

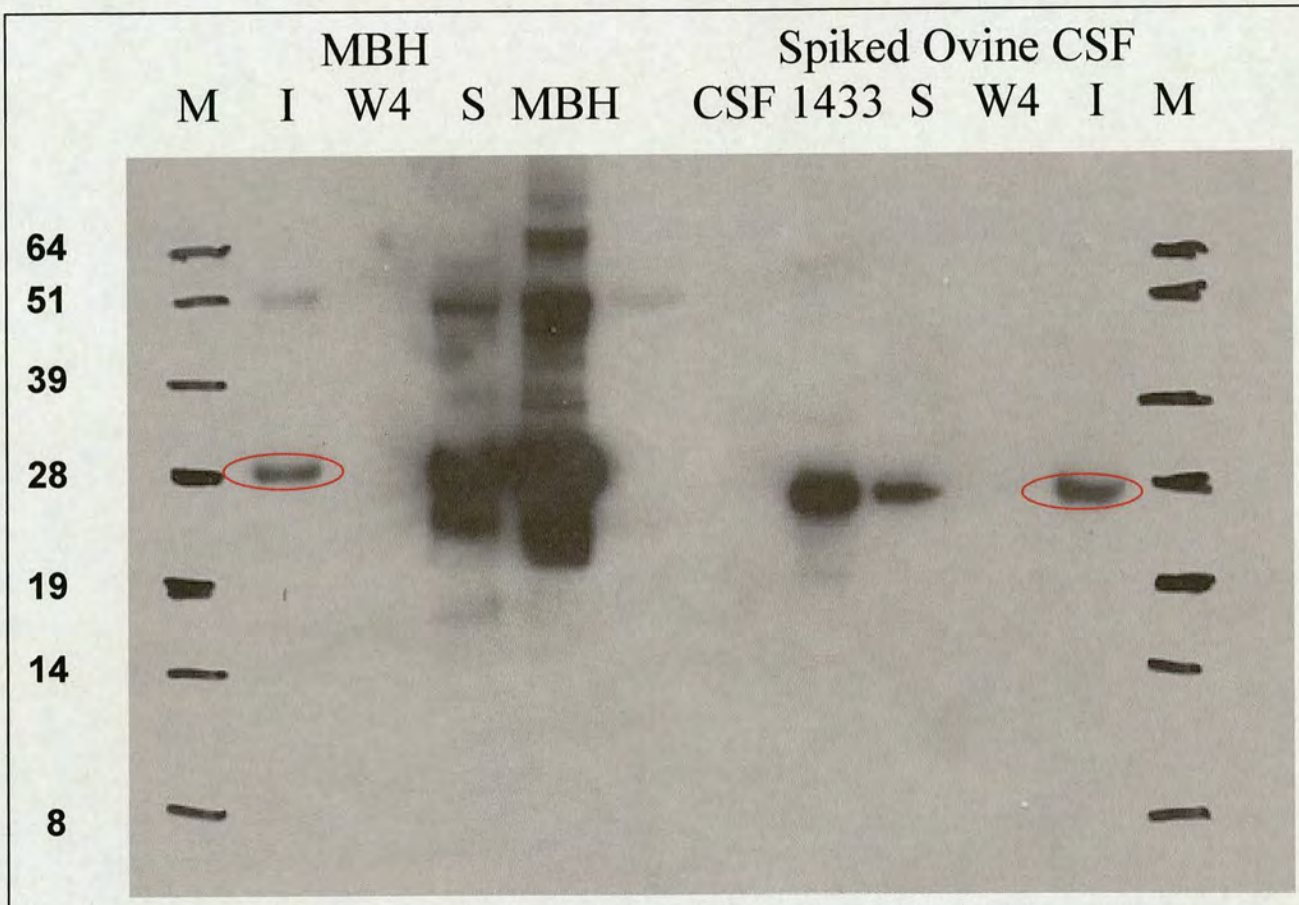

Figure 4.37: Western Blot amalgamation of the affinity purified mouse brain homogenate and spiked ovine CSF. The corresponding untransferred gels stained by GelCode blue are shown in Figures 4.35 and 4.36. Red circles highlight 14-3-3 contained in the immunoprecipitated fractions and thus the aptamer can successfully and specifically pull 14-3-3 from CSF and from mouse brain homogenate. The same abbreviations are used as that in Figures 4.35 and 4.36.

The circled bands in both Figure 4.35 and Figure 4.36, indicate a band slightly visible to the naked eye on the gel, however less apparent upon scanning on the gel. Both were extracted from the gel, digested by Trypsin (Trypsin sequencing grade, bovine pancreas, Roche) and analysed by MALDI-TOF MS. Figure 4.37, the Western blot amalgamation of 4.35 and 4.36 is a clear indication that clone S16-8 successfully

affinity purified 14-3-3 from mouse brain homogenate, and recombinant 14-3-3 γ spiked into Ovine CSF. The analysis confirmed that both were 14-3-3 proteins as was expected. The band around 50kDa was treated to the same analysis, it was found to be albumin. MALDI-MS data for the 14-3-3 protein and the albumin protein are contained in Appendix II.

4.9 Scrapie CSF Analysis

CSF from Scrapie infected sheep was obtained from H. Baxter. Scrapie is detectable using 14-3-3 as a surrogate marker.[175]

Scrapie sample F125 was analysed for 14-3-3 content using electrophoresis to separate proteins then staining or western blotting of the gels for visual analysis. The stock sample was subjected to seven doubling dilutions, from neat, to analyse what the minimum dilution necessary to visualise a 14-3-3 band. 20µl of each was boiled and then ran on gel, shown in Figure 4.38. The antibody used in the western blotting was K-19 (Santa-cruz). The figure shows in both stained and blotted images, that 14-3-3 (circled red) is slightly visible in the neat fraction but in no other samples. The large band around 64kDa, was cut from the stained gel, treated to tryptic digest and subsequent MALDI-TOF. The result of which suggested the band related to Ovine serum albumin.

Aptamer S16-8 10µl was added to Scrapie fraction F125, the solution was mixed overnight before the solution was subjected to the standard affinity purification assay. Collected wash fractions and the purified fraction were run on a Bis-Tris gel and either stained with GelCode blue or transferred to a membrane for Western blotting. The western blotting gel used the antibody K-19 as the detection agent. The stained gel and the blotted membrane are shown in Figure 4.39. All bands observed in the stained gel were excised and analysed with tryptic digest MS. The band around 60kDa was ovine serum albumin, 28kDa was 14-3-3 protein, and 10kDa was a streptavidin related protein (data shown in appendix III), presumably obtained in the process of removing the bound aptamer, involving boiling the streptavidin beads.

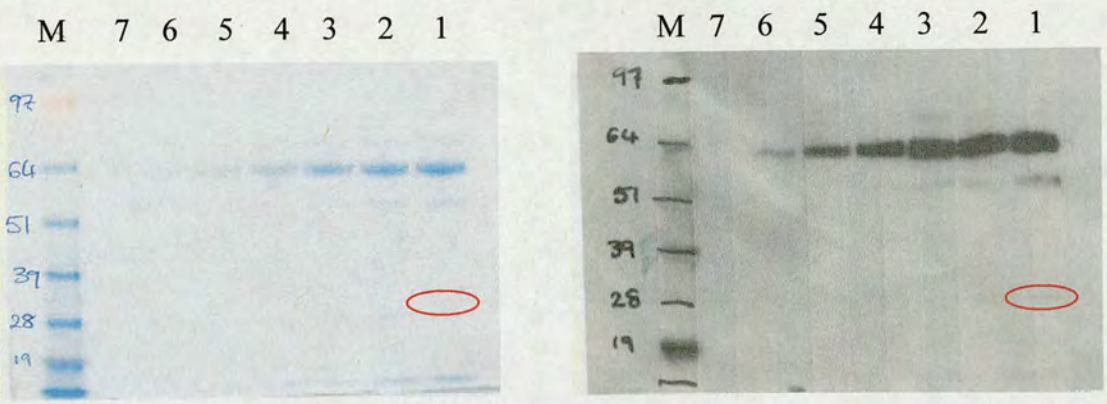

Figure 4.38: Analysis of Scrapie fraction F125. Numbered lanes indicate the diluted fractions of f125. 1-neat, 2-diluted ½, 3-diluted ¼, 4-diluted 1/8, and so forth. M indicates the marker lane. Red circles highlight the lightly visible band corresponding to 14-3-3 protein. Relevant bands were excised from the stained gel and their composition analysed by tryptic digest MS, fingerprinting observed using the SwissProt search engine.

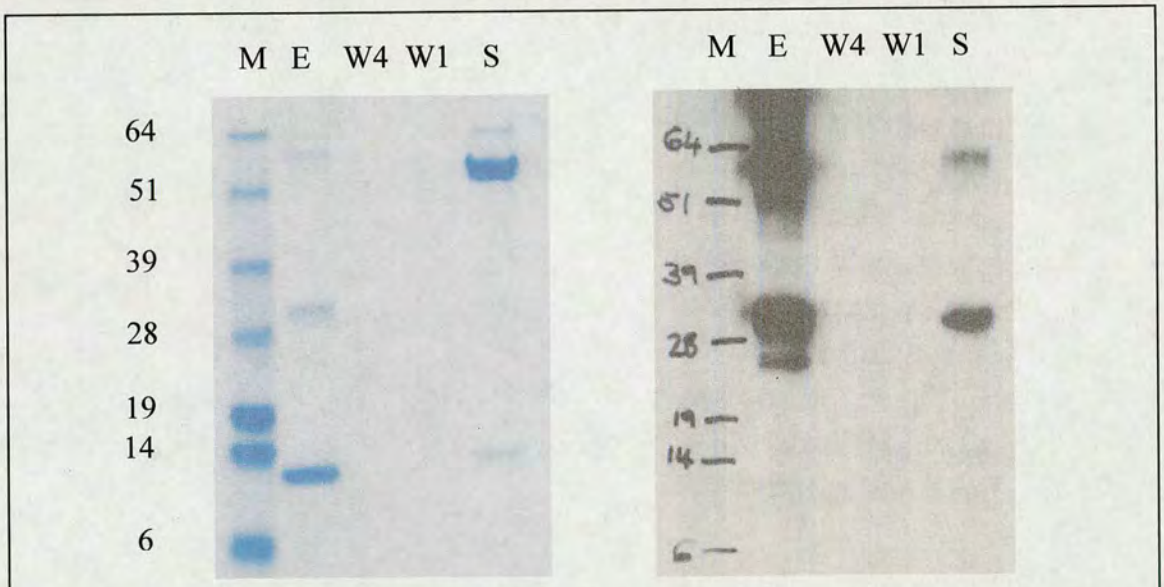

Figure 4.39: Scrapie affinity purified 14-3-3 protein. The GelCode blue and the Western blotted membrane are shown. Lanes are as follows; M-marker, E-eluted fraction, W4 and W1- wash fractions 4 and 1, and S-supernatant fraction. 14-3-3 can be shown as the band above the 28kDa marker. The prominent band below 14kDa was checked by tryptic digest MALDI-TOF, it was a streptavidin related product.

Aptamer S16-8 was successful in concentrating 14-3-3 protein in scrapie positive ovine CSF. The probe could be used to aid detection of neurodegenerative disease in a TSE.

4.10 Summary, conclusions and suggestions

In this thesis I have described the selection of members of a randomised 40 base oligodeoxynucleotide library as affinity ligands for human 14-3-3γ, the demonstration that some of these do have micromolar binding affinities for this target and to other 14-3-3 isoforms and that at least one of these can be used to selectively bind wild type 14-3-3 protein(s) in mouse brain homogenates and ovine scrapie CSF.

The preliminary steps in the project required construction of a modified gene for the N-terminal $(His)_6$ clone of 14-3-3γ and expression and purification of the tagged protein, and the synthesis of a oligonucleotide library containing *ca* 10^{15} different molecules by solid phase synthesis. The choice of N-tagging rather than C-tagging is noteworthy. Currently the better antibodies for 14-3-3 immunoassay are those raised against N-terminal epitopes which is a region which has a large degree of sequence homology across the family. It could be argued that using a N-terminal tag places might occlude this region by placing it close to the resin and allow preferential selection of ligands specific for other regions of the protein. Gratifyingly, as discussed in Chapter 4, at least one of the selected oligonucleotide ligands (S16-8) bound to 14-3-3γ without perturbing K19 antibody binding to the same protein molecule.

The SELEX process used here was adapted from, and combined techniques from, earlier work in the field. Immobilisation of the target protein to a resin (in this case a nickel resin) allowed unbound aptamers to be washed out and concentration of the bound aptamers. Molecules with an affinity for the resin or the his tag region of the protein were screened out by counter-selection. The SELEX process was monitored by incorporation of radioactivity and this allowed monitoring on a cycle by cycle basis. Basically this was adapted from the approach used by Fitzwater and Polinsky

but here I incorporated the radioactivity during the PCR step which is safer and quicker.[176] The use of resin–based selection, rather than the membrane immobilization system used previously, allowed measurement of the radioactivity by scintillation counting.[67, 160]

Since the genes for all seven of the human 14-3-3 isoforms are available it would have been possible to have built in a counter-selection step to screen out forms binding to isoforms other than γ. Since the eventual aim of the study was to enable detection of elevated 14-3-3 in diseased tissue and not that of one isoform specifically this was not considered worthwhile. Indeed, in the current protocol for vCJD diagnosis by detection of 14-3-3 in CSF by western blotting with antibodies, the levels of 14-3-3 involved are *ca* 3.1±2.9ng/ml which is lower than that found in ovine scrapie and lies at the limit of antibody detection. For this reason an oligonucleotide probe with some affinity for all the 14-3-3 isoforms would be preferred. However it should also be noted that the process could have produced a γ-isoform specific ligand even without counter-selection. Two groups have managed to select aptamers which bind to PrP^{c} and not to PrP^{Sc} without using a procedure involving a counter-selection step.[177,178] Here is should be noted that these proteins have identical sequences but differ in conformation. Another well-cited example is that of the L-arginine specific aptamer described by Geiger *et al.*[179] This aptamer was selected without counter selection for D-arginine but binds has 16,000 fold higher affinity for the L-isomer.

Although there were preliminary indications of sequence convergence after 10 cycles, the hundred oligonucleotides selected and sequenced after sixteen cycles of the SELEX procedure had very divergent sequences. However twenty of these sequences, which were all synthesized as biotinoylated probes, bound to 14-3-3 γ with K_d's in the10^{-5}-10^{-7}M range. Just why no convergence is evident is unknown. The

possibility that the library synthesis was biased enough to have a meaningful effect is unlikely. It could be argued that continuing the SELEX for several more cycles and/or using more stringent washing conditions could have seen the emergence of some consensus. However the lack of similarity between the candidate sequences after sixteen cycles suggests no clustering into 'families' and this suggests that more cycles would only have cut down the number of ligands without necessarily resulting in the emergence of one or two very high affinity types. A possibility which seems likely is that this protein has no single overwhelmingly attractive site for ssDNA binding and that we are observing several series of aptamers which dock in just slightly different conformations to a variety of sites. Ultimately only structural studies for example by X-ray crystallography or NMR will be able to throw light on this aspect. I had the opportunity to discuss this with Professor Krylov at the conference and he indicated that the phenomenon of a 'library' of DNA (or RNA) ligands with no striking sequence homology had also occurred in his laboratory.

In this work only a few (20%) of the possible aptamers have been evaluated for binding and the aptamer-protein interactions of only a few of these have been characterised further. S16-1 and S16-8 both proved to be non-selective for the γ-isoform and were shown to bind (albeit slightly less strongly) to other 14-3-3 isoforms. This justifies, to some extent, the decision not to include counter-selection steps in the SELEX procedure. The best 14-3-3 ligand examined so far, S16-8, has proven to bind wild type 14-3-3 in both brain homogenate and ovine scrapie CSF although in the latter case it also appears to show some binding with high molecular weight material which also interacts with the 14-3-3 antibody, K-19. The reason for this is unclear and this will have to be examined further.

The results obtained in this project lay the foundation for future development of assays for 14-3-3 in the diagnosis of neurodegenerative diseases. The S16 library prepared in this work may prove a valuable source of ligands which can be developed as tools for investigation of protein-DNA interactions and of non-antibody based diagnostic 14-3-3 assays.

Chapter 5: Bibliography

[1] BW Moore, V. P. "Physiological and Biochemical Aspects of Nervous Integration." (1967) Englewood Cliffs, NJ, Prentice-Hall.

[2] Ichimura, T., Isobe, T., Okuyama, T., Yamauchi, T., and Fujisawa, H. "Brain 14-3-3 protein is an activator protein that activates tryptophan 5-monooxygenase and tyrosine 3-monooxygenase in the presence of Ca2+,calmodulin-dependent protein kinase II." (1987), FEBS Lett 219, 79-82.

[3] Ichimura, T., Isobe, T., Okuyama, T., Takahashi, N., Araki, K., Kuwano, R., and Takahashi, Y. "Molecular cloning of cDNA coding for brain-specific 14-3-3 protein, a protein kinase-dependent activator of tyrosine and tryptophan hydroxylases." (1988) Proc Natl Acad Sci U S A 85, 7084-7088.

[4] Aitken, A., Ellis, C. A., Harris, A., Sellers, L. A., and Toker, A. "Kinase and neurotransmitters." (1990) Nature 344, 594.

[5] Toker, A., Ellis, C. A., Sellers, L. A., and Aitken, A. "Protein kinase C inhibitor proteins. Purification from sheep brain and sequence similarity to lipocortins and 14-3-3 protein." (1990) Eur J Biochem 191, 421-429.

[6] Morgan, A., and Burgoyne, R. D. "Exo1 and Exo2 proteins stimulate calcium-dependent exocytosis in permeabilized adrenal chromaffin cells." (1992) Nature 355, 833-836.

[7] Tzivion, G., Luo, Z., and Avruch, J. "A dimeric 14-3-3 protein is an essential cofactor for Raf kinase activity." (1998) Nature 394, 88-92.

[8] Dougherty, M. K. and Morrison D. K. "Unlocking the code of 14-3-3." (2004). J Cell Sci 117(Pt 10): 1875-84.

[9] Boston, P. F., and Jackson, P "Purification, properties, and immunohistochemical localisation of human brain 14-3-3 protein." (1982) J Neurochem 38(5): 1466-1474.

[10] Fu, H., Subramanian, R. R., and Masters, S. C. "14-3-3 proteins: structure, function, and regulation." (2000) Annu Rev Pharmacol Toxicol 40, 617-647.

[11] Toker, A., Sellers, L. A., Amess, B., Patel, Y., Harris, A., and Aitken, A. "Multiple isoforms of a protein kinase C inhibitor (KCIP-1/14-3-3) from sheep brain. Amino acid sequence of phosphorylated forms." (1992) Eur J Biochem 206, 453-461.

[12] Aitken, A., Jones, D., Soneji, Y., and Howell, S. "14-3-3 proteins: biological function and domain structure." (1995) Biochem Soc Trans 23, 605-611.

[13] Rosenquist, M., Sehnke, P., Ferl, R. J., Sommarin, M. and Larsson, C. "Evolution of the 14-3-3 protein family: does the large number of isoforms in multicellular organisms reflect functional specificity?" (2000) J Mol Evol 51, 446-458.

[14] Aitken, A. "Functional specificity in 14-3-3 isoform interactions through dimer formation and phosphorylation. Chromosome location of mammalian isoforms and variants." (2002) Plant Mol Biol 50: 993-1010.

[15] Isobe, T., Ichimura, T. and Okuyama, T. "Chemistry and cell biology of neuron- and glia-specific proteins." (1989) Arch Histol Cytol 52 Suppl: 25-32.

[16] Celis, J. E., Gesser, B., Rasmussen, H. H., Madsen, P., Leffers, H., Dejgaard, K., Honore, B., Olsen, E., Ratz, G., Lauridsen, J. B., and et al. "Comprehensive two-dimensional gel protein databases offer a global approach to the analysis of human cells: the transformed amnion cells (AMA) master database and its link to genome DNA sequence data." (1990) Electrophoresis 11, 989-1071.

[17] Nielsen, P. J., "Primary structure of a human protein kinase regulator protein." (1991) Biochim Biophys Acta 1088: 425-428.

[18] Prasad, G. L., Valverius, E. M., McDuffie, E., and Cooper, H. L. "Complementary DNA cloning of a novel epithelial cell marker protein, HME1, that may be down-regulated in neoplastic mammary cells." (1992) Cell Growth Differ 3: 507-513.

[19] Wang, W., and Shakes, D. C. "Molecular evolution of the 14-3-3 protein family." (1996) J Mol Evol 43, 384-398.

[20] Liu, D., Bienkowska, J., Petosa, C., Collier, R. J., Fu, H., and Liddington, R. "Crystal structure of the zeta isoform of the 14-3-3 protein." (1995) Nature 376, 191-194.

[21] Higgins, D. G., and Sharp, P. M. "CLUSTAL: a package for performing multiple sequence alignment on a microcomputer." (1988) Gene 73, 237-244.

[22] Xiao, B., Smerdon, S. J., Jones, D. H., Dodson, G. G., Soneji, Y., Aitken, A., and Gamblin, S. J. "Structure of a 14-3-3 protein and implications for coordination of multiple signalling pathways." (1995) Nature 376, 188-191.

[23] Yaffe, M. B., Rittinger, K., Volinia, S., Caron, P. R., Aitken, A., Leffers, H., Gamblin, S. J., Smerdon, S. J., and Cantley, L. C. "The structural basis for 14-3-3:phosphopeptide binding specificity." (1997) Cell 91, 961-971.

[24] Petosa, C., Masters, S. C., Bankston, L. A., Pohl, J., Wang, B., Fu, H., and Liddington, R. C. "14-3-3 zeta binds a phosphorylated Raf peptide and an unphosphorylated peptide via its conserved amphipathic groove." (1998) J Biol Chem 273, 16305-16310.

[25] Wang, H., Zhang, L., Liddington, R., and Fu, H. "Mutations in the hydrophobic surface of an amphipathic groove of 14-3-3zeta disrupt its interaction with Raf-1 kinase." (1998) J Biol Chem 273, 16297-16304.

[26] Wang, B., Yang, H., Liu, Y. C., Jelinek, T., Zhang, L., Ruoslahti, E., and Fu, H. "Isolation of high-affinity peptide antagonists of 14-3-3 proteins by phage display." (1999) Biochemistry 38(38): 12499-504.

[27] Hermeking, H., Lengauer, C., Polyak, K., He, T. C., Zhang, L., Thiagalingam, S., Kinzler, K. W., and Vogelstein, B. "14-3-3 sigma is a p53-regulated inhibitor of G2/M progression." (1997) Mol Cell 1, 3-11.

[28] Tzivion, G., Shen, Y. H., and Zhu, J. "14-3-3 proteins; bringing new definitions to scaffolding." (2001) Oncogene 20, 6331-6338.

[29] Muslin, A. J., Tanner, J. W., Allen, P. M., and Shaw, A. S. "Interaction of 14-3-3 with signalling proteins is mediated by the recognition of phosphoserine." (1996) Cell 84, 889-897.

[30] Yaffe, M. B., Rittinger, K., Volinia, S., Caron, P. R., Aitken, A., Leffers, H., Gamblin, S. J., Smerdon, S. J., and Cantley, L. C. "The structural basis for 14-3-3: phosphopeptide binding specificity." (1997) Cell 91, 961-971.

[31] Yaffe, M. B. "How do 14-3-3 proteins work?-- Gatekeeper phosphorylation and the molecular anvil hypothesis." (2002) FEBS Lett, 513(1): 53-57.

[32] Dubois, T., Howell, S., Amess, B., Kerai, P., Learmonth, M., Madrazo, J., Chaudhri, M., Rittinger, K., Scarabel, M., Soneji, Y., and Aitken, A. "Structure and sites of phosphorylation of 14-3-3 protein: role in coordinating signal transduction pathways." (1997) J Protein Chem 16(5): 513-22.

[33] Masters, S. C., Pederson, K. J., Zhang, L., Barbieri, J. T., and Fu, H. "Interaction of 14-3-3 with a nonphosphorylated protein ligand, exoenzyme S of Pseudomonas aeruginosa." (1999) Biochemistry 38, 5216-5221.

[34] Giles, N., Forrest, A., and Gabrielli, B. "14-3-3 acts as an intramolecular bridge to regulate cdc25B localization and activity." (2003) J Biol Chem 278, 28580-28587.

[35] Muslin, A. J., and Xing, H. "14-3-3 proteins: regulation of subcellular localization by molecular interference." (2000) Cell Signal 12, 703-709.

[36] Pozuelo Rubio, M., Geraghty, K. M., Wong, B. H., Wood, N. T., Campbell, D. G., Morrice, N., and Mackintosh, C. "14-3-3-affinity purification of over 200 human phosphoproteins reveals new links to regulation of cellular metabolism, proliferation and trafficking." (2004) Biochem J 379, 395-408.

[37] Aitken, A., Baxter, H., Dubois, T., Clokie, S., Mackie, S., Mitchell, K., Peden, A., and Zemlickova, E. "Specificity of 14-3-3 isoform dimer interactions and phosphorylation." (2002) Biochem Soc Trans 30, 351-360.

[38] Datta, S. R., Katsov, A., Hu, L., Petros, A., Fesik, S. W., Yaffe, M. B., and Greenberg, M. E. "14-3-3 proteins and survival kinases cooperate to inactivate BAD by BH3 domain phosphorylation." (2000) Mol Cell 6, 41-51.

[39] Carrasco, J. L., Castello, M. J., and Vera, P., "14-3-3 mediates transcriptional regulation by modulating nucleocytoplasmic shuttling of tobacco DNA-binding protein phosphatase-1." (2006) J Biol Chem 281(32): 22875-81.

[40] Bulavin, D. V., Higashimoto, Y., Demidenko, Z. N., Meek, S., Graves, P., Phillips, C., Zhao, H., Moody, S. A., Appella, E., Piwnica-Worms, H., and Fornace, A. J., Jr. "Dual phosphorylation controls Cdc25 phosphatases and mitotic entry." (2003) Nat Cell Biol 5, 545-551.

[41] Braselmann, S., and McCormick, F. "Bcr and Raf form a complex in vivo via 14-3-3 proteins." (1995) Embo J 14, 4839-4848.

[42] Lee, M. H., and Lozano, G. "Regulation of the p53-MDM2 pathway by 14-3-3 sigma and other proteins." (2006) Semin Cancer Biol.

[43] Thorson, J. A., Yu, L. W., Hsu, A. L., Shih, N. Y., Graves, P. R., Tanner, J. W., Allen, P. M., Piwnica-Worms, H., and Shaw, A. S. "14-3-3 proteins are required for maintenance of Raf-1 phosphorylation and kinase activity." (1998) Mol Cell Biol 18, 5229-5238.

[44] Green, A. J. "Cerebrospinal fluid brain-derived proteins in the diagnosis of Alzheimer's disease and Creutzfeldt-Jakob disease." (2002) Neuropathol Appl Neurobiol 28(6):427-440.

[45] Wilker, E., and Yaffe, M. B. "14-3-3 Proteins--a focus on cancer and human disease." (2004) J Mol Cell Cardiol 37, 633-642.

[46] Michaud, N. R., Fabian, J. R., Mathes, K. D., and Morrison, D. K., "14-3-3 is not essential for Raf-1 function: identification of Raf-1 proteins that are biologically activated in a 14-3-3- and Ras-independent manner." (1995)Mol Cell Biol 15(6): 3390-7.

[47] Wakabayashi, H., Yano, M., Tachikawa, N., Oka, S., Maeda, M., and Kido, H. "Increased concentrations of 14-3-3 epsilon, gamma and zeta isoforms in cerebrospinal fluid of AIDS patients with neuronal destruction." (2001) Clin Chim Acta 312, 97-105.

[48] Cashman, N. R., and Caughey, B. "Prion diseases--close to effective therapy?" (2004) Nat Rev Drug Discov 3, 874-884.

[49] Griffith, J. S. "Self-replication and scrapie." (1967) Nature 215, 1043-1044.

[50] Prusiner, S. B. "Novel proteinaceous infectious particles cause scrapie." (1982) Science 216, 136-144.

[51] Aguzzi, A., Montrasio, F., and Kaeser, P. S. "Prions: health scare and biological challenge." (2001) Nat Rev Mol Cell Biol 2, 118-126.

[52] Legname, G., Nguyen, H. O., Baskakov, I. V., Cohen, F. E., Dearmond, S. J., and Prusiner, S. B. "Strain-specified characteristics of mouse synthetic prions." (2005) Proc Natl Acad Sci U S A 102, 2168-2173.

[53] Castilla, J., Brun, A., Diaz-San Segundo, F., Salguero, F. J., Gutierrez-Adan, A., Pintado, B., Ramirez, M. A., del Riego, L., and Torres, J. M. "Vertical transmission of bovine spongiform encephalopathy prions evaluated in a transgenic mouse model." (2005) J Virol 79, 8665-8668.

[54] Wallace, M. "Creutzfeldt-Jakob disease: assessment and management." (1993) J Gerontol Nurs 19, 15-22.

[55] Will, R. G., Ironside, J. W., Zeidler, M., Cousens, S. N., Estibeiro, K., Alperovitch, A., Poser, S., Pocchiari, M., Hofman, A., and Smith, P. G. "A new variant of Creutzfeldt-Jakob disease in the UK." (1996) Lancet 347, 921-925.

[56] Bruce, M. E., Will, R. G., Ironside, J. W., McConnell, I., Drummond, D., Suttie, A., McCardle, L., Chree, A., Hope, J., Birkett, C., Cousens, S., Fraser, H., and Bostock, C. J. "Transmissions to mice indicate that 'new variant' CJD is caused by the BSE agent." (1997) Nature 389, 498-501.

[57] Information available from http://www.cjd.ed.ac.uk/figures.htm. The UK National Cruetzfeldt-Jakob Disease Surveillance Unit website.

[58] Safar, J. G., Scott, M., Monaghan, J., Deering, C., Didorenko, S., Vergara, J., Ball, H., Legname, G., Leclerc, E., Solforosi, L., Serban, H., Groth, D., Burton, D. R., Prusiner, S. B., and Williamson, R. A. "Measuring prions causing bovine spongiform encephalopathy or chronic wasting disease by immunoassays and transgenic mice." (2002) Nat Biotechnol 20, 1147-1150.

[59] Zerr, I., Pocchiari, M., Collins, S., Brandel, J. P., de Pedro Cuesta, J., Knight, R. S., Bernheimer, H., Cardone, F., Delasnerie-Laupretre, N., Cuadrado Corrales, N., Ladogana, A., Bodemer, M., Fletcher, A., Awan, T., Ruiz Bremon, A., Budka, H., Laplanche, J. L., Will, R. G., and Poser, S. "Analysis of EEG and CSF 14-3-3 proteins as aids to the diagnosis of Creutzfeldt-Jakob disease." (2000) Neurology 55, 811-815.

[60] Baxter, H. C., Fraser, J. R., Liu, W. G., Forster, J. L., Clokie, S., Steinacker, P., Otto, M., Bahn, E., Wiltfang, J., and Aitken, A. "Specific 14-3-3 isoform detection and immunolocalization in prion diseases." (2002) Biochem Soc Trans 30, 387-391.

[61] Green, A. J., Ramljak, S., Muller, W. E., Knight, R. S., and Schroder, H. C. "Use of 14-3-3 in the diagnosis of Creutzfeldt-Jakob disease." (2002) Neurosci Lett 324, 57-60.

[62] Chapman, T., McKeel, D. W., Jr., and Morris, J. C. "Misleading results with the 14-3-3 assay for the diagnosis of Creutzfeldt-Jakob disease." (2000) Neurology 55, 1396-1397.

[63] Kenney, K. Brechtel, C. Takahashi, H. Kurohara, K. Anderson, P. and Gibbs, C J. Jr. "An enzyme-linked immunosorbent assay to quantify 14-3-3 proteins in the cerebrospinal fluid of suspected Creutzfeldt-Jakob disease patients." (2000) Ann Neurol 48(3), 395-398.

[64] Wiltfang, J., Otto, M., Baxter, H. C., Bodemer, M., Steinacker, P., Bahn, E., Zerr, I., Kornhuber, J., Kretzschmar, H. A., Poser, S., Ruther, E., and Aitken, A. "Isoform pattern of 14-3-3 proteins in the cerebrospinal fluid of patients with Creutzfeldt-Jakob disease." (1999) J Neurochem 73, 2485-2490.

[65] Van Everbroeck, B. R., Boons, J., and Cras, P. "14-3-3 {gamma}-isoform detection distinguishes sporadic Creutzfeldt-Jakob disease from other dementias." (2005) J Neurol Neurosurg Psychiatry 76, 100-102.

[66] Green, A. J., Ramljak, S., Muller, W. E., Knight, R. S., and Schroder, H. C. "14-3-3 in the cerebrospinal fluid of patients with variant and sporadic Creutzfeldt-Jakob disease measured using capture assay able to detect low levels of 14-3-3 protein." (2002) Neurosci Lett 324, 57-60.

[67] Tuerk, C., and Gold, L. "Systematic evolution of ligands by exponential enrichment: RNA ligands to bacteriophage T4 DNA polymerase." (1990) Science 249, 505-510.

[68] Ellington, A. D., and Szostak, J. W. "In vitro selection of RNA molecules that bind specific ligands." (1990) Nature 346, 818-822.

[69] Sullenger, B. A., Gallardo, H. F., Ungers, G. E., and Gilboa, E. "Overexpression of TAR sequences renders cells resistant to human immunodeficiency virus replication." (1990) Cell 63, 601-608.

[70] He, Y. Y., Stockley, P. G., and Gold, L. "In vitro evolution of the DNA binding sites of Escherichia coli methionine repressor, MetJ." (1996) J Mol Biol 255, 55-66.

[71] Hermann, T., and Patel, D. J. "Adaptive recognition by nucleic acid aptamers." (2000) Science 287, 820-825.

[72] Pagratis, N. C., Bell, C., Chang, Y. F., Jennings, S., Fitzwater, T., Jellinek, D., and Dang, C. "Potent 2'-amino-, and 2'-fluoro-2'-deoxyribonucleotide RNA inhibitors of keratinocyte growth factor." (1997) Nat Biotechnol 15, 68-73.

[73] Zimmermann, G. R., Jenison, R. D., Wick, C. L., Simorre, J. P., and Pardi, A. "Interlocking structural motifs mediate molecular discrimination by a theophylline-binding RNA." (1997) Nat Struct Biol 4, 644-649.

[74] Fan, P., Suri, A. K., Fiala, R., Live, D., and Patel, D. J."Molecular recognition in the FMN-RNA aptamer complex." (1996) J Mol Biol 258(3): 480-500.

[75] Lin, C. H., and Patel, D. J. "Structural basis of DNA folding and recognition in an AMP-DNA aptamer complex: distinct architectures but common recognition motifs for DNA and RNA aptamers complexed to AMP." (1997) Chem Biol 4, 817-832.

[76] Jiang, F., Kumar, R. A., Jones, R. A., and Patel, D. J. "Structural basis of RNA folding and recognition in an AMP-RNA aptamer complex." (1996) Nature 382, 183-186.

[77] Dieckmann, T., Suzuki, E., Nakamura, G. K., and Feigon, J. "Solution structure of an ATP-binding RNA aptamer reveals a novel fold." (1996) Rna 2, 628-640.

[78] Lin, C. H., and Patel, D. J. Encapsulating an amino acid in a DNA fold." (1996) Nat Struct Biol 3, 1046-1050.

[79] Lin, C. H., Wang, W., Jones, R. A., and Patel, D. J. "Formation of an amino-acid-binding pocket through adaptive zippering-up of a large DNA hairpin loop." (1998) Chem Biol 5, 555-572.

[80] Yang, Y., Kochoyan, M., Burgstaller, P., Westhof, E., and Famulok, M. "Structural basis of ligand discrimination by two related RNA aptamers resolved by NMR spectroscopy." (1996) Science 272, 1343-1347.

[81] Jiang, L., Suri, A. K., Fiala, R., and Patel, D. J. "Saccharide-RNA recognition in an aminoglycoside antibiotic-RNA aptamer complex." (1997) Chem Biol 4, 35-50.

[82]Jiang, L., and Patel, D. J. "Solution structure of the tobramycin-RNA aptamer complex." (1998) Nat Struct Biol 5, 769-774.

[83] Jiang, L., Majumdar, A., Hu, W., Jaishree, T. J., Xu, W., and Patel, D. J. "Saccharide-RNA recognition in a complex formed between neomycin B and an RNA aptamer." (1999) Structure 7, 817-827.

[84] Ye, X., Gorin, A., Ellington, A. D., and Patel, D. J. "Deep penetration of an alpha-helix into a widened RNA major groove in the HIV-1 rev peptide-RNA aptamer complex." (1996) Nat Struct Biol 3, 1026-1033.

[85] Baskerville, S., Zapp, M., and Ellington, A. D. "Anti-Rex aptamers as mimics of the Rex-binding element." (1999) J Virol 73, 4962-4971.

[86] Convery, M. A., Rowsell, S., Stonehouse, N. J., Ellington, A. D., Hirao, I., Murray, J. B., Peabody, D. S., Phillips, S. E., and Stockley, P. G. "Crystal structure of an RNA aptamer-protein complex at 2.8 A resolution." (1998) Nat Struct Biol 5, 133-139.

[87] Wang, K. Y., McCurdy, S., Shea, R. G., Swaminathan, S., and Bolton, P. H. "A DNA aptamer which binds to and inhibits thrombin exhibits a new structural motif for DNA." (1993) Biochemistry 32, 1899-1904.

[88] Padmanabhan, K., Padmanabhan, K. P., Ferrara, J. D., Sadler, J. E., and Tulinsky, A. "The structure of alpha-thrombin inhibited by a 15-mer single-stranded DNA aptamer." (1993) J Biol Chem 268, 17651-17654.

[89] Robertson, S. A., Harada, K., Frankel, A. D., and Wemmer, D. E. "Structure determination and binding kinetics of a DNA aptamer-argininamide complex." (2000) Biochemistry 39, 946-954.

[90] Sussman, D., Nix, J. C., and Wilson, C. "The structural basis for molecular recognition by the vitamin B 12 RNA aptamer." (2000) Nat Struct Biol 7, 53-57.

[91] Baugh, C., Grate, D., and Wilson, C. "2.8 Å crystal structure of the malachite green aptamer." (2000) J Mol Biol 301, 117-128.

[92] Nix, J., Sussman, D., and Wilson, C. "The 1.3 Å crystal structure of a biotin-binding pseudoknot and the basis for RNA molecular recognition." (2000) J Mol Biol 296, 1235-1244.

[93] Katahira, M., Kobayashi, S., Matsugami, A., Ouhashi, K., Uesugi, S., Yamamoto, R., Taira, K., Nishikawa, S., and Kumar, P. "Structural study of an RNA aptamer for a Tat protein complexed with ligands." (1999) Nucleic Acids Symp Ser, 269-270.

[94] Piganeau, N., and Schroeder, R. "Aptamer structures: a preview into regulatory pathways?" (2003) Chem Biol 10, 103-104.

[95] Huang, D. B., Vu, D., Cassiday, L. A., Zimmerman, J. M., Maher, L. J., 3rd, and Ghosh, G. "Crystal structure of NF-kappaB (p50)2 complexed to a high-affinity RNA aptamer." (2003) Proc Natl Acad Sci U S A 100, 9268-9273.

[96] Shafer, R. H., and Smirnov, I. "Biological aspects of DNA/RNA quadruplexes." (2000) Biopolymers 56, 209-227.

[97] Mandal, M., and Breaker, R. R. "Gene regulation by riboswitches." (2004) Nat Rev Mol Cell Biol 5, 451-463.

[98] Dewey, T. M., Mundt, A., Crouch G. J., Zyzniewski, M. C., and Eaton, B. E., "New Uridine Derivatives for Systematic Evolution of RNA Ligands by Exponential Enrichment" (1995) J Am Chem Soc 117, (32) 8474-8475.

[99] Eaton, B. E. "The joys of in vitro selection: chemically dressing oligonucleotides to satiate protein targets." (1997) Curr Opin Chem Biol 1, 10-16.

[100] Eaton, B. E., and Pieken, W. A. "Ribonucleosides and RNA." (1995) Annu Rev Biochem 64, 837-863.

[101] Klussmann, S., Nolte, A., Bald, R., Erdmann, V. A., and Furste, J. P. "Mirror-image RNA that binds D-adenosine." (1996) Nat Biotechnol 14, 1112-1115.

[102] Cesareni, G. "Peptide display on filamentous phage capsids. A new powerful tool to study protein-ligand interaction." (1992) FEBS Lett 307, 66-70.

[103] James, W. "Aptamers." (2000) Encyclopedia of Analytical Chemistry :4848–4871.

[104] Wallace, S. T., and Schroeder, R. "In vitro selection and characterization of streptomycin-binding RNAs: recognition discrimination between antibiotics." (1998) Rna 4, 112-123.

[105] Bock, L. C., Griffin, L. C., Latham, J. A., Vermaas, E. H., and Toole, J. J. "Selection of single-stranded DNA molecules that bind and inhibit human thrombin." (1992) Nature 355, 564-566.

[106] Gal, S. W., Amontov, S., Urvil, P. T., Vishnuvardhan, D., Nishikawa, F., Kumar, P. K., and Nishikawa, S. "Selection of a RNA aptamer that binds to human activated protein C and inhibits its protease function." (1998) Eur J Biochem 252, 553-562.

[107] Jayasena, S. D. "Aptamers: an emerging class of molecules that rival antibodies in diagnostics." (1999) Clin Chem 45, 1628-1650.

[108] Breaker, R. R. "DNA aptamers and DNA enzymes." (1997) Curr Opin Chem Biol 1, 26-31.

[109] Famulok, M., Mayer, G., and Blind, M. "Nucleic acid aptamers-from selection in vitro to applications in vivo." (2000) Acc Chem Res 33, 591-599.

[110] Carey, J., Cameron, V., de Haseth, P. L., and Uhlenbeck, O. C. "Sequence-specific interaction of R17 coat protein with its ribonucleic acid binding site." (1983) Biochemistry 22, 2601-2610.

[111] Cox, J. C., Rajendran, M., Riedel, T., Davidson, E. A., Sooter, L. J., Bayer, T. S., Schmitz-Brown, M., and Ellington, A. D. "Automated acquisition of aptamer sequences." (2002) Comb Chem High Throughput Screen 5, 289-299.

[112] Mendonsa, S. D., and Bowser, M. T. "In vitro selection of high-affinity DNA ligands for human IgE using capillary electrophoresis." (2004) Anal Chem 76, 5387-5392.

[113] Espelund, M., Stacy, R. A., and Jakobsen, K. S. "A simple method for generating single-stranded DNA probes labeled to high activities." (1990) Nucleic Acids Res 18, 6157-6158.

[114] Fukusaki, E., Hasunuma, T., Kajiyama, S., Okazawa, A., Itoh, T. J., and Kobayashi, A. "SELEX for tubulin affords specific T-rich DNA aptamers. Systematic evolution of ligands by exponeential enrichment." (2001) Bioorg Med Chem Lett 11, 2927-2930.

[115] Jeter, M. L., Ly, L. V., Fortenberry, Y. M., Whinna, H. C., White, R. R., Rusconi, C. P., Sullenger, B. A., and Church, F. C. "RNA aptamer to thrombin binds anion-binding exosite-2 and alters protease inhibition by heparin-binding serpins." (2004) FEBS Lett 568, 10-14.

[116] Burke, D. H., and Gold, L. "RNA aptamers to the adenosine moiety of S-adenosyl methionine: structural inferences from variations on a theme and the reproducibility of SELEX." (1997) Nucleic Acids Res 25, 2020-2024.

[117] Patel, D. J., Suri, A. K., Jiang, F., Jiang, L., Fan, P., Kumar, R. A., and Nonin, S. "Structure, recognition and adaptive binding in RNA aptamer complexes." (1997) J Mol Biol 272, 645-664.

[118] Griffin, L. C., Toole, J. J., and Leung, L. L. "The discovery and characterization of a novel nucleotide-based thrombin inhibitor." (1993) Gene 137, 25-31.

[119] Kohler, G. and Milstein, C. "Continuous cultures of fused cells secreting antibody of predefined specificity." (1975) Nature 256(5517): 495-497.

[120] White, R., Rusconi, C., Scardino, E., Wolberg, A., Lawson, J., Hoffman, M., and Sullenger, B. "Generation of species cross-reactive aptamers using "toggle" SELEX." (2001) Mol Ther 4, 567-573.

[121] Tobin, K. A. Macugen treatment for wet age-related macular degeneration." (2006) Insight 31, 11-14.

[122] Nimjee, S. M., Rusconi, C. P., and Sullenger, B. A. "Aptamers: an emerging class of therapeutics." (2005) Annu Rev Med 56, 555-583.

[123] Yamamoto, R., Katahira, M., Nishikawa, S., Baba, T., Taira, K., and Kumar, P. K. "A novel RNA motif that binds efficiently and specifically to the Ttat protein of HIV and inhibits the trans-activation by Tat of transcription in vitro and in vivo." (2000) Genes Cells 5, 371-388.

[124] Browning, C. M., Cagnon, L., Good, P. D., Rossi, J., Engelke, D. R., and Markovitz, D. M. "Potent inhibition of human immunodeficiency virus type 1 (HIV-1) gene expression and virus production by an HIV-2 tat activation-response RNA decoy." (1999) J Virol 73, 5191-5195

[125] Kohn, D. B., Bauer, G., Rice, C. R., Rothschild, J. C., Carbonaro, D. A., Valdez, P., Hao, Q., Zhou, C., Bahner, I., Kearns, K., Brody, K., Fox, S., Haden, E., Wilson, K., Salata, C., Dolan, C., Wetter, C., Aguilar-Cordova, E., and Church, J. "A clinical trial of retroviral-mediated transfer of a rev-responsive element decoy gene into CD34(+) cells from the bone marrow of human immunodeficiency virus-1-infected children." (1999) Blood 94, 368-371

[126] Kumar, P. K., Machida, K., Urvil, P. T., Kakiuchi, N., Vishnuvardhan, D., Shimotohno, K., Taira, K., and Nishikawa, S. "Isolation of RNA aptamers specific to

the NS3 protein of hepatitis C virus from a pool of completely random RNA." (1997) Virology 237, 270-282.

[127] Proske, D., Gilch, S., Wopfner, F., Schatzl, H. M., Winnacker, E. L., and Famulok, M. "Prion-protein-specific aptamer reduces PrPSc formation." (2002) Chembiochem 3, 717-725.

[128] DeAnda, A., Jr., Coutre, S. E., Moon, M. R., Vial, C. M., Griffin, L. C., Law, V. S., Komeda, M., Leung, L. L., and Miller, D. C. "Pilot study of the efficacy of a thrombin inhibitor for use during cardiopulmonary bypass." (1994) Ann Thorac Surg 58, 344-350.

[129] Eyetech Study Group "Preclinical and phase 1A clinical evaluation of an anti-VEGF pegylated aptamer (EYE001) for the treatment of exudative age-related macular degeneration." (2002) Retina 22(2): 143-152.

[130] Pietras, K., Ostman, A., Sjoquist, M., Buchdunger, E., Reed, R. K., Heldin, C. H., and Rubin, K. "Inhibition of platelet-derived growth factor receptors reduces interstitial hypertension and increases transcapillary transport in tumors." (2001) Cancer Res 61, 2929-2934.

[131] Mann, M. J., Whittemore, A. D., Donaldson, M. C., Belkin, M., Conte, M. S., Polak, J. F., Orav, E. J., Ehsan, A., Dell'Acqua, G., and Dzau, V. J. "Ex-vivo gene therapy of human vascular bypass grafts with E2F decoy: the PREVENT single-centre, randomised, controlled trial." (1999) Lancet 354, 1493-1498.

[132] Santulli-Marotto, S., Nair, S. K., Rusconi, C., Sullenger, B., and Gilboa, E. "Multivalent RNA aptamers that inhibit CTLA-4 and enhance tumor immunity." (2003) Cancer Res 63, 7483-7489.

[133] Ravelet, C., Boulkedid, R., Ravel, A., Grosset, C., Villet, A., Fize, J., and Peyrin, E. "A L-RNA aptamer chiral stationary phase for the resolution of target and related compounds." (2005) J Chromatogr A 1076, 62-70.

[134] Michaud, M., Jourdan, E., Villet, A., Ravel, A., Grosset, C., and Peyrin, E. "A DNA aptamer as a new target-specific chiral selector for HPLC." (2003) J Am Chem Soc 125, 8672-8679.

[135] Romig, T. S., Bell, C., and Drolet, D. W. "Aptamer affinity chromatography: combinatorial chemistry applied to protein purification." (1999) J Chromatogr B Biomed Sci Appl 731, 275-284.

[136] Engvall, E., Jonsson, K., and Perlmann, P. "Enzyme-linked immunosorbent assay. II. Quantitative assay of protein antigen, immunoglobulin G, by means of enzyme-labelled antigen and antibody-coated tubes." (1971) Biochim Biophys Acta 251, 427-434.

[137] Drolet, D. W., Moon-McDermott, L., and Romig, T. S. "An enzyme-linked oligonucleotide assay." (1996) Nat Biotechnol 14, 1021-1025.

[138] Dick, L. W., Jr., and McGown, L. B. "Aptamer-enhanced laser desorption/ionization for affinity mass spectrometry." (2004) Anal Chem 76, 3037-3041.

[139] Connor, A. C., Frederick, K. A., Morgan, E. J., and McGown, L. B. "Insulin capture by an insulin-linked polymorphic region G-quadruplex DNA oligonucleotide." (2006) J Am Chem Soc 128, 4986-4991.

[140] Rajendran, M., and Ellington, A. D. "In vitro selection of molecular beacons." (2003) Nucleic Acids Res 31, 5700-5713.

[141] Hamaguchi, N., Ellington, A., and Stanton, M. "Aptamer beacons for the direct detection of proteins." (2001) Anal Biochem 294, 126-131.

[142] Khati, M., Schuman, M., Ibrahim, J., Sattentau, Q., Gordon, S., and James, W. "Neutralization of infectivity of diverse R5 clinical isolates of human immunodeficiency virus type 1 by gp120-binding 2'F-RNA aptamers." (2003) J Virol 77, 12692-12698.

[143] Misono, T. S., and Kumar, P. K. "Selection of RNA aptamers against human influenza virus hemagglutinin using surface plasmon resonance." (2005) Anal Biochem 342, 312-317.

[144] Huang, C. C., Huang, Y. F., Cao, Z., Tan, W., and Chang, H. T. "Aptamer-modified gold nanoparticles for colorimetric determination of platelet-derived growth factors and their receptors." (2005) Anal Chem 77, 5735-5741.

[145] Tartof, K.D. and Hobbs, C. A. "New cloning vectors and techniques for easy and rapid restriction mapping." (1988) Gene 67(2), 169-182.

[146] Sanger, F. Donelson, J. E. Coulson, A. R. Kossel, H. Fisher, D. "Determination of a nucleotide sequence in bacteriophage f1 DNA by primed synthesis with DNA polymerase." (1974) J Mol Biol 90, 315-333.

[147] Sambrook, J., Fritsch, E.F., and Maniatis, T. "in Molecular Cloning: A Laboratory Manual" (1989) Cold Spring Harbor Laboratory Press, NY, Vol. 1,2,3.

[148] King, J. and Laemmli U. K. "Polypeptides of the tail fibres of bacteriophage T4" (1971) J Mol Biol 62, 465-477.

[149] Bradford, M. M. "A rapid and sensitive method for the quantitation of microgram quantities of protein utilizing the principle of protein-dye binding." (1976) Anal Biochem 72, 248-254.

[150] Jones, D. H., Martin, H., Madrazo, J., Robinson, K. A., Nielsen, P., Roseboom, P. H., Patel, Y., Howell, S. A., and Aitken, A. "Expression and structural analysis of 14-3-3 proteins." (1995) J Mol Biol 245, 375-384.

[151] Zhan, Y., Song, X., and Zhou, G. W. "Structural analysis of regulatory protein domains using GST-fusion proteins." (2001) Gene 281, 1-9.

[152] Gasteiger E., Gattiker A., Hoogland C., Ivanyi I., Appel R.D., and Bairoch A. "ExPASy: the proteomics server for in-depth protein knowledge and analysis" (2003) Nucleic Acids Res. 31:3784-3788.

[153] Wang, C., Zhang, M., Yang, G., Zhang, D., Ding, H., Wang, H., Fan, M., Shen, B., and Shao, N. "Single-stranded DNA aptamers that bind differentiated but not parental cells: subtractive systematic evolution of ligands by exponential enrichment." (2003) J Biotechnol 102, 15-22.

[154] Kelly, S. M. and Price N. C. "The use of circular dichroism in the investigation of protein structure and function." (2000) Curr Protein Pept Sci 1(4): 349-384.

[155] Lobley, A., L. Whitmore, et al. (2002). "DICHROWEB: an interactive website for the analysis of protein secondary structure from circular dichroism spectra." Bioinformatics 18(1): 211-2.

[156] Robinson, K., Jones, D., Patel, Y., Martin, H., Madrazo, J., Martin, S., Howell, S., Elmore, M., Finnen, M. J., and Aitken, A. "Mechanism of inhibition of protein kinase C by 14-3-3 isoforms. 14-3-3 isoforms do not have phospholipase A2 activity." (1994) Biochem J 299 (Pt 3), 853-861.

[157] Brigham-Burke, M. Edwards, J. R. and O'Shannessy, D. J. "Detection of receptor-ligand interactions using surface plasmon resonance: model studies employing the HIV-1 gp120/CD4 interaction." (1992) Anal Biochem (205)1:125-131.

[158] Murphy, M. B., Fuller, S. T., Richardson, P. M., and Doyle, S. A. "An improved method for the in vitro evolution of aptamers and applications in protein detection and purification." (2003) Nucleic Acids Res 31, e110.

[159] Green, L. S., Jellinek, D., Jenison, R., Ostman, A., Heldin, C. H., and Janjic, N. "Inhibitory DNA ligands to platelet-derived growth factor B-chain." (1996) Biochemistry 35, 14413-14424.

[160] Sinha, N. D., Biernat, J., McManus, J., and Koster, H. "Polymer support oligonucleotide synthesis XVIII: use of beta-cyanoethyl-N,N-dialkylamino-/N-morpholino phosphoramidite of deoxynucleosides for the synthesis of DNA fragments simplifying deprotection and isolation of the final product." (1984) Nucleic Acids Res 12, 4539-4557.

[161] Irvine, D., Tuerk, C., and Gold, L. "SELEXION. Systematic evolution of ligands by exponential enrichment with integrated optimization by non-linear analysis." (1991) J Mol Biol 222, 739-761.

[162] Vianini, E., Palumbo, M., and Gatto, B. "In vitro selection of DNA aptamers that bind L-tyrosinamide." (2001) Bioorg Med Chem 9, 2543-2548.

[163] Thompson, J. D., Higgins, D. G., and Gibson, T. J. "CLUSTAL W: improving the sensitivity of progressive multiple sequence alignment through sequence weighting, position-specific gap penalties and weight matrix choice." (1994) Nucleic Acids Res 22, 4673-4680.

[164] Zuker, M. "Mfold web server for nucleic acid folding and hybridization prediction." (2003) Nucleic Acids Res 31, 3406-3415.

[165] Saitou, N., and Nei, M. "The neighbor-joining method: a new method for reconstructing phylogenetic trees." (1987) Mol Biol Evol 4, 406-425.

[166] Sayer, N., Ibrahim, J., Turner, K., Tahiri-Alaoui, A., and James, W. "Structural characterization of a 2'F-RNA aptamer that binds a HIV-1 SU glycoprotein, gp120." (2002) Biochem Biophys Res Commun 293, 924-931.

[167] Guthrie, J. W., Hamula, C. L., Zhang, H., and Le, X. C. "Assays for cytokines using aptamers." (2006) Methods 38, 324-330.

[168] Tang, J., Xie, J., Shao, N., and Yan, Y. "The DNA aptamers that specifically recognize ricin toxin are selected by two in vitro selection methods." (2006) Electrophoresis 27, 1303-1311.

[169] Moreno, M., Rincon, E., Pineiro, D., Fernandez, G., Domingo, A., Jimenez-Ruiz, A., Salinas, M., and Gonzalez, V. M. "Selection of aptamers against KMP-11 using colloidal gold during the SELEX process." (2003) Biochem Biophys Res Commun 308, 214-218.

[170] Missailidis, S., Thomaidou, D., Borbas, K. E., and Price, M. R. "Selection of aptamers with high affinity and high specificity against C595, an anti-MUC1 IgG3 monoclonal antibody, for antibody targeting." (2005) J Immunol Methods 296, 45-62.

[171] Liliom, K., Orosz, F., Horvath, L., and Ovadi, J. "Quantitative evaluation of indirect ELISA. Effect of calmodulin antagonists on antibody binding to calmodulin." (1991) J Immunol Methods 143, 119-125.

[172] Orosz, F., and Ovadi, J. "A simple method for the determination of dissociation constants by displacement ELISA." (2002) J Immunol Methods 270, 155-162.

[173] Bachler, M., Schroeder, R., and von Ahsen, U. "StreptoTag: a novel method for the isolation of RNA-binding proteins." (1999) Rna 5, 1509-1516.

[174] Locker, N., Easton, L. E., and Lukavsky, P. J. "Affinity purification of eukaryotic 48S initiation complexes." (2006) Rna 12, 683-690.

[175] Hsich, G., Kenney, K., Gibbs, C. J., Lee, K. H., and Harrington, M. G. "The 14-3-3 brain protein in cerebrospinal fluid as a marker for transmissible spongiform encephalopathies." (1996) N Engl J Med 335, 924-930.

[176] Fitzwater, T., and Polisky, B. "A SELEX primer." (1996) Methods Enzymol 267, 275-301.

[177] Sayer, N. M., Cubin, M., Rhie, A., Bullock, M., Tahiri-Alaoui, A., and James, W. "Structural determinants of conformationally selective, prion-binding aptamers." (2004) J Biol Chem 279, 13102-13109.

[178] Weiss, S., Proske, D., Neumann, M., Groschup, M. H., Kretzschmar, H. A., Famulok, M., and Winnacker, E. L. "RNA aptamers specifically interact with the prion protein PrP." (1997) J Virol 71, 8790-8797.

[179] Geiger, A., Burgstaller, P., von der Eltz, H., Roeder, A., and Famulok, M. "RNA aptamers that bind L-arginine with sub-micromolar dissociation constants and high enantioselectivity." (1996) Nucleic Acids Res 24, 1029-1036.

[181] Shi, B., Stevenson, R., Campopiano, D. J., and Greaney, M. F. "Discovery of glutathione S-transferase inhibitors using dynamic combinatorial chemistry" (2006) J Am Chem Soc 128(26), 8259-8267.

Appendix I: Structural Comparison of CLONES

Questions posed by this study are (a) why do the selected aptamers interact with 14-3-3 proteins? (b) Why different aptamers show different association to 14-3-3 proteins? The answer to both questions may be related to the tertiary structure adopted by each aptamer species. The tertiary structure can be obtained by either analysing the X-ray crystal structure of the protein/aptamer complex, or the NMR result observed for the complex. Ideally the interaction of S16-8 with $(His)_6$14-3-3γ could have been analysed using either method.

A possible secondary structure for ssDNA folding can be anticipated using the mfold algorithm and as such, the structures of the two best aptamers, S16-8 and S16-1 had their possible secondary structures computed (shown in **Figure I**).

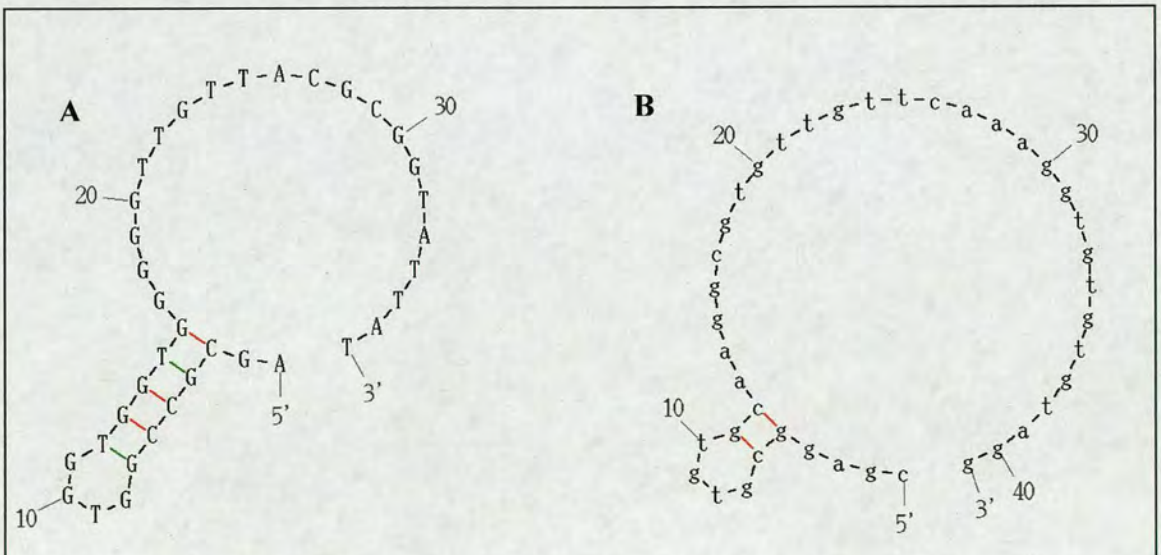

Figure I: Aptamer S16.1 and S16.8. The folded S16.1 (A) structure has a dG -1.53 kcal/mol and was the aptamer used in the above SPR analysis. S16.8 (B) was a clone that consistently showed promise in the aptamer linked enzyme assay dG -1.12.kcal/mol.

The actual secondary structures may differ from those presented. There may be a number of weaker stabilising interactions, not considered by the mfold algorithm that

relies heavily on Watson-Crick pairing when calculating the secondary structure of ssDNA. Sequence S16-1and S16-8 look to provide scope for G-quartets although of all possible mfold structures, none contain that motif. The algorithm used in mfold does not allow for g-quartets.

S16-1; agcg ccgg tggt ggtg gggg ttgt tacg cggt atta t.

S16-8; cgag gcgt gtgc aagg cgtg ttgt tcaa aggt gtgt gtag g

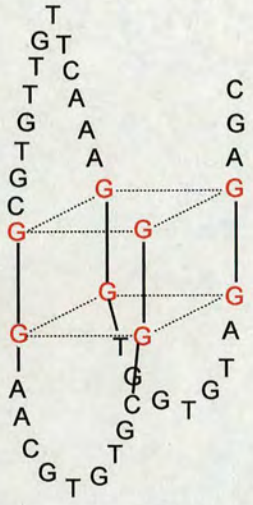

Fig II: A diagrammatical representation of aptamer S16-8 forming a g-quartet structure. The g-quartet is highlighted in red, is to emphasise one of many possible secondary structures.

While analysing the cycle 16 sequencing data, an aptamer not synthetically produced for further analysis, stood out due to its high guanine content. Sequence S16-28, looks to potentially provide a g-quartet structure although this is not suggested by the mfold algorithim The structure that is predicted, does still had a strong secondary structure however (dG -6.57 kcal/mol).

S16-28; gagc gggg gctc gggc tgga acac ggag gccc ggga cgta

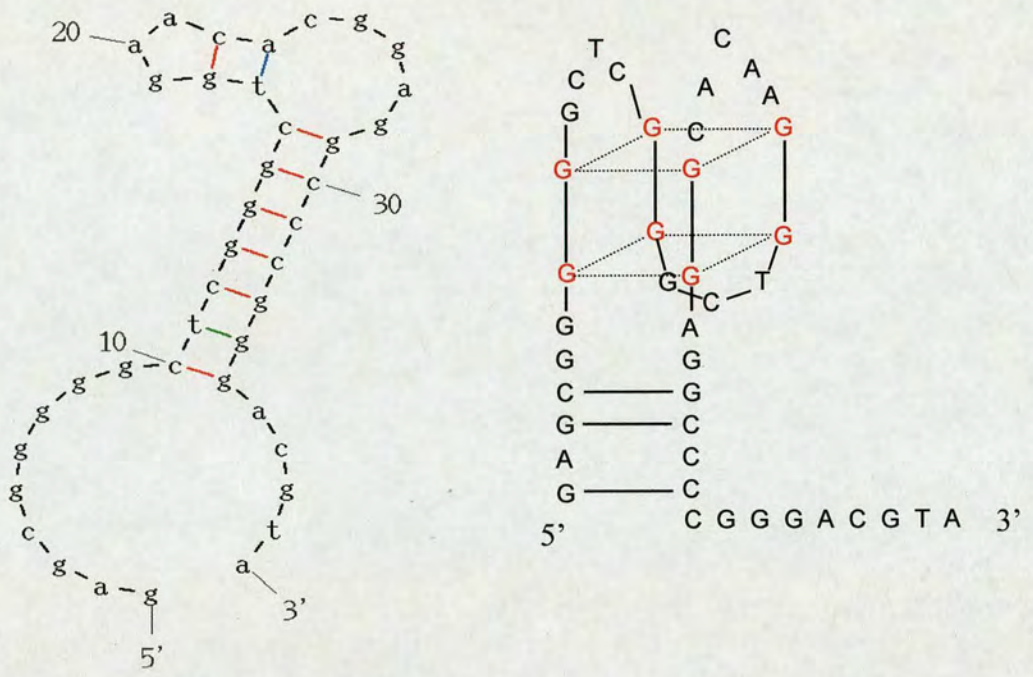

Figure III: The mfold predicted structure for S16-28 and diagrammatical representation of a possible G-Quartet structure. The structure has a dG -6.57kcal/mol, and a more definite structure than S16-1 and S16-8.

The example of S16-28, provides the kind of result that hoped for at the start of the SELEX process. S16-8 is not however, is not representative of the remaining aptamer pool in general and was perhaps undeserving of additional attention. The SELEX process had dictated which aptamers were to be successful and all those collected at the end of cycle 16 have a realistic chance of having the best association to the expressed 14-3-3γ. Trying to second guess what aptamers may be best from a probable structure was unlikely to yield profitable results. A far more effective method was likely to be finding out binding by SPR or by ELONA.

Appendix II – Tryptic digest MS Data

Analysis of the bands removed from the MBH affinity purification and the scrapie affinity purification led to the following results.

Database searched: **SwissProt.200406**
Molecular weight search (**1000 - 100000 Da**) selects **187433** entries.
Full pI range: **198834** entries.
Combined molecular weight and pI searches select **187433** entries.
MS-Fit search selects **2933** entries (results displayed for top **15** matches).

– **Result Summary**

1	**5.56e+007**	**12/98 (12%)**	**69188.7 / 5.80**	SHEEP	**P14639** Serum albumin precursor
2	**1.21e+005**	**8/98 (8%)**	**69293.9 / 5.82**	BOVIN	**P02769** Serum albumin precursor (Allergen Bos d 6) (BSA)
3	**3.72e+004**	**8/98 (8%)**	**80364.1 / 5.97**	MOUSE	**Q9D6Y9** 1,4-alpha-glucan branching enzyme (Glycogen branching enzyme) (Brancher enzyme)
4	**2.21e+004**	**9/98 (9%)**	**99428.2 / 4.95**	RAT	**O35550** Rab GTPase-binding effector protein 1 (Rabaptin-5) (Rabaptin-5alpha)
5	**2.2e+004**	**9/98 (9%)**	**99552.4 / 4.97**	MOUSE	**O35551** Rab GTPase-binding effector protein 1 (Rabaptin- 5) (Rabaptin-5alpha)

Detailed Results
1. 12/98 matches (12%). 69188.7 Da, pI = 5.80. Acc. # P14639. SHEEP. Serum albumin precursor.

Database searched: **SwissProt.200406**
Molecular weight search (**1000 - 100000 Da**) selects **187433** entries.
Full pI range: **198834** entries.
Combined molecular weight and pI searches select **187433** entries.
MS-Fit search selects **2933** entries (results displayed for top **5** matches).

– **Result Summary**

1	**6.09e+006**	**11/82 (13%)**	**28252.7 / 4.80**	BOVIN	**P68252** 14-3-3 protein gamma (Protein kinase C inhibitor protein 1) (KCIP-1)
2	**6.08e+006**	**11/82 (13%)**	**28302.7 / 4.80**	RAT	**P61983** 14-3-3 protein gammagi|48428722|sp|P61982|1433G_MOUSE 14-3-3 protein gammagi|48428721|sp|P61981|1433G_HUMAN 14-3-3 protein gamma (Protein kinase C inhibitor protein 1) (KCIP-1)gi|68565133|sp|Q5RC20|1433G_PONPY 14-3-3 protein gamma
3	**5.78e+005**	**10/82 (12%)**	**28230.7 / 4.84**	CHICK	**Q5F3W6** 14-3-3 protein gamma
4	**9.23e+004**	**9/82 (10%)**	**28244.7 / 4.80**	XENLA	**Q6NRY9** 14-3-3 protein gamma-B
5	**9.22e+004**	**9/82 (10%)**	**28273.7 / 4.80**	XENLA	**Q6PCG0** 14-3-3 protein gamma-A

Detailed Results
1. 11/82 matches (13%). 28252.7 Da, pI = 4.80. Acc. # P68252. BOVIN. 14-3-3 protein gamma (Protein kinase C inhibitor protein 1) (KCIP-1).

Figure IV: MALDI ToF data from affinity purified gel. The bands excised from the gel, figure 4.35, with a molecular weights around 60kDa and 30kDa were identified following tryptic digest MS as ovine serum albumin and 14-3-3 γ, respectively.

Database searched: **SwissProt.200406**
Molecular weight search (**1000 - 100000 Da**) selects **187433** entries.
Full pI range: **198834** entries.
Combined molecular weight and pI searches select **187433** entries.
MS-Fit search selects **2933** entries (results displayed for top **5** matches).

– **Result Summary**

1	**9.37e+005**	**6/69 (8%)**	**18833.8 / 7.94**	STRAV	**P22629** Streptavidin precursor
2	**2.45e+005**	**5/69 (7%)**	**10051.4 / 5.83**	RICCO	**O04066** Acyl-CoA-binding protein (ACBP)
3	**4.91e+004**	**7/69 (10%)**	**79898.5 / 6.05**	HUMAN	**Q9NVU0** DNA-directed RNA polymerases III 80 kDa polypeptide (RNA polymerase III subunit 5) (RPC5)
4	**4.85e+004**	**4/69 (5%)**	**10018.5 / 5.83**	GOSHI	**Q39779** Acyl-CoA-binding protein (ACBP)
5	**4.2e+004**	**8/69 (11%)**	**86877.5 / 6.54**	MOUSE	**Q9D4H8** Cullin-2 (CUL-2)

Detailed Results
1. 6/69 matches (8%). 18833.8 Da, pI = 7.94. Acc. # P22629. STRAV. Streptavidin precursor.

Figure V: MALDI ToF data from scrapie affinity purified gel. The band excised from the gel, figure 4.39, with a molecular weight around 10kDa was identified following tryptic digest MS as a streptavidin precursor. The streptavidin beads were boiled to remove bound biotinylated aptamer during the process, releasing streptavidin which was detected after separation by electrophoresis and staining.

APPENDIX III: Publication

Discovery of glutathione S-transferase inhibitors using dynamic combinatorial chemistry

Balou Shi, Ross Stevenson, Dominic J. Campopiano, Mike F. Greaney

Journal of the American Chemical Society, 2006 Jul 5, 128(26):8259-67

During the course of my PhD studies I have researched and published work on glutathione S-transferase and its inhibitors[181].

The paper is attached at back of thesis.

Appendix IV: Training Record

Oral Presentations

Departmental Residential meeting, Firbush, April 2005.

1st Annual EASTChem Biorganic Conference, Firbush, Jun 2005.

Departmental Group Talks, 2002-2005.

Poster Presentations

The Protein Society Annual Conference, Boston Ma, USA, August 2005.

Departmental Residential Meeting, Firbush, April 2004.

Conferences Attended

11th Royal Society of Chemistry Bioorganic Committee Firbush.

meeting/Carbohydrate Group Autumn Meeting, Firbush, September 2004.

Royal Society of Chemistry: Perkin Division, Dundee 2002, Edinburgh 2003, St Andrews 2004.

Scottish TSE Network Meetings 2004 -2005.

UK Joint Funders TSE Conference, York, September 2004.

Departmental Residential Meetings, Firbush, 2002-2005.

Teaching and Demonstrating

Supervised Final Year Undergraduate Students, 2003-2005.

Supervised Nuffield Student, 2004.

Demonstrated First Year Undergraduate Laboratory Sessions, 2002-2005.

Courses and Lectures Attended

Departmental Organic Research Seminars, 2002-2005.

Departmental Symposiums and Colloquia, 2002-2005.

Walker Memorial Lectures, 2002-2005.

Fire Safety Training, 2002.

Radiation Protection Course, 2002.

J|A|C|S
ARTICLES
Published on Web 06/09/2006

Discovery of Glutathione S-Transferase Inhibitors Using Dynamic Combinatorial Chemistry

Baolu Shi, Ross Stevenson, Dominic J. Campopiano,* and Michael F. Greaney*

Contribution from the School of Chemistry, University of Edinburgh, The King's Buildings, West Mains Road, Edinburgh EH9 3JJ, United Kingdom

Received November 27, 2005; E-mail: Michael.Greaney@ed.ac.uk; Dominic.Campopiano@ed.ac.uk

Abstract: Protein-directed dynamic combinatorial chemistry (DCC) relies on reversible chemical reactions that can function under the near-physiological conditions required by the biological target. Few classes of reaction have so far proven effective at generating dynamic combinatorial libraries (DCLs) under such constraints. In this study, we establish the conjugate addition of thiols to enones as a reaction well-suited for the synthesis of dynamic combinatorial libraries (DCLs) directed by the active site of the enzyme glutathione S-transferase (GST). The reaction is fast, freely reversible at basic pH, and easily interfaced with the protein, which is a target for the design of inhibitors in cancer therapy and the treatment of parasitic diseases such as schistosomiasis. We have synthesized DCLs based on glutathione (GSH, **1**) and the enone ethacrynic acid, **2a**. By varying either set of components, we can choose to probe either the GSH binding region ("G site") or the adjacent hydrophobic acceptor binding region ("H site") of the GST active site. In both cases the strongest binding DCL components are identified due to molecular amplification by GST which, in the latter system, leads to the identification of two new inhibitors for the GST enzyme.

Introduction

Dynamic Combinatorial Chemistry (DCC) is a powerful approach to the discovery of small molecule ligands for large biomolecules.[1] The method uses the biomolecular target to direct the reversible, in situ assembly of a small molecule library and as such can be considered, in the wider context of target-guided synthesis (TGS), an umbrella term that covers a variety of systems that feature small-molecule synthesis orchestrated by a large biomolecule (usually a protein).[2−10] DCC contrasts with the majority of TGS methods by using reversible reactions to assemble the prospective ligands. Whereas kinetic methods use the interior of proteins to direct and accelerate an irreversible reaction, usually between isolated sets of reactants, a dynamic combinatorial library (DCL) of compounds is designed such that it can equilibrate in the presence of the target. Since the library population distribution is under thermodynamic control, stabilization of one member through selective binding to the protein is expected to amplify that species at the expense of other (nonbinding) species, generating hit structures that can be identified through analysis of the DCL population distribution. DCC thus bridges the gap between chemical synthesis of drug candidates and their biological binding assay, meshing the two operations into a single process whereby the structure of the biological target directs the assembly of its own best inhibitor in situ.

The set of chemical reactions that have been successfully applied to the construction of DCLs in the presence of a biological target is currently rather small, centering on C=N and S−S bond-forming processes.[11−14] This lack of diversity

(1) Reviews: (a) Cheeseman, J. D.; Corbett, A. D.; Gleason, J. L.; Kazlauskas, R. J. *Chem.—Eur. J.* **2005**, *11*, 1708−1716. (b) Otto, S. *Curr. Opin. Drug Discovery Dev.* **2003**, *6*, 509−520. (c) Otto, S.; Furlan, R. L. E.; Sanders, J. K. M. *Curr. Opin. Chem. Biol.* **2002**, *6*, 321−327. (d) Lehn, J.-M. *Chem.—Eur. J.* **1999**, *5*, 2455−2463.
(2) Rideout, D. *Science* **1986**, *233*, 561−563.
(3) Nguyen, R.; Huc, I. *Angew. Chem., Int. Ed.* **2001**, *40*, 1774−1776.
(4) Nicolaou, K. C.; Hughes, R.; Cho, S. Y.; Winssinger, N.; Smethurst, C.; Labischinski, H.; Endermann, R. *Angew. Chem., Int. Ed.* **2000**, *39*, 3823−3828.
(5) Nicolaou, K. C.; Hughes, R.; Cho, S. Y.; Winssinger, N.; Labischinski, H.; Endermann, R. *Chem.—Eur. J.* **2001**, *7*, 3824−3843.
(6) Erlanson, D. A.; Braisted, A. C.; Raphael, D. R.; Randal, M.; Stroud, R. M.; Gordon, E. M.; Wells, J. A. *Proc. Natl. Acad. Sci. U.S.A.* **2000**, *97*, 9367−9372.
(7) Lewis, W. G.; Green, L. G.; Grynszpan, F.; Radić, Z.; Carlier, P. R.; Taylor, P.; Finn, M. G.; Sharpless, K. B. *Angew. Chem., Int. Ed.* **2002**, *41*, 1053−1057.
(8) Mocharla, V. P.; Colasson, B.; Lee, L. V.; Röper, S.; Sharpless, K. B.; Wong, C.-H.; Kolb, H. C. *Angew. Chem., Int. Ed.* **2005**, *44*, 116−120.
(9) Bourne, Y.; Kolb, H. C.; Radić, Z.; Sharpless, K. B.; Taylor, P.; Marchot, P. *Proc. Natl. Acad. Sci. U.S.A.* **2004**, *101*, 1449−1454.
(10) Krasinski, A.; Radić, Z.; Manetsch, R.; Raushel, J.; Taylor, P.; Sharpless, K. B.; Kolb, H. C. *J. Am. Chem. Soc.* **2005**, *127*, 6686−6692.
(11) C=N bond formation: (a) Huc, I.; Lehn, J.-M. *Proc. Nat. Acad. Sci. U.S.A.* **1997**, *94*, 2106−2110. (b) Bunyapaiboonsri, T.; Ramström, O.; Lohmann, S.; Lehn, J.-M.; Peng, L.; Goeldner, M. *ChemBioChem* **2001**, *2*, 438−444. (c) Hochgürtel, M.; Kroth, H.; Piecha, D.; Hofmann, M. W.; Nicolau, C.; Krause, S.; Schaaf, O.; Sonnenmoser, G.; Eliseev, A. V. *Proc. Nat. Acad. Sci. U.S.A.* **2002**, *99*, 3382−3387. (d) Gerber-Lemaire, S.; Popowycz, F.; Rodriguez-Garcia, E.; Asenjo, A. T. C.; Robina, I.; Vogel, P. *ChemBioChem* **2002**, *3*, 466−470. (e) Ramström, O.; Lohmann, S.; Bunyapaiboonsri, T.; Lehn, J.-M. *Chem.—Eur. J.* **2004**, 10, 1711−1715. (f) Bugaut, A.; Toulmé, J.-J.; Rayner, B. *Angew. Chem., Int. Ed.* **2004**, *43*, 3144−3147. (g) Zameo, S.; Vauzeilles, B.; Beau, J.-M. *Angew. Chem., Int. Ed.* **2005**, *44*, 965−969. (h) Bugaut, A.; Bathany, K.; Schmitter, J.-M.; Rayner, B. *Tetrahedron Lett.* **2005**, *46*, 687−690.
(12) S−S bond formation: (a) Ramström, O.; Lehn, J.-M. *ChemBioChem* **2000**, *1*, 41−48. (b) Krishnan-Ghosh, Y.; Balasubramanian, S. *Angew. Chem., Int. Ed.* **2003**, *42*, 2171−2173. (c) Whitney, A. M.; Ladame, S.; Balasubramanian, S. *Angew. Chem., Int. Ed.* **2004**, *43*, 1143−1146. (d) Hotchkiss, T.; Kramer, H. B.; Doores, K. J.; Gamblin, D. P.; Oldham, N. J.; Davis, B. G. *Chem. Commun.* **2005**, 4264−4266. (e) Ladame, S.; Whitney, A. M.; Balasubramanian, S. *Angew. Chem., Int. Ed.* **2005**, *44*, 5736−5739.
(13) Thioester formation: Larsson, R.; Pei, Z.; Ramström, O. *Angew. Chem., Int. Ed.* **2004**, *43*, 3716−3718.

10.1021/ja058049y CCC: $33.50

Scheme 1. DCL Composed of EA Analogues and GSH, **1**[a]

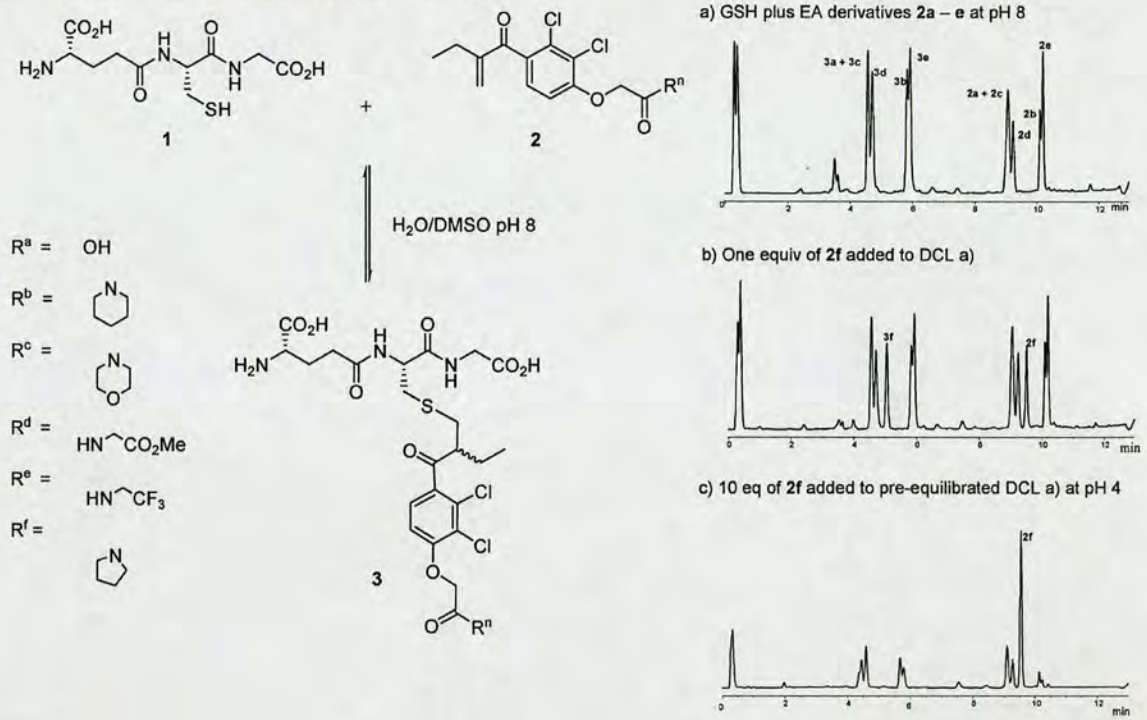

[a] Glutathione, **1**, adds to the five enones **2a**−**e** to set up a DCL that has an equitable distribution of thiol conjugates **3a**−**e** and starting enones (chromatogram a). The reversibility of the DCL is proven by adding an additional enone component, **2f**, to the pre-equilibrated library and observing the incorporation of adduct **3f** (chromatogram b). The pH control of the DCL is illustrated by pre-equilibration, acidification to pH 4, and subsequent addition of a large excess of enone **2f**, which is not incorporated into the library as the conjugate addition reaction has been switched off (chromatogram c).

is unsurprising, as the successful reaction must meet two sets of exacting criteria; it must proceed under the near physiological conditions required by the protein target as well as fulfilling the thermodynamic condition of reversibility inherent to the DCC process. An increase in the number of chemical reactions available for DCC is necessary to enable greater functional group diversity and increased applicability of DCLs as a target-guided synthesis methodology. With this in mind, we have recently introduced the conjugate addition of thiols to enones as a new method for DCL synthesis.[15] The reaction is well-suited to DCC being fast, freely reversible, responsive to pH change, and proceeding in water under mild conditions with no external reagents (Scheme 1). In addition, the choice of the tripeptide glutathione (γ-Glu-Cys-Gly, GSH, **1**) as the thiol in our preliminary studies creates DCLs that are biologically relevant and amenable to targeting by a variety of proteins, the most relevant being the enzymes responsible for mediating the conjugate addition chemistry of GSH in the cell: the glutathione S-transferases (GSTs).

The GSTs are a large family of dimeric enzymes responsible for cell detoxification, thereby protecting the cell from cytotoxic and oxidative stress.[16,17] They catalyze the conjugation of GSH to a wide variety of xenobiotic electrophiles such as quinones, prostaglandins, and base propenals, making them more water soluble and easily eliminated from the cell. The GSTs are potential drug targets in cancer therapy, where resistance to chemotherapeutic drugs has been directly correlated with the overexpression of GSTs in tumor cells, and parastic diseases such as malaria and schistosomiasis.[18] We now describe the application of our GSH-based DCLs to the discovery of GST inhibitors.

Results and Discussion

We initially designed a biased DCL to examine the compatibility of our conjugate addition methodology with GST and to see whether the enzyme could effectively amplify the best binding component from a DCL. Since DCL synthesis requires large amounts of highly purified enzyme, we selected GST from the helminth worm *Schistosoma japonica* (SjGST, 26kDa monomer) as our target transferase, as it is well characterized and amenable to recombinant overexpression in *E. coli* as an affinity-tagged construct.[19] The DCL is shown in Scheme 2 and consists of GSH, **1**, three tripeptide GSH analogues **4**−**6**, and the enone ethacrynic acid, **2a** (EA). The tripeptide analogues were synthesized using standard solid-phase synthesis methods and differ from GSH at the γ-glutamyl residue. As a result, the three analogues are expected to be poor fits for the GSH binding region of the GST active site, as the γ-glutamyl residue is thought to be critical for binding,[20] thus biasing the DCL toward

(14) Enzymatic aldol reaction: (a) Lins, R. J.; Flitsch, S. L.; Turner, N. J.; Irving, E.; Brown, S. A. *Angew. Chem., Int. Ed.* **2002**, *41*, 3405−3407. (b) Lins, R.; Flitsch, S. L.; Turner, N. J.; Irving, E.; Brown, S. A. *Tetrahedron* **2004**, *60*, 771−780.
(15) Shi, B.; Greaney, M. F. *Chem. Commun.* **2005**, 886−888.
(16) Mannervik, B.; Danielson, U. H. *CRC Crit. Rev. Biochem.* **1988**, *23*, 283−337.
(17) Hayes, J. D.; Flanagan, J. U.; Jowsey, I. R. *Annu. Rev. Pharmacol. Toxicol.* **2005**, *45*, 51−88.
(18) Mahajan, S.; Atkins, W. M. *Cell. Mol. Life Sci.* **2005**, *62*, 1221−1233.
(19) Waugh, D. S. *Trends Biotechnol.* **2005**, *23*, 316−320.
(20) Andersson, C.; Mosialou, E.; Adang, A. E.; Mulder, G. J.; van Der Gen, A.; Morgenstern, R. *J. Biol. Chem.* **1991**, *266*, 2076−2079.

Scheme 2. DCL Composed of GSH Analogues and EA, **2a**[a]

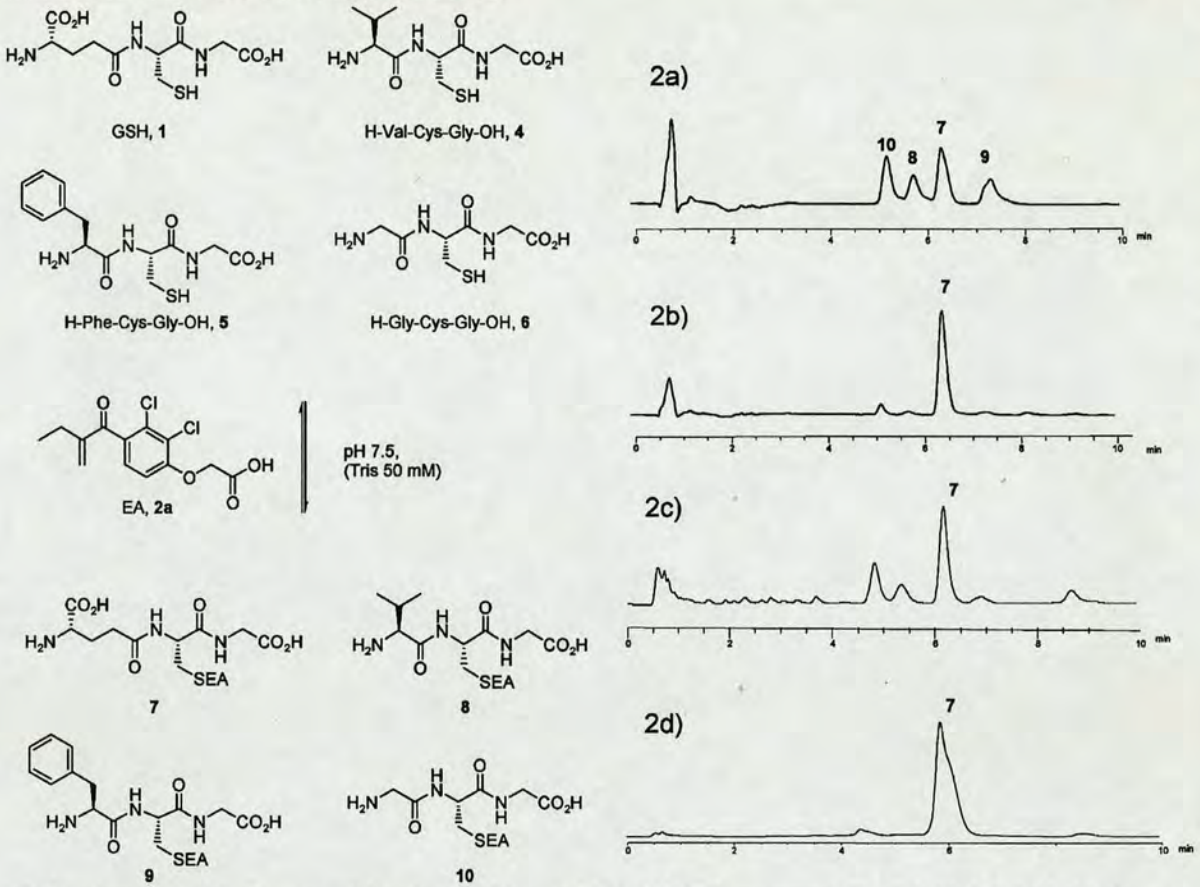

[a] The four tripeptides **1**, **4**−**6** undergo reversible conjugate addition to EA, **2a**, at pH 7.5. Chromatogram (a) shows the blank DCL after 1 h; chromatogram (b) shows the DCL after 10 min in the presence of SjGST; chromatogram (c) shows the DCL after pre-equilibration and *then* addition of SjGST, after 2 days; chromatogram (d) shows the same system as (c) after 6 days. Although each EA adduct is formed as a mixture of diastereoisomers upon conjugate addition, giving a total of eight adducts in the DCL, the diasteromeric adducts are not separable under the LC conditions.

the GSH adduct **7**. The enone ethacrynic acid is a known inhibitor of GSTs and provides a motif for further structural elaboration.

The blank DCL, assembled in the absence of any enzyme, equilibrates in 1 h to give the distribution of each of the four conjugates **7**−**10** shown in chromatogram 2a (Scheme 2). Upon incubation of the same components with 0.8 equiv of SjGST for 10 min, the DCL collapsed to essentially one adduct, the expected GS-EA, **7** (chromatogram 2b), and remained unchanged thereafter. The rapid equilibration in the presence of SjGST indicates that the enzyme is accelerating the conjugate addition, as would be expected given its catalytic function as a transferase in GSH biochemistry. To verify that the composition shown in chromatogram 2b represented true equilibrium and not a metastable distribution generated by target-accelerated synthesis in the presence of the enzyme, we added SjGST to the pre-equilibrated DCL shown in chromatogram 2a. Strong amplification of adduct **7** was again observed, but at a far slower rate. After 2 days **7** was present in 55% of total adduct concentration (chromatogram 2c), and after 6 days the DCL had equilibrated to an identical distribution to that of chromatogram 2b, where adduct **7** is by far the dominant species. These results indicate that catalysis of the conjugate addition reaction by SjGST does not effect the equilibrium distribution of the DCL and that the amplified compound **7** is the thermodynamically preferred binder.

The expected adduct **7** has been amplified from 35% of total conjugate concentration to 92% at equilibrium, a large amplification that ought to reflect correspondingly large differences in binding affinity between **7** and those peptides lacking the γ-glutamyl residue. To verify that amplification and binding affinity are indeed correlated in this system, we quantified the inhibitory activity of **7** and **10** for SjGST using the standard chlorodinitrobenzene (CDNB) GST inhibition assay.[21] Measured IC_{50} values of 0.32 μM for **7** and 88 μM for **10** differ by over 2 orders of magnitude, demonstrating that the extent of molecular amplification for each component in the biased DCL can be clearly related to their binding affinity for the protein target. Similar strong amplification was also observed in slightly larger DCLs based upon seven starting tripeptides (vide infra). Control experiments using bovine serum albumin as the protein target in place of SjGST produced no changes to the blank DCL composition, indicating that the active site of SjGST is directing the amplification of the DCL. The success of these biased DCLs

(21) (a) Habig, W. H.; Pabst, M. J.; Jakoby, W. B. *J. Biol. Chem.* **1974**, *249*, 7130−7139. (b) Burg, D.; Filippov, D. V.; Hermanns, R.; van der Marel, G. A.; van Boom, J. H.; Mulder, G. J. *Bioorg. Med. Chem.* **2002**, *10*, 195−205.

Scheme 3. A DCL Made from GSH and 14 EA Analogues

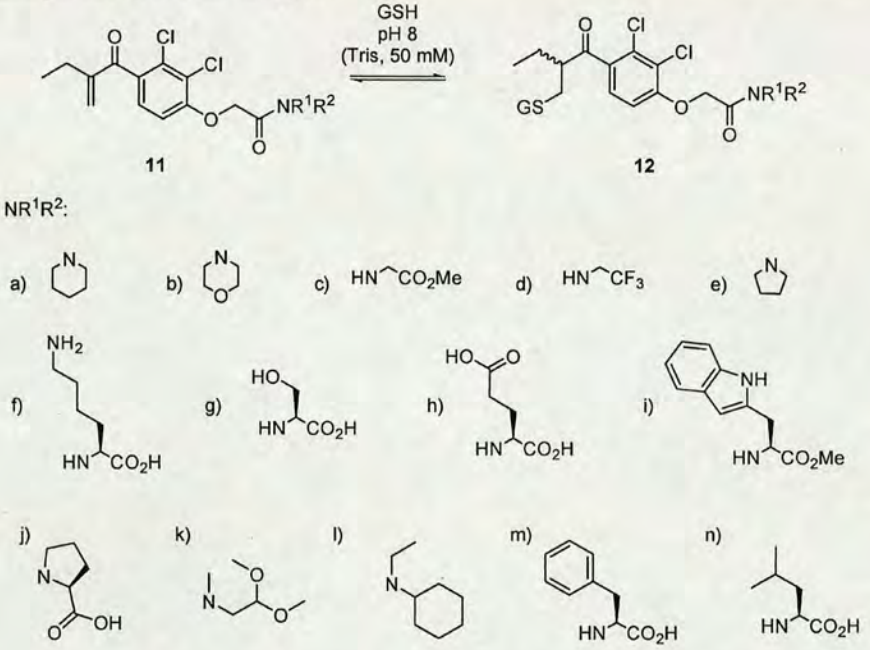

encouraged us to extend the thiol addition methodology to the discovery of new GST inhibitors through the synthesis of larger, nonbiased DCLs.

All GSTs contain two recognition areas for GS−R conjugates: a highly conserved GSH binding site and a hydrophobic binding region for the electrophilic substrate, called the H-site, which varies across the different GST isoforms. The design of inhibitors which target the H-site is a promising strategy in terms of isozyme discrimination,[18] so we elected to use DCC to explore the H-site of SjGST with a series of EA analogues. We prepared a DCL with reversed stoichiometry from that in Scheme 2, whereby *n* EA analogues react with GSH to afford *n* GS-EA adducts. The EA analogues were prepared from EA via EDC-mediated amide bond formation at the carboxylic acid group, producing a series of compounds **11a**−**n** that display a variety of randomly selected functional groups (Scheme 3). The fourteen EA analogues were equilibrated with GSH in both the absence and presence of SjGST (2 equiv). Figure 1 shows the LC traces of each DCL, along with an overlay for comparison purposes. The large peak eluting at ~5.9 min in the amplified trace is due to trace amounts of SjGST still present in the reaction mixture. We verified that all of the expected GSH conjugates were present in the DCL using ESI-MS analysis and then looked to identify only those components that have been amplified by the enzyme.

Looking at the overlay trace in the area of the GSH conjugates we can see that a single peak has been amplified, marked with a star at $R_T = 4.8$ min. This amplification is at the expense of the first peak at $R_T = 3.3$ min, which is reduced in intensity. MS analysis of the amplified peak indicated four adducts, **12a**, **d**, **m**, and **n**, while the reduced peak is due to adduct **12f**.

Deconvolution studies established that each of the adducts **12a**, **m**, and **n** were being amplified in the presence of SjGST, whereas **12d** was not.[22] Identical amplification results were obtained when SjGST was added to the pre-equilibrated DCL, indicating that the thermodynamic reversibility inherent to the thiol conjugate addition in the absence of any target is maintained in the presence of GST. To ascertain whether the hit structures generated from DCC were in fact active inhibitors of SjGST, we synthesized the amplified adducts **12a** and **12n**, a nonamplified adduct **12b**, and the depreciated adduct **12f** separately and measured their IC_{50} values (Figure 2).

Both piperidine (**12a**) and leucine (**12n**) derivatives of EA inhibit SjGST at the low micromolar/high nanomolar level, with the piperidine derivative **12a** being slightly more potent (IC_{50} = 0.61 μM versus IC_{50} = 1.40 μM). The more polar lysine amide **12f** is, as expected, the least active, with an IC_{50} value more than 10-fold lower than **12a** at 8.20 μM. The morpholine amide **12b** lies halfway between **12a** and **12f** with an IC_{50} value of 4.30 μM, approximately 7-fold lower than the piperidine amide. These figures indicate that the extent of DCL amplification not only reflects the relative binding affinities of DCL components for the protein target but is also discriminatory across an order of magnitude range of IC_{50} values. The piperidine and leucine amides **12a** and **12n** are amplified from the library at the expense of the lysine amide **12f**, which being an approximately 10-fold weaker binder is removed from the equilibrium composition of the DCL. The reversibility inherent to the thiol conjugate addition is enabling the SjGST target to amplify relatively weak-binding compounds from a nonbiased selection of small molecules, demonstrating that this TGS methodology can be applied in a medicinal chemistry lead-finding context.

As EA is known to inhibit GSTs both on its own and as a GSH conjugate,[23] we were interested in acquiring IC_{50} data for some of the enone starting materials. We assayed the five enones **2a**, **11a**, **11b**, **11f**, and **11n**, the corresponding Michael acceptors

(22) See Supporting Information.

(23) Oakley, A. J.; Rossjohn, J.; Lo Bello, M.; Caccuri, A. M.; Federici, G.; Parker, M. W. *Biochemistry* **1997**, *36*, 576−585.

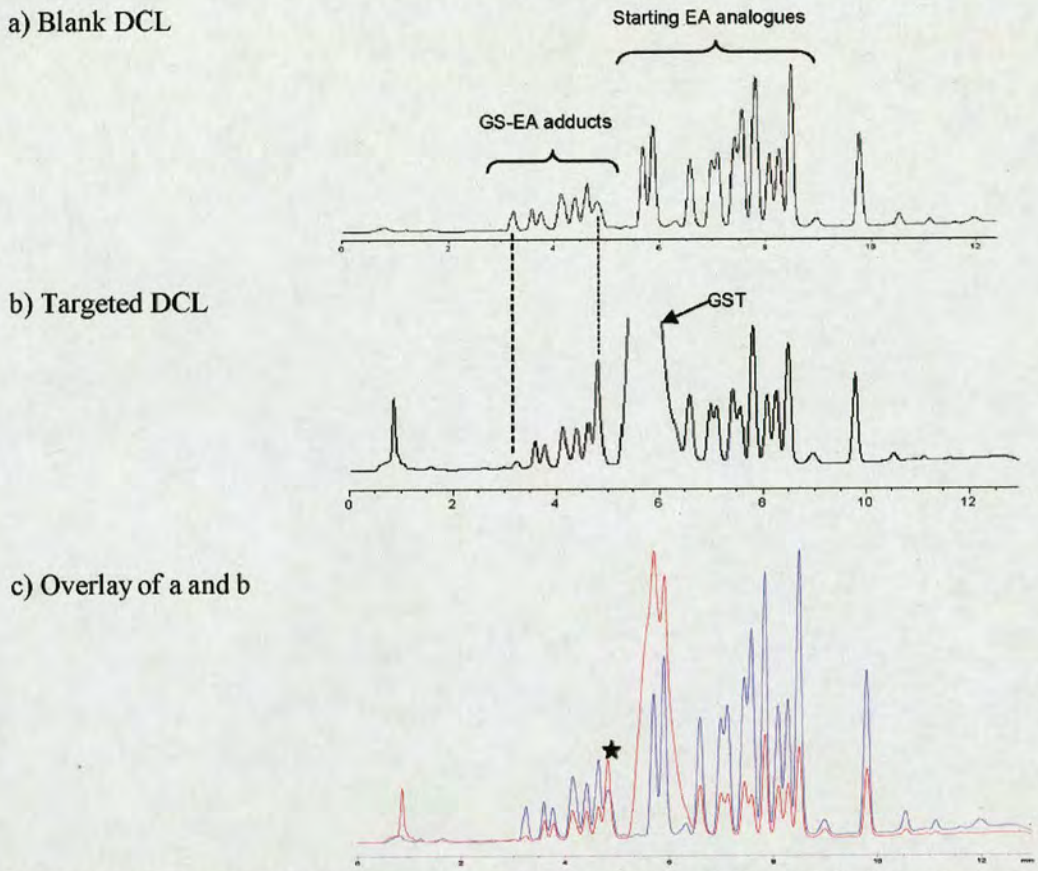

Figure 1. HPLC chromatograms for the targeted DCL of EA analogues. Chromatogram (a) shows the blank DCL distribution after 1 h, chromatogram (b) shows the DCL composition in the presence of SjGST after 30 min and chromatogram (c) shows an overlay of (a) and (b). The two dotted lines indicate the peak that is reduced in intensity on addition of the enzyme, at $R_T = 3.3$ min, along with the peak that is amplified upon enzyme addition, at $R_T = 4.8$ min.

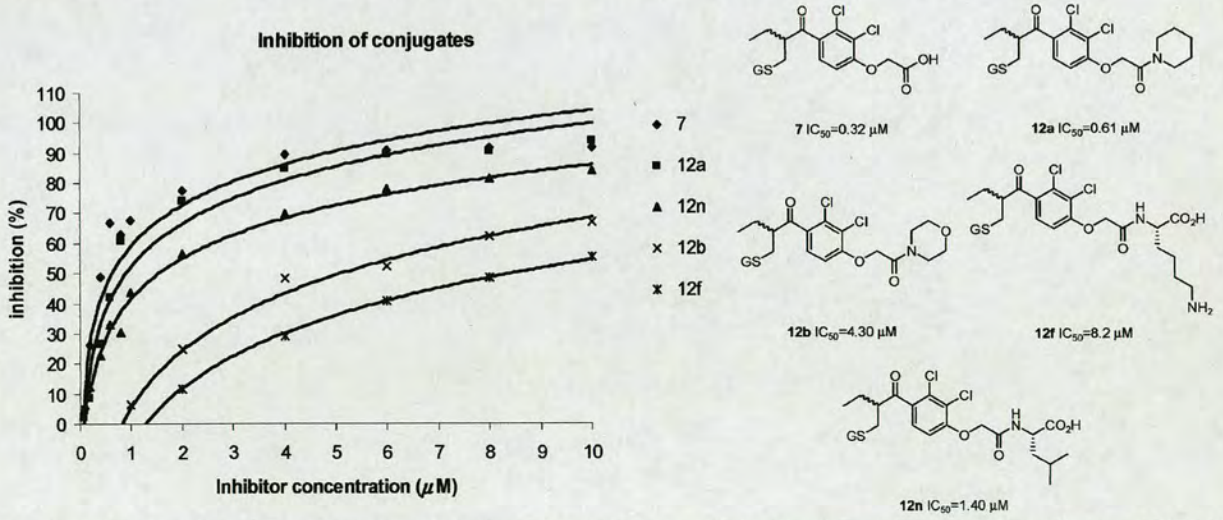

Figure 2. Inhibition profiles and IC_{50} values for amplified adducts **12a** and **12n**, nonamplified adduct **12b**, and depreciated adduct **12f** along with GS−EA, **7**, for comparison purposes.

to the five GSH conjugates we had previously investigated. The inhibition data are shown in Figure 3 and follow a similar trend to that of the conjugates, with **2a** ≈ **11a** > **11n** > **11b** > **11f**. Additionally, the quantitative IC_{50} values are similar for each enone and its corresponding GSH conjugate, a common observation across a number of GST isozymes.[23−25] The absence of any significant augmentation of binding in the case of the GS−EA conjugates relative to the EA analogues suggests that the EA moiety of the conjugate may bind in different orientations and/or positions within the H-site relative to the parent

(24) Ploemen, J. H. T. M.; van Ommen, B.; van Bladeren, P. J. *Biochem. Pharmacol.* **1990**, *40*, 1631−1635.
(25) Awasthi, S.; Srivastava, S. K.; Ahmad, F.; Ahmad, H.; Ansari, G. A. S. *Biochim. Biophys. Acta* **1993**, *1164*, 173−178.

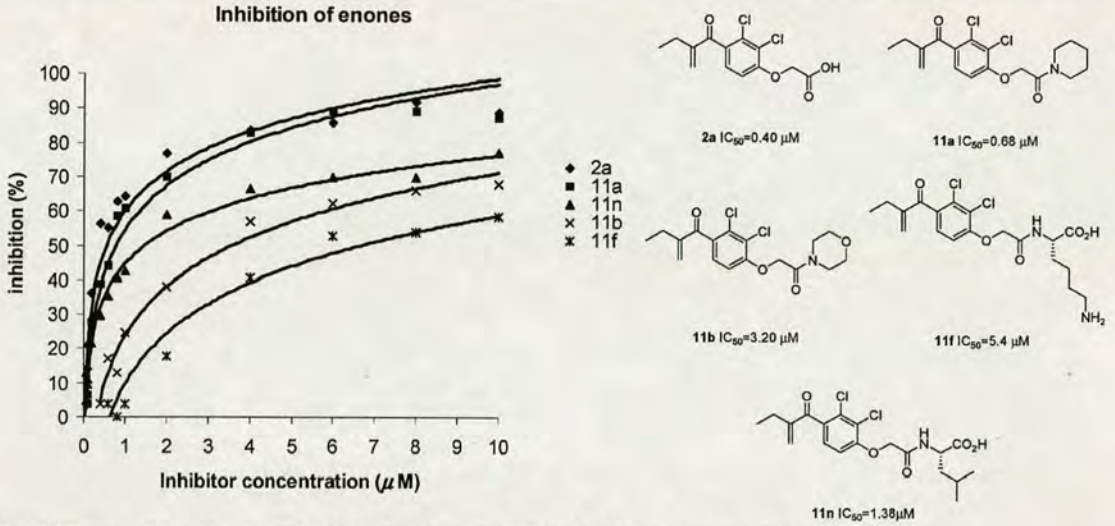

Figure 3. Inhibition profiles and IC_{50} values for enone starting materials **11a**, **b**, **f**, and **n** along with EA, **2a**.

compound. This phenomenon has been observed in the crystal structures of EA and GS−EA bound into the active site of GSTP1-1[23] and is perhaps to be expected, given that the two binding fragments of GSH and EA are linked in the conjugate by a single covalent bond which offers little flexibility for the EA group to explore analogous optimal binding modes to the individual enones.

It is important to note that GST assays use the non-natural CDNB as a substrate and the exact nature of binding of this substrate to SjGST is not known. Moreover, the details of GSH-EA binding to SjGST are also lacking since a high-resolution structure of the SjGST/GS−EA complex has not been determined. A model structure of the SjGST GSH EA Michaelis complex was recently proposed based on structures of SjGST bound to a series of glutathione derivatives (glutathione sulfonate, *S*-hexyl glutathione, and *S*-2-iodobenzyl glutathione).[26] This model identifies a series of residues (Arg103, Tyr111, Ser107, Gln 204) that could interact with the EA carboxylic acid group and proposes that the enzyme must undergo conformational changes to allow conjugate addition of the GSH thiol onto the enone of EA. Interestingly, our identification of the amplified amide compounds **12a** and **12n** from our DCLs indicates that the carboxylic acid group of EA is not essential for binding in the SjGST H site and may be successfully extended without significant loss of inhibitory activity.

Conclusions

We have established the conjugate addition reaction of thiols to enones as a new reaction for enzyme-directed DCC. Using the enzyme SjGST, we could investigate either the GSH- or the H-regions of the enzyme active site by varying DCL stoichiometry between *n* thiols/one enone and one thiol/*n* enones. DCL amplification was successful for both approaches, with the amplified compounds corresponding to the best inhibitors as measured by a competition assay. While the degree of amplification from the EA-based DCL is quantitatively far lower than that observed in the biased GSH-based DCLs, it represents a more significant application of DCC. The power of DCC as a TGS method in medicinal chemistry will likely be realized early in the drug discovery process, where libraries of weak-binding compounds can be rapidly screened to produce lead structures for further development. The ability of SjGST to amplify the low micromolar inhibitors **12a** and **12n** from a nonbiased thiol conjugate DCL, at the expense of compound **12f** which differs in IC_{50} by only a single order of magnitude, illustrates this discovery process in a microcosm and demonstrates the power of TGS in combining the chemical synthesis, discovery, and biological binding assay of enzyme inhibitors into a single operation. Future work will extend our GSH-based DCL methodology to the discovery of novel inhibitors for a range of human GST isoforms.

Experimental Section

General. All reagents were purchased from commercial suppliers and used as received. Dichloromethane (DCM) was distilled from CaH_2. TLC was performed with Merck aluminum plates silica gel 60 F_{254}. Melting points were recorded on a Gallenkamp melting point instrument and are uncorrected. ^1H and ^{13}C NMR spectra were recorded on a Bruker DPX360 MHz NMR spectrometer unless otherwise specified. Chemical shifts δ are quoted in ppm relative to the $CDCl_3$ signal as reference. Coupling constants are given in Hz. Optical rotations were measured on a POLAAR 20 automatic polarimeter using a 2 mL cell. Mass spectra were obtained from the EPSRC National Mass Spectrometry Service Centre, University of Wales, Swansea.

Analytical HPLC was performed on an HP1100 instrument and analytical HPLC-MS on a Waters 2790 HPLC with a micromass Platform II quadrupole mass spectrometer. Enzyme concentrations were determined by Bradford assay on a UNICAM UV−visible spectrometer with bovine serum albumin as a standard.[27] Enzyme activity assays were conducted on a CARY 300 SCAN UV−visible spectrometer.

Synthesis of Library Components. A. General Protocol for Peptide Syntheses: Tripeptides **4**−**6**, **13**−**15** were prepared using standard Fmoc solid-phase synthesis methods. The preparation of H-Val-Cys-Gly-OH (**4**) is illustrative: Fmoc-Gly-Wang (0.6 mmol/g) was swollen in DCM at rt for 10 min. The resin was drained and treated with 20% piperidine in dry DMF. The reaction was agitated with nitrogen at rt and monitored by Kaiser test. After completion, the resin was washed with DMF, DCM, and MeOH and dried in vacuo. The

(26) Cardoso, R. M. F.; Daniels, D. S.; Bruns, C. M.; Tainer, J. A. *Proteins* **2003**, *51*, 137−146.

(27) Bradford, M. *Anal. Biochem.* **1976**, *72*, 248−254.

resulting H-Gly-Wang resin was then swollen in DCM at rt for 10 min and drained. Fmoc-Cys(Trt)-OH (5 equiv), HBTU (4.9 equiv), and HOBt·H_2O (5 equiv) were mixed in dry DMF and added to the resin. The mixture was agitated with nitrogen, while DIPEA (10 equiv) was added. The reaction was monitored by Kaiser test. After completion, the resin was washed with DMF, DCM, and MeOH and dried in vacuo to afford Fmoc-Cys(Trt)-Gly-Wang. Fmoc removal from the cysteine residue was accomplished as described for the deprotection of Gly, followed by coupling to Fmoc-Val under the same conditions as those used for coupling to cysteine with the exception that DIPEA was added to the mixture of peptide, HBTU, and HOBt·H_2O for the activation. Fmoc removal from Fmoc-Val-Cys(Trt)-Gly-Wang was carried out as before, and the resin finally dried in vacuo over KOH. Cleavage and deprotection were accomplished by adding aqueous TFA solution (94.5% TFA, 2.5% H_2O, 2.5% EDT, 1% TIS) to the resin followed by gentle filtration and washing with TFA solution (×2). All of the filtrate was collected and added dropwise to a 10-fold excess of cold ether in a centrifuge tube. After centrifugation, ether was carefully decanted, and the centrifugation was repeated twice. Water was then added to the white residue, and the aqueous solution was transferred to a separatory funnel. The aqueous phase was washed with DCM 3 times and then lyophilized to give the pure tripeptide **4** (11 mg, 35%) as a fluffy white solid: ^{1}H NMR (360 MHz, D_2O) δ = 1.06 (6H, dd, J = 6.5, 6.5 Hz, Val $(CH_3)_2$), 2.27 (1H, m, Val CH), 2.91−3.04 (2H, m, Cys CH_2), 3.91 (1H, d, J = 5.8 Hz, Val CH), 3.97−4.08 (2H, m, Gly CH_2), 4.53 (1H, t, J = 6.5 Hz, Cys CH); ^{13}C NMR (91 MHz, D_2O) δ = 17.8, 18.6, 26.2, 31.1, 42.4, 56.8, 59.4, 170.4, 172.7, 174.3; HRMS (ES+) calcd for $C_{10}H_{20}O_4N_3S$ $[M + H]^+$ 278.1169, found 278.1171.

B. Synthesis of EA derivatives. EA derivatives were synthesized according to the coupling procedure described in ref 15, followed by Boc cleavage with TFA. The preparation of **11g** is illustrative: Ethacrynic acid (151.6 mg, 0.50 mmol), HOBt·H_2O (84.2 mg, 0.55 mmol), EDCI (105.4 mg, 0.55 mmol), H-Ser(*t*Bu~)-O*t*Bu·HCl (139.6 mg, 0.55 mmol), and DIPEA (428 μl, 2.50 mmol) were dissolved in DCM (10 mL), and the reaction was left to stir at room temperature overnight. The reaction was worked up in the usual fashion, followed by flash column chromatography (SiO_2, DCM/EtOAc 9:1) to yield the *tert*-butyl-protected amide (156 mg, 62%) as a colorless oil; R_f = 0.3 (SiO_2, DCM/EtOAc 9:1); ^{1}H NMR (360 MHz, $CDCl_3$) δ = 1.09−1.16 (12H, m, Ser *t*Butyl + CH_3), 1.45 (9H, s, Ser *t*Butyl), 2.45 (2H, q, J = 7.4, methylene CH_2), 3.54 (1H, dd, Ser CH_2, J_1 = 8.7 Hz, J_2 = 3.1 Hz), 3.85 (1H, dd, Ser CH_2, J_1 = 8.7 Hz, J_2 = 2.7 Hz), 4.54−4.61 (2H, m, OCH_2), 4.66 (1H, m, Ser CH), 5.57 (1H, s, enone H), 5.93 (1H, s, enone H), 6.85 (1H, d, J = 8.5 Hz, Ph H), 7.17 (1H, d, J = 8.5 Hz, Ph H), 7.58 (1H, d, J = 8.7 Hz, amide H); ^{13}C NMR (91 MHz, $CDCl_3$ + CD_3OD) δ = 13.4, 24.4, 28.3, 29.0, 53.8, 63.0, 69.0, 74.2, 83.1, 111.8, 124.1, 128.2, 129.8, 132.4, 135.0, 151.2, 155.6, 167.6, 169.8, 196.7; HRMS (ES+) calcd for $C_{24}H_{34}O_6NCl_2$ $[M + H]^+$ 502.1758, found 502.1748; $[\alpha]^{20}_D$ = +11° (c = 2.72, chloroform). The amide was then taken up into dry DCM (5−10 mL), and TFA (5 mL) was added. The reaction was allowed to stir under nitrogen at rt for 1 day, after which time it was partitioned between water and DCM and the organic phase was extracted (×3). Drying over $MgSO_4$ and concentration in vacuo yielded the acid **11g** (66 mg, 54%) as a white solid; mp 144−146 °C; ^{1}H NMR (360 MHz, $CDCl_3$ + CD_3OD) δ = 1.03 (3H, t, J = 7.4 Hz, CH_3), 2.34 (2H, q, J = 7.4 Hz, methylene CH_2), 3.78−3.93 (2H, m, Ser CH_2), 4.49−4.57 (3H, m, OCH_2 + Ser CH), 5.50 (1H, s, enone H), 5.87 (1H, s, enone H), 6.83 (1H, d, J = 8.5 Hz, Ph H), 7.07 (1H, d, J = 8.5 Hz, Ph H); ^{13}C NMR (91 MHz, $CDCl_3$ + CD_3OD) δ = 17.2, 28.3, 59.4, 66.9, 72.9, 116.1, 128.1, 132.1, 134.2, 136.2, 138.8, 155.0, 159.7, 172.7, 201.2; HRMS (ES+) calcd for $C_{16}H_{21}O_6N_2Cl_2$ $[M + NH_4]^+$ 407.0771, found 407.0771; $[\alpha]^{21}_D$ = +28.1° (c = 1.32, chloroform/methanol 9:1).

Protein Synthesis. A. Cloning of SjGST as a His-Tagged Fusion. The pET-6His-SjGST plasmid was designed to have SjGST fused to a 6His N-terminal tag which facilitates purification of the SjGST on nickel metal-affinity resin, rather than glutathione-affinity resins which are typically used to purify GST isoforms. This strategy thus provided large amounts of SjGST free from large amounts of glutathione (GSH) which could interfere with dynamic combinatorial library (DCL) synthesis. The *Schistosoma japonica gst* gene was amplified by PCR using pGEX6P-1 (Amersham Biosciences, Genbank Accession Number U78872) plasmid DNA as a template with primers GST-FOR (5′ GGA AAC AAG CTT **CAT GA**C CCC TAT 3′) which incorporated a *Bsp*HI site (in bold) and GST-REV (5′ GAA CTT CGG **GGA TCC** CAT GGG CCC 3′) which incorporated a *Bam*HI site (in bold). The PCR products were cloned into plasmid pUC19, sequenced to confirm the fidelity of the cloned DNA, and then cloned into plasmid pET-6His plasmid DNA digested with appropriate restriction enzymes (*Nco*I and *Bam*HI for the pET plasmid and *Bsp*HI and *Bam*HI for pUC19/SjGST). Clones containing the correct insert were isolated and sequenced to confirm the identity of the pET-6His-SjGST plasmid.

B. Expression and Purification of GST. Overexpression of *Schistosoma japonica* GST was achieved by transforming *E. coli* BL21(DE3) (Novagen) cells with the plasmid pET-6His-SjGST. A single colony was used to inoculate 50 mL of LB broth supplemented with ampicillin (100 μg/mL) and grown overnight at 37 °C with shaking. This overnight seed culture was then used to inoculate 2 L of fresh growth medium and grown at 37 °C to OD_{600} = 0.8 before induction with isopropyl thio-β-D-galactoside (IPTG) (1.0 mM final concentration). After a further 3 h agitation at 37 °C, the cells were harvested by centrifugation (6000 g for 15 min at 4 °C) and frozen at −20 °C for 16 h. The defrosted cells were resuspended in 50 mL of binding buffer (10 mM Tris/HCl, pH 7.5, 10 mM NaCl, containing one tablet of Complete Protease Inhibitor Cocktail (Roche)) and gently agitated for 1 h at 4 °C. The cells were disrupted by sonication (15 pulses of 30 s at 30-s intervals, on ice), and the cell debris was removed by centrifugation at 27 000 g for 20 min at 4 °C after which the cell lysate supernatant was filtered through a 0.45-μm membrane prior to chromatography.

The cell lysate was applied to a HisTrap HP column (5 mL, Amersham Biosciences) pre-equilibrated with binding buffer (50 mM Tris/HCl, 0.5 M NaCl, 5 mM imidazole, pH 7.5). The column was then washed with 20 column volumes of binding buffer (100 mL) before bound material was eluted using a linear gradient of 0−100% elution buffer (50 mM Tris/HCl, 0.5 M NaCl, 0.5 M imidazole, pH 7.5, over 20 column columns, 100 mL; see Figure S5.1 in the Supporting Information). Fractions were analyzed by SDS-PAGE, and those containing GST were pooled and dialyzed overnight against 4 L of 10 mM Tris/HCl (pH 7.5) at 4 °C. SDS-PAGE analysis suggested that the protein was greater than 95% pure (Figure S5.2 in the Supporting Information). Further purification was achieved using MonoQ anion exchange (1 mL, Amersham Biosciences). The protein was loaded onto the column, washed with 50 mM Tris, pH 7.5, and then eluted with a linear 0−1 M NaCl gradient over 20 mL. Fractions were analyzed by SDS-PAGE, and the purest GST fractions were pooled, concentrated by ultrafiltration (10 kDa cutoff), and frozen. A 1 mg aliquot of the isolated 6His-SjGST was analyzed by gel filtration chromatography (Sephacryl HR-75, Amersham Bioscience) to confirm that it was dimeric in solution.

Electrospray mass spectrometry (ESI-MS) analysis of the pure enzyme gave the molecular mass of the 6His-SjGST as 28 068 Da (±5 Da), in good agreement with the predicted value of 28 057 Da for the monomer. The final yield of GST using this method was ~20 mg per L of bacterial culture, and this protein was used for all subsequent library synthesis and inhibition assays.

Dynamic Combinatorial Chemistry. Representative procedure for GSH analogue DCL: The seven GSH tripeptides **1**, **4**−**6**, **13**−**15** (7 × 8.2 μL, 10 mM aqueous) and ethacrynic acid (0.82 μl, 0.1 M in DMSO) were added to tris buffer (200 μL, 50 mM, pH 7.5). The DCL was allowed to stand at rt with occasional gentle shaking and monitored by HPLC at regular intervals to establish the blank DCL composition

Scheme 4. HPLC Analysis of DCL Made from Seven GSH-Based Tripeptides **1**, **4**–**6**, **13**–**15**[a]

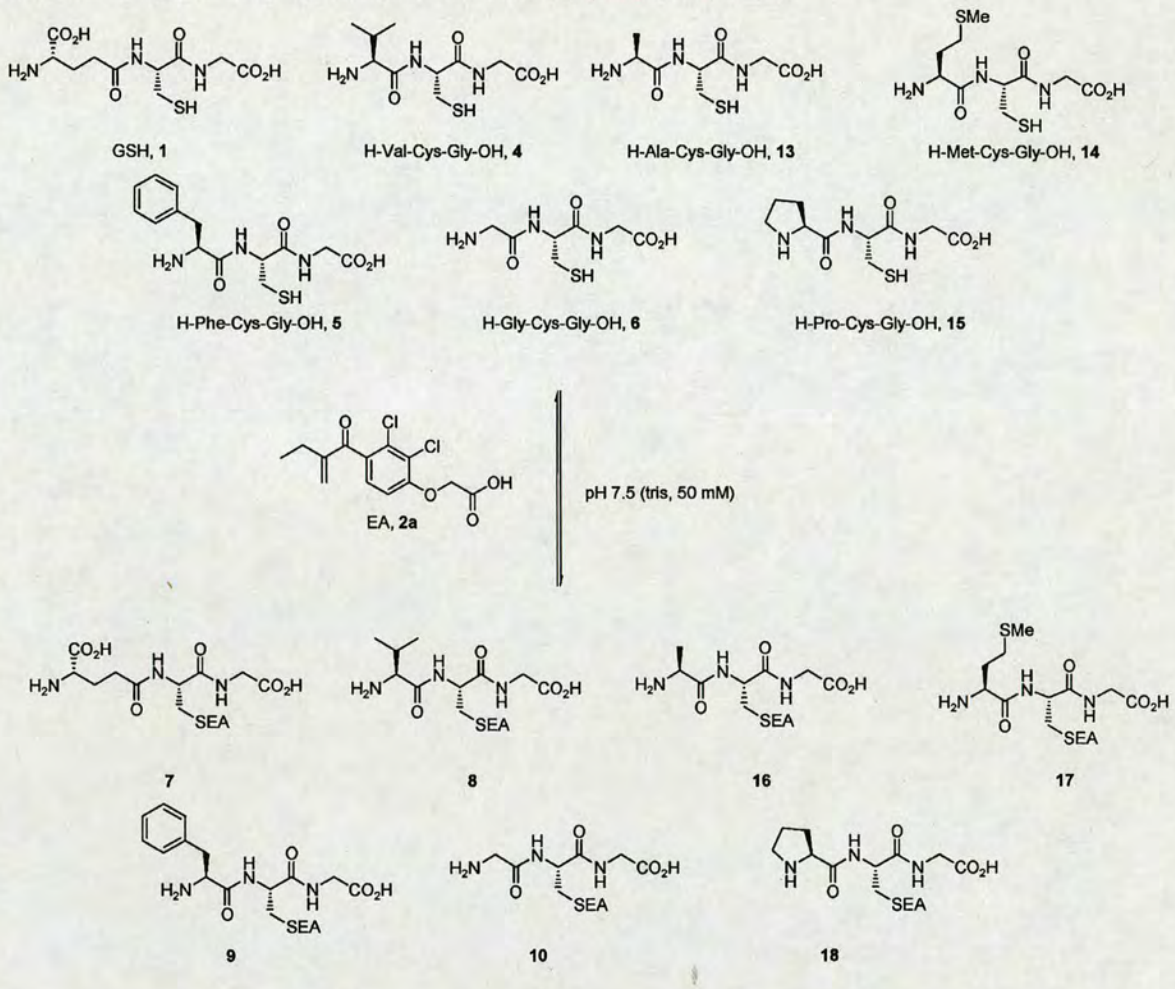

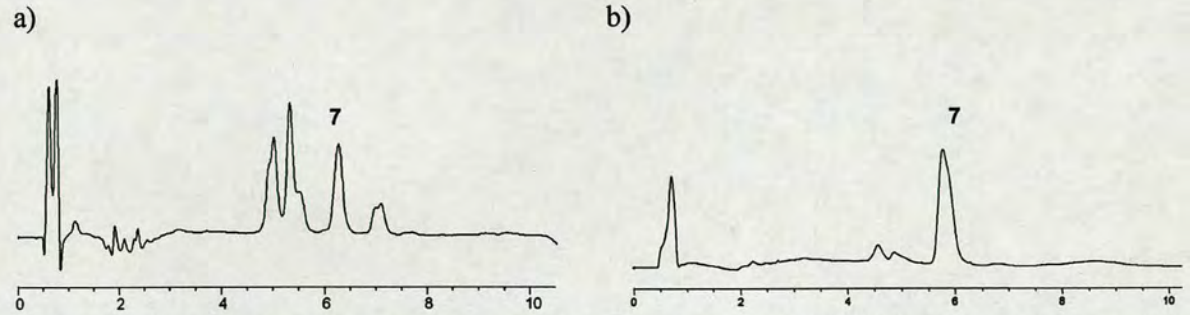

[a] Chromatogram (a) shows the blank DCL, and chromatogram (b) shows the DCL in the presence of SjGST. The GSH–EA adduct **7** is amplified from 35% of total adduct concentration to 88%.

(HPLC conditions: Column: Luna 5 μ C18(2) 30 mm × 4.60 mm, flow rate 1 mL min^{-1}, wavelength 254 nm, temperature 23 °C, gradient H_2O/MeCN (0.01% TFA) from 80% to 70% over 8 min, then to 40% over 1 min eventually to 20% over 2 min).

The DCL was then resynthesized in the presence of SjGST (200 μl, 160 μM in 50 mM tris buffer pH 7.5), and the HPLC trace was compared to that of the blank (Scheme 4). The DCL composition was identical in the case of addition of SjGST from the start and the case of SjGST addition to a pre-equilibrated library.

Representative procedure for EA analogue DCL: Reduced glutathione (20 μL, 10 mM aqueous) and the 14 ethacrynic acid derivatives **11a**–**n** (14 × 2 μL, 0.1 M in DMSO) were added to tris buffer (3.3 mL, 50 mM, pH 8). The DCL was allowed to stand with occasional gentle shakes at rt and monitored by HPLC at regular intervals. LC–MS verified that each of the expected adducts was present in the blank DCL (Figure S6.1). HPLC conditions: Column: Luna 5 μ C18(2) 30 mm × 4.60 mm, flow rate 1 mL min^{-1}, wavelength 254 nm, temperature 23 °C, gradient H_2O/MeCN (0.01% TFA) from 80% to 5% over 10 min.

The DCL was then resynthesized in the presence of SjGST (1.1 mL, 180 μM in 50 mM tris buffer pH 7.5) and added to tris buffer (2.2 mL, 50 mM, pH 8), and the HPLC traces were compared (Figure 1). The

DCL composition was identical in the case of addition of SjGST from the start and the case of SjGST addition to a pre-equilibrated library.

Inhibition Assays. To a 500 μL cuvette were added phosphate buffer (415 μL, 0.1 M pH 6.6), GST (10 μL, 0.148 mg/mL), and inhibitor (12.5 μL in DMSO), and the solution was mixed well. After incubation at ambient temperature for 5 min, CDNB (12.5 μl, 40 mM in EtOH) and GSH (50 μl, 10 mM) were added and quickly mixed well. Absorbance was measured at 340 nm at 20 °C for 5 min. Prior to each experiment, the baseline of the UV spectrometer was corrected by replacing GST solution with phosphate buffer. For each inhibitor, a group of experiments were conducted by varying inhibitor concentrations (0.02−10 μM). After each experiment absorbance against time graphs were plotted such that the initial gradients as velocities were worked out. To calculate the IC_{50} of each inhibitor, the ratio of these velocities and the velocity without any inhibitor were plotted against inhibitor concentrations.

Acknowledgment. We thank the HFSP for the award of a postdoctoral fellowship to Dr. Shi, AstraZeneca and Pfizer for research support grants, and the EPSRC mass spectrometry service at the University of Swansea.

Supporting Information Available: Characterization data for all compounds and analyses of GST protein purity. This material is available free of charge via the Internet at http://pubs.acs.org.

JA058049Y